Intelligent Charging Strategies for Battery Electric Vehicles

Submitted by Leonhard Menz to the University of Exeter
as a thesis for the degree of
Doctor of Philosophy in Computer Science
in November 2019

I certify that all material in this thesis which is not my own work has been identified and that no material has previously been submitted and approved for the award of a degree by this or any other University.

Signature: 

Abstract

Given the relevance of mobility in a globalised world, the development of *sustainable* mobility describes one of the most prominent challenges of modern societies. Electric mobility in conjunction with renewable energy (RE) generation can contribute to the reduction of transportation-related greenhouse gas (GHG) emissions. The combination of RE generation and electric mobility is a nontrivial task. Fluctuations in RE generation and mobility-related energy demand are the products of independent processes. Among other objectives, "smart charging" concepts aim to align these processes by shifting electric vehicle (EV) charging into sensible periods, for instance during excessive RE availability.

The original purpose of EVs, which is to provide mobility to their users, is significantly affected by charging events. EVs cannot fulfil their purpose for as long as they are charging. Hence, shifting charging into periods in which a user wants to be mobile would contradict the concept of electric mobility.

Existing smart charging solutions often consider EV energy demand as generic input that needs to be provided by the user. A smart charging solution's dependency on user input, however, limits its applicability. To eliminate the necessity of manual charging data provision and promote a widespread application of smart charging solutions, this dissertation demonstrates how smart charging can be enhanced by individual user mobility prediction.

As part of a joint framework, the thesis explores an improved method for human mobility prediction. The method combines a Markov model-based prediction scheme with kernel density estimation for departure time prediction. A neural network-based prediction method for atypical travel behaviour further enhances the framework's prediction performance. It is demonstrated that a generic scheduling scheme can schedule EV charging based on predicted mobility under consideration of existing charging infrastructure.

The applicability of a smart charging framework on real-world data is used to demonstrate that it can avoid disutility and a user's adaption in mobility behaviour due to EV-related constraints is not necessary. The resulting framework does not only contribute to the wider adoption of smart charging but can also improve EV acceptance. Improved smart charging usability serves

multiple higher purposes as it accelerates prevalent adoption to EV, advances sustainable mobility, reduces transportation-related GHG emissions and saves resources.

Furthermore, insights about individual mobility behaviour are aggregated to gain knowledge about collective behaviour, which will be valuable information for utilities, grid operators and government energy policymakers.

Contents

List of Figures

List of Tables

List of publications originated from this research:

- Menz, L., Kehl, S., Grill, F., Gerlicher, A. (2016, November) Challenges in the Implementation of Intelligent Charging Strategies. In the VDE-Congress - Internet of Things, Mannheim

- Menz, L., Herberth, R., Luo, C., Gauterin, F., Gerlicher, A., and Wang, Q. (2018, April). An improved method for mobility prediction using a Markov model and density estimation. In Wireless Communications and Networking Conference (WCNC), 2018 IEEE (pp. 1-6). IEEE.

- Menz. L., Herberth, R., Koerper, S., Luo, C., Gauterin, F., Gerlicher, A., and Wang, Q. (2019, October) Identifying Atypical Travel Patterns for Improved Medium-Term Mobility Prediction. In IEEE Transactions on Intelligent Transportation Systems (T-ITS)

Chapter 1: Introduction

The automobile industry is facing the greatest transformation in its history. A market that has been dominated by internal combustion engine vehicles (ICEVs) is now determined to change into a market that will be predominantly based on vehicles that are propelled by electric power units. The transition is mainly driven by efforts to reduce road vehicle-related emissions of greenhouse gases (GHG) [1]. Being the second greatest source, transportation accounted for 15% of the global GHG emissions in 2017 [2].

Electric vehicles (EV) can be operated without local emissions and have the potential to contribute to a more efficient and clean transportation sector [3]. Nevertheless, the energy to charge EVs needs to be generated somehow, which is why some sources argue that electric mobility shifts pollution to the location of power production [4] [5] [6].

The discussions around the environmental impact of EVs were the starting point for several types of research, which investigated how the well-to-wheel emissions of EVs could be determined and minimised [7]. Well-to-wheel emissions describe how much pollution is generated in the process of generating the power to operate an EV. Several independent studies imply that an EV only creates any emission-related benefit over an ICEV if it is charged with renewable energy [8] [9].

Power generation for charging EVs is not the only aspect that is discussed controversially in the fields of electric energy generation and transportation. With an increased EV market penetration, the impact of charging EVs on local power grids becomes a relevant detail. The lower energy density of existing battery technology compared with fossil fuel (11800 - 12800 Wh/kg for petrol and diesel vs. 200 Wh/kg for EV batteries [10]) is often compensated with large capacity traction batteries, which can be charged with high power rates to achieve a short charging time. A load of several hundred kilowatts (kW) that a single charging EV can generate on a power grid is significantly higher than from any other domestic device [11].

Many research projects focus on the challenges brought by the increasing power

demand caused by charging EV and the corresponding loads on power grids. Thereby multiple aspects can be summarised into two key aspects that need to be addressed in particular:

- Single and especially multiple simultaneously charging EVs can create higher loads than any other device within private infrastructures. Hence, power grid branches that originally were not designed to cope with high loads could easily be overstrained.

- The growing utilisation of volatile renewable energy in conjunction with load peaks created by charging EVs increases the risk of local blackouts.

The motivation to maximise the proportion of renewable energy for EV charging and indications for negative grid impact of charging EVs are the main drivers for the development of smart charging solutions. The mitigation of the impact of charging EVs on the power grid includes shifting charging events into periods of renewable power generation, whereas it is avoided to charge at the time when high grid loads are already expected.

Smart charging describes a process in which an EV and a charging infrastructure negotiate a charging event in consideration of the aforementioned factors. The strategy that guides the negotiation can vary, depending on different optimisation targets. To this end, a communication channel is used to transmit a vehicle's charging need in form of energy demand and a "target time", at which charging should be finished. An infrastructure can provide a set of parameters that informs the vehicle about the available charging power and additional information, such as time-dependent power or energy prices.

Both the vehicle's energy demand and the point in time at which charging should be finished are mandatory for a smart charging event, independent from the optimisation scheme. Both parameters are required to compute a "schedule" that takes into account an infrastructure's capabilities and, for instance, the expected renewable energy availability. Also, both values are required to reflect an EV user's mobility wishes. The "required energy" parameter ensures that the vehicle can pro-

vide the desired range within the limits of its battery capacity. The "target time" ensures a sufficient charge at the time of departure.

A major shortcoming of existing smart charging proposals is that a user's charging demand, e.g. the required energy and target time must be provided manually. An EV's energy demand is the result of its user's mobility wishes. Hence, an EV's charging demand is dependant from its current state of charge (SOC), its current position/location and the current time as a reference to the next departure.

Apart from handing over energy demand and departure time to the system, it is an EV user's task to determine a *sensible* input to the smart charging system. For instance, it could be sensible to charge a vehicle just enough to reach a location at which charging might be more efficient or less expensive. In most existing smart charging proposals, this task can be complicated if external information such as flexible power prices, renewable energy generation, charging infrastructure availability and possibly others must be taken into the equation. To date, the technology that is required for sustainable EV charging creates significantly more user involvement than operating a conventional vehicle.

The transition to EVs and the introduction of EV charging technology should be critically assessed from a user's perspective. A significant number of individuals report being uncomfortable with technological change and the associated uncertainty [12]. Studies about the predisposition towards new technologies found out that 50% of Americans are "technology pessimists" [13] and stick to "notions of tradition and familiarity..." in their buying decisions [14] [15].

The following research question is brought up, if the conservative attitude towards new technology is taken into account: What motivates an individual, which is already required to adapt to EV technology, to participate in smart charging, rather than charging whenever it is possible?

Existing smart charging proposals refer to monetary benefits by charging automatically in the time of cheap power provision. However, as will be shown in this research, the actual achievable benefit is neglectable with current tariff structures. The limitations of existing smart charging solutions are used to formulate the first

research question of this thesis:

- How can existing smart charging solutions be advanced by being more user-friendly to promote their use and to contribute to a user-friendly application?

The assessment of existing smart charging solutions is used to illustrate existing shortcomings and to design a conceptual framework for an advanced smart charging system. Apart from creating a user experience improvement, an advanced system must be able to provide vehicle-related charging demand automatically and without the necessity of manual user input. A challenge for such a system is to provide charging inputs that reflect a user's demand, without causing disutility. For example, if a system schedules charging until 9:00 a.m. and the EV user plans to departure at 8:00 a.m.. The assessment of the first research question will illustrate, that a user-centric smart charging solution must relate to an EV user's travel behaviour. The research question that arises from this challenge is:

- What characterises human travel behaviour and are these characteristics eligible to make useful assumptions about smart charging parameters?

Deduced from these two questions and building upon findings of human travel behaviour prediction, one objective of this thesis is to answer the question:

- How can existing prediction schemes be enhanced to provide spatio-temporal mobility predictions which can be used to schedule smart charging events based on prediction?

The prediction of mobility and corresponding energy demand is one of at least two requirements which must be fulfilled to provide an advanced smart charging system. The second step is characterised by a scheme that schedules necessary charging periods in the sequence of predicted mobility events, leading to the following research question:

- What characterises a scheduling scheme that combines individual predicted mobility, predicted energy demand, and charging infrastructure features to a smart "charging schedule"?

Motivated by the need, identified in Chapter 2, to improve existing smart charging solutions, this thesis explores how individual human travel behaviour can be predicted as part of an advanced smart charging framework. Supported by the relevance of a successful transition to sustainable electric mobility, this thesis proposes an adaptive system, which provides full spatio-temporal user mobility prediction and can be considered as an extension to existing smart charging proposals.

Building upon the first research questions the objective of this research is to investigate possibilities to predict mobility characteristics aiming to automate smart charging to a degree at which a user is relieved from general residual planning or scheduling task.

Chapter 3 assesses a purposely collected data set to investigate vehicle-related travel data. The analyses of characteristic trip length, departure times, points of interest (POI), trip sequences and dwell times provide the basis for the design of an advanced prediction mechanism. The investigation of travel data includes the assessment of typical travel patterns, which follow a weekly cycle and atypical travel patterns, which do not follow a weekly periodicity.

Building upon findings of Chapter 3, Chapter 4 explores different combinations of Markovian mobility prediction mechanisms and combines them to a prediction framework, which identifies and predicts typical and atypical travel patterns. The prediction method is supplemented by density estimation based departure time prediction.

Chapter 5 introduces a generic scheduling scheme that is designed to schedule charging events according to different priorities. The scheduling scheme allows the deduction of parameters that are required to make use of smart charging technology. More specifically, the scheduling scheme can be used to transfer *relevant* departure time and predict energy demands to a smart charging infrastructure, which eliminates manual user input.

Referring to the initial question, "What motivates a user to participate in smart charging?" is answered by the proposal of a smart charging framework, which potentially eliminates a user's involvement in the smart charging process. An EV driver

could experience the system as a user-centric recommendation system, which gives individualised notifications for "smart" charging events. The proposed framework achieves two greater goals. It promotes the necessary application of smart charging for secure and sustainable EV charging and contributes to positive EV user experience.

1.1 Contributions

Given the importance of smart charging for a sustainable transition to electromobility, this research provides several original contributions:

- This work contains a detailed review of the concepts of existing smart charging solutions. The review in Chapter 2 reveals that the majority of existing smart charging solutions rely on a user's price sensitivity to make use of smart charging technology. Simulation with real-world mobility data and power tariffs will demonstrate, that most existing smart charging proposals miss convincing motivations for an EV user to participate in balanced grid operation. The discussion in Chapter 2 is used to propose a conceptual approach that promotes the application of smart charging by eliminating user involvement.

- The analysis of travel data outlines the need for and benefits of a smart charging solution that is largely independent of a user's interactions. Chapter 3 introduces a method for EV-related data processing and mobility prediction. The collected data, as well as an accessible data set of anonymised smartphone data, is used to characterise human travel behaviour. In the subsequent Chapters 4 and 5, the aggregated data set is used to demonstrate the applicability of the introduced prediction and scheduling schemes.

- This work introduces an improved method for travel pattern prediction based on a Markov model and probability density estimation (PDE) for accurate departure and arrival time prediction. Furthermore, a method is introduced that utilises a clustering method for categorical data and an artificial neural network (ANN) for day sequence prediction, which enhances the framework's

prediction accuracy. This contribution, which is presented in Chapter 4, provides a travel pattern prediction that sets the groundwork for the subsequent generation of smart charging schedules.

- To the author's knowledge, this thesis is the first that combines individual travel pattern prediction with smart charging solutions. Hence, it is hoped that with the introduction of the proposed smart charging framework, this thesis contributes to the scientific communities of EV charging, power production, and human mobility prediction.

1.2 Thesis Outline

The outline of this thesis is depicted in Figure 1. Because the proposed methods and framework adopt and build upon existing methods, Chapter 2 introduces existing concepts for EV smart charging and human mobility prediction.

Chapter 3 describes the field study that has been conducted as part of this work to a) capture different travel patterns and b) validate the introduced smart charging framework on a real-world data set in later chapters. Human travel behaviour is further analysed with the help of a set of smartphone data that is processed and analysed in Chapter 3 to enlarge the accessible database.

Chapter 4 derives the requirements that mobility prediction in the context of smart charging creates and introduces an improved method for travel pattern prediction. To this end, different prediction methods are explored and combined to ensure that the framework provides reliable predictions for a great variety of different travel patterns.

Chapter 5 introduces a generic rating algorithm to create *predicted schedules*. These schedules combine predicted travel behaviour, energy demand, flexible tariffs and charging infrastructure availability to an user-centric proposal of smart charging events.

Chapter 6 concludes this work and gives an outlook for further research.

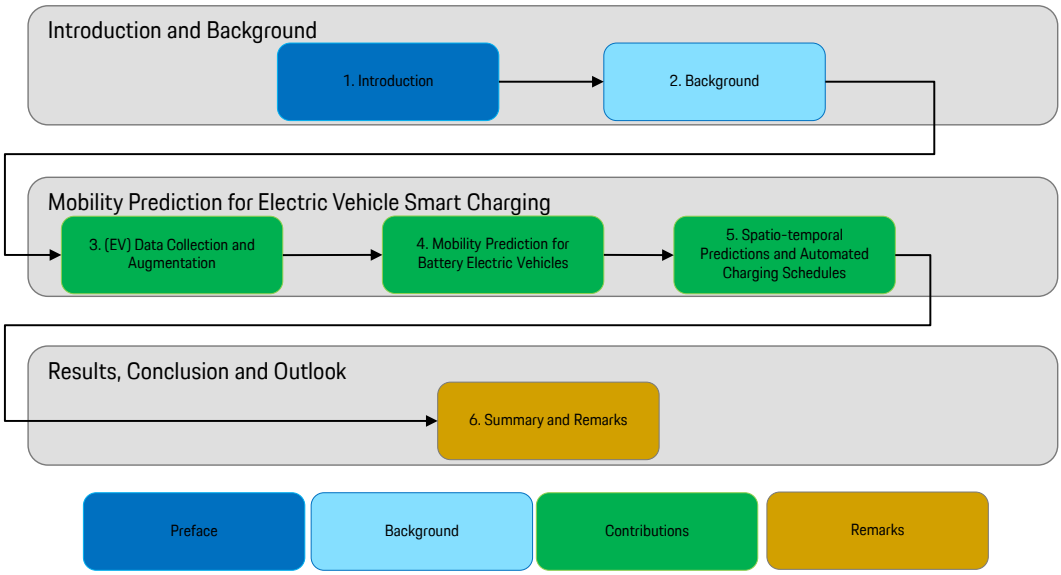

Figure 1: Outline of this thesis

Chapter 2: Background

Chapter 1 pointed out that an advanced smart charging concept should consider an EV user's "travel demand". "Travel demand" can be described as a subtopic of "human travel behaviour" and marks a dedicated research topic. Hence, the design of an advanced smart charging system combines the scientific fields of human travel behaviour and EV (smart) charging. Existing literature, however, treats both aspects as independent scientific fields. To assess their compatibility and address the central research question, 'how to utilise mobility prediction for smart charging', this chapter gives background information about existing smart charging and mobility prediction concepts. The reviewed prediction concepts target private persons in contrast to, for instance, public transportation systems. Section 2.1 gives an overview of the emerging relevance of electro-mobility. Section 2.2 comments on effects and corresponding challenges of uncoordinated EV charging. Section 2.3 explains existing smart charging concepts to mitigate the impact of uncoordinated charging. Section 2.4 gives an overview of existing concepts of travel pattern analysis and trajectory data mining. Section 2.4.6 describes the challenges that are created by mobility prediction in the context of electro-mobility. Section 2.5 summarises this chapter and discusses the compatibility of travel pattern prediction and smart charging.

2.1 Electro-Mobility

Being responsible for approximately 15% of the global greenhouse gas emission[1], the transportation sector in its current state is unsustainable [14]. To create an alternative to vehicles that release GHG by the combustion of fossil fuels, almost all global active vehicle manufacturers are investing in the development of EVs.

However, currently, widespread distribution of EVs is hindered due to various reasons. The most obvious aspect is the comparably high cost of ownership for EVs. Dallinger [16] estimated that the additional investment for an EV to a comparable

[1] https://www.iea.org/weo/, 2019, IEA

ICEV is between 4585 Euros and 8067 Euros. Duvall et al. estimated that the extra cost of owning a hybrid electric vehicle (HEV) ranges between $2500 and $14,000 compared to ICEV [17]. Disregarding the possibility to compensate higher initial investment costs over a vehicle's lifetime [18], incentives in several countries were introduced to promote sales of EVs.

According to the International Organisation of Motor Vehicle Manufacturers (OICA[2]), in 2015, the number of passenger and commercial vehicles worldwide reached almost 1.3 billion units. Around 746000 of these units were battery electric vehicles (BEV), which utilise electric power for propulsion. The required electric power can be obtained by different sources, such as hydrogen cells or vehicle integrated combustion engines [19]. This thesis focuses on battery electric vehicles, which obtain their energy from a power grid by using charging equipment to charge so-called traction batteries, also referred to as plug-in electric vehicles (PEV). Figure 2 illustrates the rising numbers of registered EVs worldwide from 2012 to 2018.

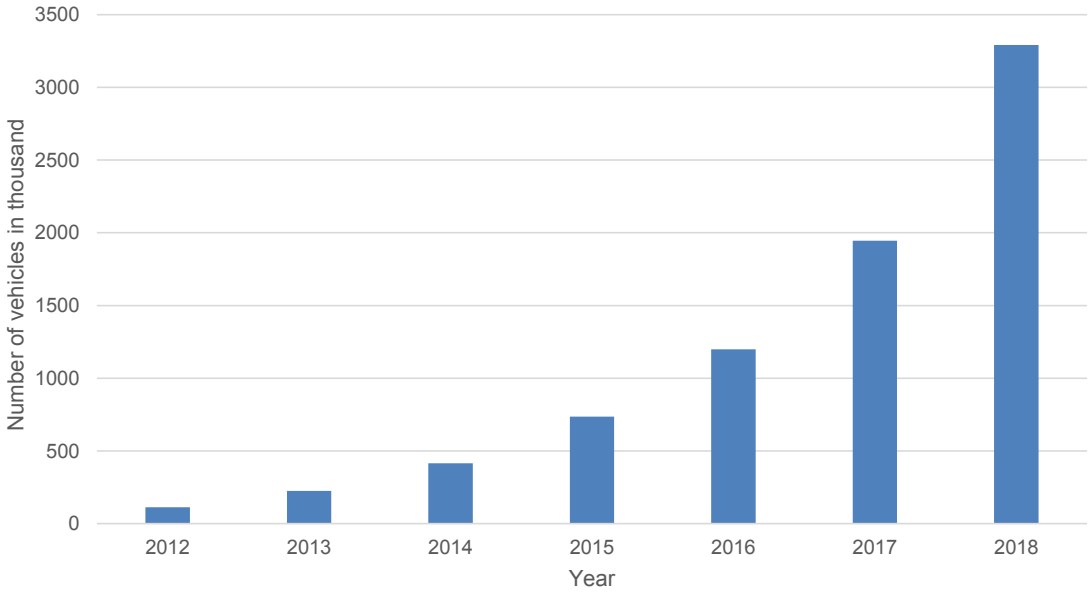

Figure 2: Number of registered electric vehicles (2012-2018) [20]

Besides the absence of local emissions, electric engines and drive trains are superior to combustion engines in term of efficiency and can help to reduce the overall

[2]http://www.oica.net/category/vehicles-in-use/, 2019, OICA

power demand for transportation [21] [22].

2.1.1 Trends in Electro-Mobility

Electro-mobility has gained increased attention in recent years. Emission limits frequently being exceeded inside city centres caused several countries to pass legislation that prohibits combustion engines in general [23] [24]. The Netherlands as well as India plan to stop the registration of vehicles with combustion engines in 2030, Great Britain and France aim for a prohibition in 2040. In Norway, a prohibition could start in 2025, at the same time being one of the fastest growing markets for EVs within the last decade[3]. Figure 3 illustrates the rapid increase of EV-registrations (BEV and "plug-in electric vehicles" (PHEV)) in Norway from 2008 to 2017.

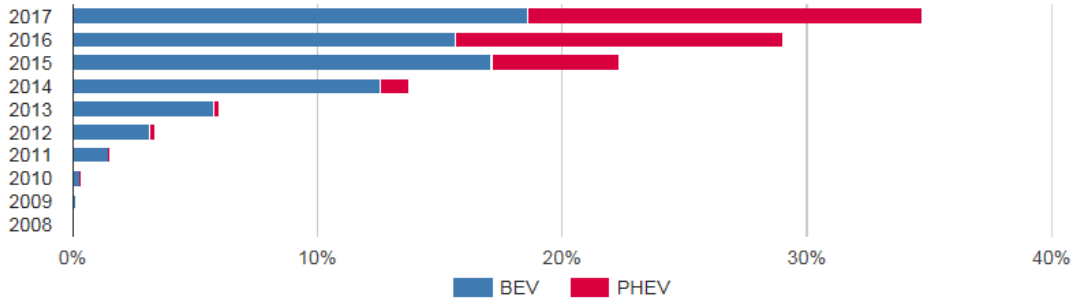

Figure 3: Electric vehicle registration in Norway

The ongoing discussion about banning combustion engine vehicles from city centres, financial incentives [25] and increasing customer acceptance [26] motivate vehicle manufacturers to revise their product lines. As a consequence, the number of available hybrid or fully electric vehicles is constantly rising. Trends in sales of EVs as well as the declared adoption of their product lines of multiple vehicle manufacturers imply that the global market share of EVs will grow.

Both Norway and China established world-leading positions in the electrification of passenger traffic. Both countries installed strong monetary and non-monetary incentives for both, investments in charging infrastructure and vehicles. This led to an increase of EV market penetration from 0.3% to 2.2% in China and 11% to 32% in Norway between 2014 and 2018 [27]. These trends indicate the growing relevance

[3]http://www.eafo.eu/content/norway

of EVs and demonstrate how quickly a relevant proportion of transportation-related energy demand could be shifted from fossil fuels to electric power. With global sales of more than one million units in 2017, EV sales are expected to reach up to 4.5 million by 2020 [27].

2.1.2 Battery Electric Vehicle Components

EVs are categorised according to different factors. Vehicles that combine combustion engines with electric engines but cannot be charged via the electric power grid are called "hybrid electric vehicle" (HEV) or "mild hybrids". Hybrid vehicles that can be charged via the electric power grid are called "plug-in hybrid electric vehicle". Pure electric driven vehicles are often referred to as "battery electric vehicles" (BEV). In the remainder of this work, if not stated differently, "EV" refers to BEV.

HEV carry an internal combustion engine in addition to an electric engine. Hence, their battery capacity is usually smaller than in BEV, as the majority of energy is provided by fossil fuel. Table 1 gives an overview of typical battery sizes of some currently available PHEV.

Table 1: Capacity and range of some currently available PHEV

Vehicle	**Battery capacity [kWh]**	**Rated electric range [km]**
Porsche Panamera 4 e-hybrid	14.1	50
Mercedes Benz S 560 e	13.5	50
Toyota Prius	8.8	20

Compared with plug-in hybrid electric vehicles, full battery electric vehicles rely solely on electric energy provided by the traction battery and therefore carry larger batteries with greater capacities to provide a range up to several hundred kilometres. A vehicle's battery size affects the potential impact that a vehicle can create on the power grid that it is connected to while charging. Not only the energy that is related to a charging event is greater for vehicles with larger batteries but also the

potential load it creates while charging can be higher. Table 2 gives an overview of some currently available full electric vehicles and their battery sizes according to the manufacturer's homepages. The capacity is in most cases significantly higher compared to PHEV batteries, as illustrated in Table 1.

Table 2: Capacity and range of some currently available EV

Vehicle	**Battery capacity [kWh]**	**Rated electric range [km]**
Fiat 500e	24	135
Honda Clarity EV	25.5	143
Hyundai Ioniq EV	28	200
Ford Focus Electric	33.5	185
Volkswagen e-Golf	35.8	201
Nissan LEAF II	40	243
BMW i3	42	246
Tesla Model 3 SR	50	354
Chevrolet Bolt EV	60	383
Tesla Model 3 MR	62	425
Hyundai Kona EV	64	415
Kia Niro Electric	64	379
Tesla Model 3 LR	78	499
Tesla Model SD	75	416
Tesla Model XD	75	381
Jaguar i-Pace	90	377
Audi e-tron	95	399
Tesla Model SD	100	539
Tesla Model XD	100	475

An EV's traction battery consists of multiple battery cells connected in parallel and series. By connecting battery cells in series, it is possible to increase the voltage output as the overall voltage is the sum of all cell voltages connected in series. In

contrast, a traction battery's overall capacity is the sum of all cell capacities, that are connected in parallel [28]. This property is used to create a battery setup that provides the required battery output and the desired capacity.

To date, most available EVs are built with traction batteries that provide a mean voltage output of 400 V [29]. More recent developments increase the voltage output to 800 V [30] [31]. By increasing the voltage, the current can be decreased while maintaining the power output but with smaller cable diameters for the high voltage system, which helps reduce an EV's overall weight.

2.1.2.1 Battery State of Charge

The State of Charge (SOC) is used to express the present battery capacity as a percentage of its maximum capacity [32]. It is often differentiated between technical SOC and "usable" SOC. While the technical SOC is derived from the cell's current to indicate the change in battery capacity over time, the "usable" SOC is used to indicate the range of charge of a battery that can be exploited without creating extended wear on the battery cell chemistry (e.g. 6%-96%) [33] [34] [35] [36]. For this thesis, a more applicable indicator is a battery's State of Energy (SOE), because the SOE is independent of a battery specific capacity. The SOE is indicated in kilowatt hours (kWh) and describes a battery's actual energy content [37]. The amount of energy stored in the battery defines the spatial constraints of an EV [38]. In the remainder of this thesis, simulations and calculations regarding a vehicle's range and energy demand will be based on a vehicle's (simulated) SOE.

2.1.2.2 Electric Vehicle Charging Components

To operate an electric motor, EVs are equipped with power electronics (Inverters) that convert direct current (DC) provided by a battery to a three-phase alternating current (AC) [39]. Inverters also modulate AC in frequency and voltage to control the electric motor's power output corresponding to the requested power output from the driver.

An EV's battery can be charged in two different ways. If the vehicle is coasting, the electric motor(s) can be used to convert the vehicle's kinetic energy to a three-

phase current. In this state, the inverter will convert AC, created by the motor, into DC to charge the traction battery. This process is referred to as "recuperation". The second option is to charge the battery via an external power source. Today most charging infrastructures provide AC (see Section 2.1.3 for detailed discussion). While in theory, the inverter could also be used to convert externally obtained AC, a so-called onboard charger (OBC) is used to provide the battery required DC [29] [40]. An OBC converts AC on different power levels between 3.6 kW and 22 kW. OBCs, in contrast to inverters, are galvanically isolated from the power grid and therefore require fewer safety measures to be operated [41] [42]. Figure 4 gives a schematic overview of some EV-components and their connections.

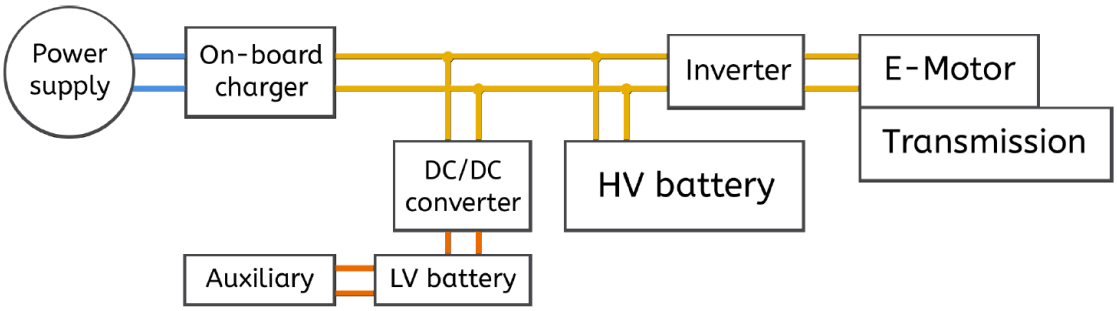

Figure 4: Conceptual illustration of EV components. The blue lines represent the interface to an external power supply. Figure adapted from [43].

2.1.3 Charging Infrastructure

The charging infrastructure is often referred to as the enabler of electric traffic and acts as a physical interface between vehicle and power source [14]. The achievable power output depends on the available voltage and current, which can be different depending on the national power grid [44]. Charging infrastructure with both AC and DC exists [40] [45]. While AC has the advantage of being available in private infrastructure, it is limited to the maximum power output of the local low voltage (LV) grid. In contrast, DC is usually not available in private infrastructure, but offers higher charging power and is not required to be converted to match the battery's requirements. DC charging infrastructure is connected to the distribution grid and is responsible for power conversion instead of the vehicle's inverter [45].

The following paragraphs categorise charging infrastructure in three different classes.

2.1.3.1 Private Charging Infrastructure

Private infrastructures are usually designed to cope with the average load of a household, which normally range up to 5 kW in peak [11]. Figure 5 gives an overview of loads of domestic appliance and the typical frequency of use. Referring to charging at home with up to 22 kW (Mode 4 according to IEC 62196, see Subsection 5.1.4), EVs can generate substantially higher loads than other currently available devices in private households.

Charging in private infrastructure is expected to be the most popular way of charging EVs and has been the favourable charging location in surveys and field trials [46] [47] [48]. This is an important finding as private vehicles often remain parked at home for the longest part of the day [49]. Hence charging at home offers the highest potential to be optimised, as it can be delayed or scheduled with a lower risk of compromising the user's required range [50]. A key feature, that makes charging at home attractive, is that an EV user must not fear waiting time to start charging due to charging point occupation.

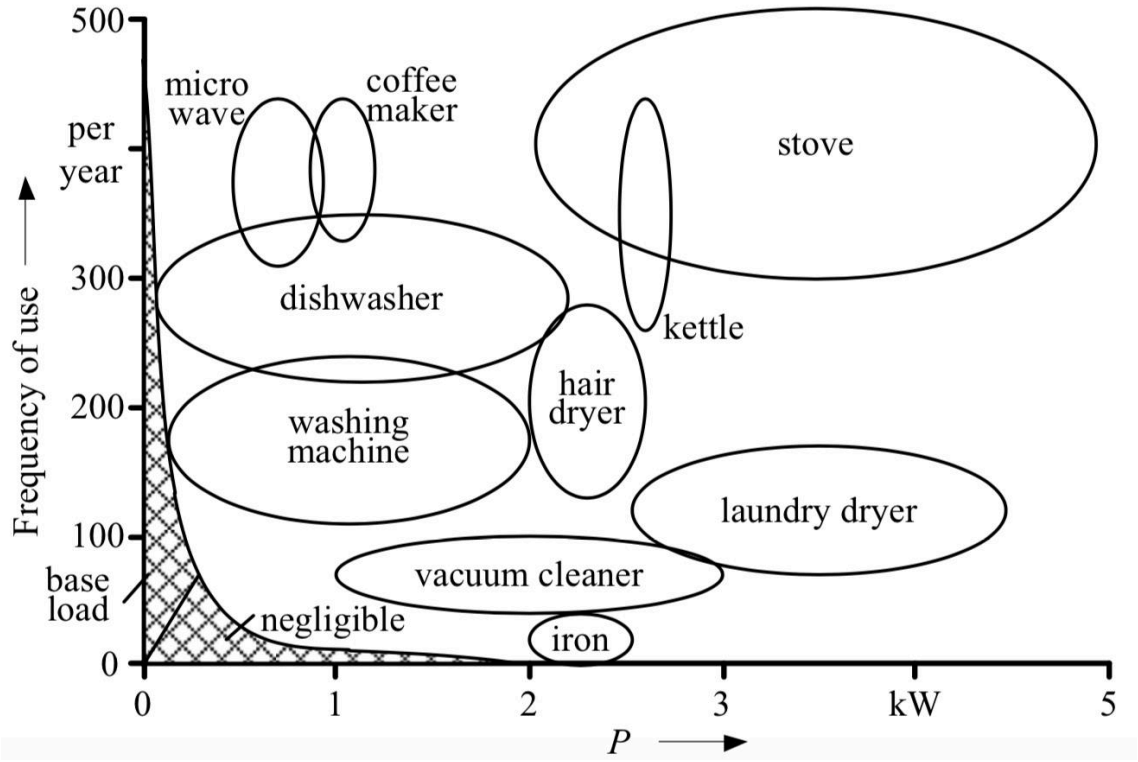

Figure 5: House loads and the corresponding frequency of use [11].

2.1.3.2 Semi-Public Charging Infrastructure

Charging infrastructure that is not private but offers limited access to a specific group of customers or users is referred to as semi-public charging infrastructure. Examples of such kind of charging infrastructures are charging installations for airport service vehicles or EVs for public transportation.

Charging infrastructure for this group of vehicles is likely to be used less randomly as public infrastructure since the duty cycles and the corresponding energy demand of a distinctive group of vehicles can be analysed more easily [51]. In addition to that, charging events are bound to specific locations which help dimension the charging infrastructure to the expected load accordingly.

2.1.3.3 Public Charging Infrastructure

If a trip length exceeds an EV's range, is it required to be charged during the trip. In this situation, charging times of several hours would not be accepted. To avoid long charging sessions, vehicles need to be equipped with DC charging technology

that enables fast charging with high power [52]. Charging on a trip, which is usually conducted on public infrastructure, intends to be as fast as possible to avoid waiting time. To this end, DC fast charging infrastructure is designed to cope with high loads [45]. To date, there is a great variety of different public AC charging infrastructures, which, at the time of writing, is limited to around 22 kW [14]. Due to the necessity of AC to DC conversion AC charging is limited to relatively small charging power which results in charging sessions of up to several hours.

As the intention to charge instantly and as quickly as possible suspends the concept of smart charging, charging at public fast-charging infrastructure is neglected from the consideration of a smart charging framework.

Taking into account human travel and usage behaviour related to personal vehicles, AC charging offers more potential to be optimised. This is emphasised in Chapter 3, which will show that for the majority of EV users fast charging would not be required, as the length of parking periods are more than sufficient to cover the energy demand of private vehicles, even with low power outputs.

2.2 Uncoordinated Charging Schemes

The relevance of smart charging solutions can be illustrated by assessing the effects of multiple uncoordinated charging EVs on the power grid.

The following sources refer to "uncoordinated charging" as a process in which vehicles are either charged immediately after their last trip or immediately after the last trip of the day. Furthermore, these charging events are conducted without any kind of communication between the EV and the power grid. They are referred to as "uncoordinated" as the sum of required charging energy would require a coordinated grid load allocation to avoid local power grid congestion.

An example that is frequently used to illustrate the event of uncoordinated charging is the scenario of EV owners arriving at home in the afternoon. After finishing the final trip of the day, the scenario assumes that a great number of EV owners will start to charge their vehicles on a private power outlet.

Since humans tend to follow similar and repetitive activity patterns during the

day, there is an increased risk of simultaneously charging EVs in periods in which workers arrive at home [53] (see Section 2.4.1 for a review of human travel patterns). Assuming an uncoordinated charging behaviour as described above is expected to create a significant load impact on corresponding power grids. Details of the effects have been investigated in several research projects [54][55][56][57][58][59][60][61].

Disregarding the different data sets that were used for the impact assessments of charging EVs, all investigations conclude the same results with different magnitudes concerning their impact: uncoordinated charging can have negative effects on power grids in form of losses [59], harmonic distortions and DC offsets [60] as well as voltage drops and deviations [61]. Based on the description of uncoordinated vehicle charging, the effects are most significant for charging events in private infrastructure.

A broad consensus can be identified regarding the criticality of large quantities of *simultaneously* charging vehicles. In this case, the sum of power that is required to charge every vehicle is greater than the infrastructure's capacity. To determine periods in which critical situations probably occur, different approaches were presented. Steen et al. [59] used demographic data of a case study in Sweden to determine points in time in which a large proportion of people usually arrive at work or at home. Assuming they would connect a large quantity of EVs for charging in a short period would result in a critical increase in power demand in these periods.

In contrast, Ma et al. [62] used a surveyed dataset of "Mobility in Germany 2008" to model EV user behaviour and estimate accumulated and time-dependent energy and power demand for EV charging. By having access to the regular trip starting and ending times in conjunction with simulated energy demands, the authors addressed the risk of operating the power grid outside of the permissible power limit, if vehicles are charged without any coordinated schedule.

Real EV charging patterns were evaluated by Jiang et al. [63] from a dataset of 64 EVs that were observed for a period of more than twelve months. The results in [63] are different to the previously mentioned sources, as the observed load peak caused by charging events was observed between 3:00 p.m. - 5:00 p.m. rather than expected peak loads between 3:00 p.m. and 8:00 p.m. of other researches [64] [65].

Further impact assessments concluding a critical increase in load due simultaneously charging EVs were conducted in [66][60][67][63].

Differences regarding the magnitude of EV related grid impacts can be explained by the great number of dynamic influences. Two examples are the assumption of different EV market penetration scenarios and the differences in the expected time dependant charging locations. For instance, Jiang et al. [63] focused on the impact of charging at public charging stations, located in the vicinity of working places. Other research projects expect the largest proportion of EV-charging in private infrastructure. The assumption that many users charge their vehicles during the working time naturally results in different load peak compared to charging after the commute in the evening.

2.2.1 Charging Considerations

A charging event is characterised by several aspects. The following subsection will introduce the dominating influencing factors, according to the prominent literature. Relevant aspects can be separated into two groups:

- vehicle related
- grid-related.

Power grids are separated into *Transmission Grid* in which utilities feed generated power, *Distribution Grid* and *Low Voltage Systems*, on which the consumer is connected to the grid [68] [44].

Different grid levels are interconnected via transformers which transform high voltage (Transmission Grid) to medium voltage (Distribution Grid) and low voltage (Low Voltage Systems) for consumers. In some cases, great power consumers, such as industrial facilities which surpass country-specific load limits, are connected to the distribution grid directly to reduce stress on the low voltage distribution infrastructure. Same applies for power generating facilities such as wind farms [69] and photovoltaics [70].

DC charging infrastructure, for instance charging parks that offer high charging power for multiple EVs simultaneously, can surpass local grid constraints. In

this case, the charging infrastructures are, similar to industrial facilities, directly connected to the distribution grid.

2.2.1.1 Charging Location

Depending on the assumption *where* an EV would be charged, the results of the assessments of EV charging impacts on a power grid vary. As discussed in Section 2.1.3, EVs can be connected to the grid via different types of infrastructure. The tendency of humans to travel alongside different locations during the day implies that users pass by or visit different charging infrastructure types during their daily journeys. Accordingly, the user's decision to use one of the available charging possibilities does change the corresponding grid impact in terms of load and location.

To anticipate a realistic EV penetration scenario, Pederson et al. clustered parking locations of vehicles to provide geospatial details for load simulation of charging EVs. The goal of the investigation was to find out how the charging location could affect different branches of a power grid [71]. A shortcoming of the investigation is the assumption that EVs would be connected to the grid every time they are stationary. This assumption would be supported by opportunistic charging behaviour, which has been concluded for a majority of EV users in [50]. However, it is not considered to be realistic to find a charging infrastructure at every parking location. Furthermore, driving data which did not imply a typical "home-work-home" schedule was excluded from the analysis in [71]. Nevertheless, Pederson et al. were able to illustrate a correlation between mobility behaviour, potential charging behaviour and the corresponding impact of a charging location to the power grid.

Besides the relevance of the question: "where to charge?" for an EV user, the location of a critical number of simultaneously conducted charging events is of relevance for a secure grid operation [61] [72]. This applies especially to charging events that are not conducted on dedicated charging infrastructure, for example at an EV user's home. Recall that dedicated charging infrastructure is designed to cope high loads, as has been described in Section 2.1.3. In residential areas, which have

not been dimensioned for simultaneously charging EVs, grid operators will benefit from information about expected loads, as it offers the possibility to utilise shifting potential of flexible loads [73].

2.2.1.2 Charging Time of Day

The time of a charging event plays an important role for utilities, as power needs to be generated at the moment it is needed. To prepare power grid and power generation facilities, utilities create load profiles [74]. These profiles show the average power demand of a sufficient number of households and indicate the expected grid load [75]. Figure 6 illustrates a standard load profile of a residential power consumer in Germany [76]. Separate profiles can be created for commercial and industrial power consumers. Figure 6 emphasises that residential power demand is characterised by peaks in the morning and evening hours, presumably when residents are awake and follow activities at home. Based on this forecast, utilities organise their resources.

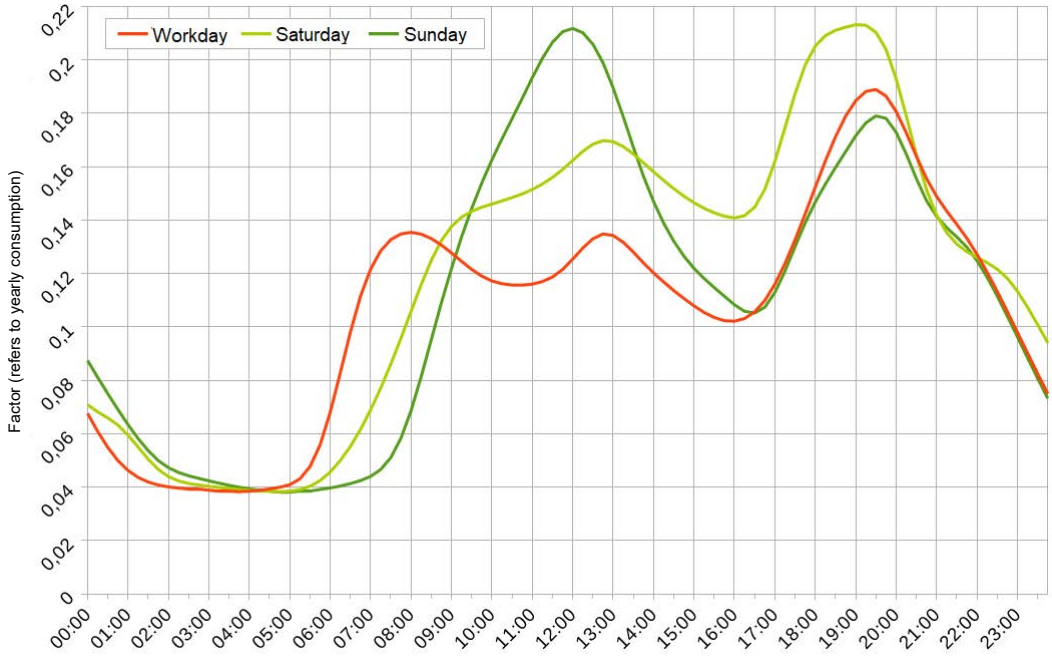

Figure 6: Load profiles for working days (red), Saturday (light green) and Sunday (green). Illustration adapted from [76].

Taking into account the energy and power demand of EVs, the charging time of a sufficient number of EVs changes existing load profiles [77]. An assessment

of the impact of charging EV has been conducted in [59] and [78] to show the influence of charging vehicles on standard load profiles. Investigations regarding the impact of uncontrolled charging have been conducted for different regions and countries, e.g. among others, Germany [79], United Kingdom [50], Belgium [80], USA [81], Canada [82], Portugal [77], Sweden [83], Denmark [71] and Norway [84]. The impact regarding the maximum load created by charging vehicles is sensitive to the assumed EV market penetration, as different results of impact assessments suggest.

Load profiles illustrate the challenges that must be expected when EVs are charged in a manner that most researchers assume, which is at home and right after the arrival in the afternoon/evening. Charging EVs in private infrastructure is usually limited to 22 kW, which is already a higher load than most existing devices create in private infrastructures. The sum of simultaneously charging vehicles, especially on a local level [72], could increase the peak in power demand between 5:00 p.m. and 9:00 p.m. significantly.

The risk of overloading a power grid always exists. For instance, the excessive additional load of air conditioners causes critical stress on California's power grid during hot summer days [85] [86]. Established tools such as load profiles, that are based on historical data and experience, cannot prevent situations where demand excels the capacity of the grid, however, they can forecast critical situations and initiate counteractions. Applicable tools in these situations are control mechanisms like Time-of-use (TOU) [87], Real-time-pricing (RTP) [88] or critical peak pricing (CPP) tariffs [85], which will be explained in more detail in Subsection 2.3. As the dispatch decision is made by the consumer, these mechanisms are referred to as "indirect control mechanisms" or "customer-driven control" mechanisms. In contrast, a direct control dispatch decision, sometimes described as "direct load control" (DLC), can be taken by the service provider [89] [90]. Details about the advantages and disadvantages of different dispatch allocations are given in [16].

2.2.2 Effects of Vehicle Charging on Power Grids

Charging an EV has different impacts on a power grid. Despite creating a significant load, these impacts may cause problems which have been investigated in several research projects.

Focusing on AC charging with 16-32 A current, Farkas et al. investigated possibilities to protect distribution and transmission grids from overloads and power quality issues, caused by charging EVs [91]. For their investigation, Farkas et al. focused on single-phased and three-phased chargers and pointed out, that single-phase chargers can create a voltage asymmetry on the low voltage grid. It should be added that this applies for any single-phase device, however, established devices in household create smaller loads and their effects are accordingly less relevant. In addition to that, the effects should be eased by the random distribution of single phased devices over all three phases. Similar effects were investigated and demonstrated in [60].

Focusing on investigating the impact of DC fast charging on the distribution grid, Yanus et al. [92] compared stochastic and deterministic modelling approaches to elaborate on the effects and possible mitigation measures. Unsurprisingly their findings confirmed that fast charging (with up to 250 kW in their simulation) can have negative effects on distribution transformer loading and system bus voltage profiles. However, it is also demonstrated that local energy storage and voltage conditioning devices, such as Static Var Compensators (SVC), can be used to handle the identified issues.

To gain a better understanding of the influence of onboard chargers on power quality (PQ) in a larger city context, the authors in [60] used a joint research platform. In their findings, Bass et al. illustrate that onboard chargers, more specifically charge controllers, can sometimes create high levels of total harmonic distortions (DTH)[4] which are amplified with a greater number of simultaneously charging vehicles. Similar findings were investigated and presented in [93] and [81].

The previously cited investigations demonstrate that EVs have a measurable

[4]Harmonic distortions describe deviations from the sinusoidal shape of a current or voltage [60].

impact on PQ. To this end, the degree of allowed disturbances, caused by an EV's OBC, is defined in national norms and standards. However, the goal of this dissertation's smart charging framework is to minimise the impact of charging vehicles in terms of loads and not to mitigate the PQ-issues that were presented in the previously mentioned sources. It is assumed that the combination of previously described PQ standards and an early provision of charging needs (based on predicted charging demand and location) will help utilities and grid operators to prepare and allocate grid resources in a manner that minimises the aforementioned negative effects.

2.2.3 Charging Behaviour Case Studies

A charging event's location and time are determined by an EV user's decision to charge or more specifically a result of user-specific charging behaviour. Comparably little is known about the actual charging behaviour of private EV owners. To this end, data extracted from the *SwitchEV* project has been analysed in [94]. The *SwitchEV* project used 49 EVs to collect driving and charging data from a total of 125 users over a period of four years. 23 of these individuals used the vehicle for private purposes and had access to charging infrastructure at home as well as to the *Charge Your Car* (CYC) project, which operates a charging network of 850 charging posts in public, work and home locations [48].

The survey in [48] used data loggers to record vehicle data and smart meter data to record charging related loads. Figure 7 illustrates the average SOC change of 3332 charging events that took place in the residential infrastructure. The plot gives insight into users' charging behaviour at home. It reveals that most charging events are not conducted because they appeared to be necessary. Instead, it draws the picture of an opportunistic charging behaviour, in which charging is conducted due to the availability of charging infrastructure, rather than due to a charging need. This observation is supported by a qualitative survey, conducted in the context of the *SwitchEV* project, in which users stated to *"charge it whether it needs it or not. Just to max up the miles."* [95].

An analysis of 19000 charging events, including public charging, is given in Fig-

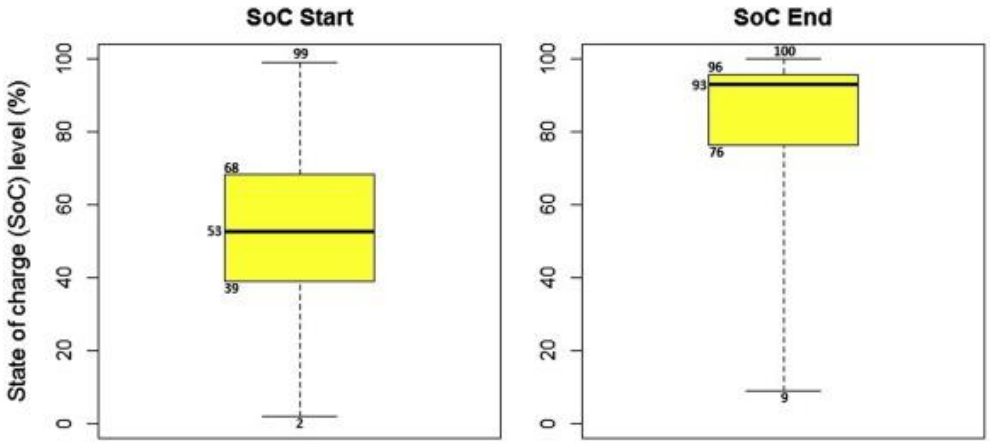

Figure 7: Start and end SOC for 3332 charging events in residential infrastructure. The box indicates the area between the 25th and 75th percentile of data. The bold lines indicate the median. The whiskers indicate the maximum and minimum of all observations [95].

ure 8. The boxplot indicates that when public charging infrastructure is taken into account, the median Start SOC is slightly higher but in general similar to the charging behaviour in private infrastructure [48]. Figure 8 also illustrates that 50% of charging events are used to charge batteries between 15% to 40%. The trial gives

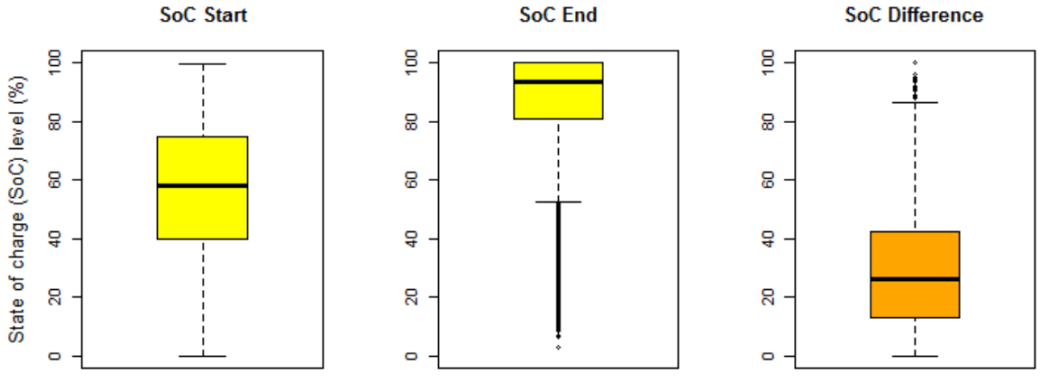

Figure 8: Start and end SOC as well as the corresponding SOC difference for 19000 charging events [95].

valuable insight into charging behaviour. However, the indicated numbers must be assessed carefully and should not be generalised. The vehicles used in the *SwitchEV* study carried traction batteries with capacities between 15 kWh and 24 kWh (Nissan Leaf - 24 kWh for MY 2011-2015, Avid Cue-V - 22 kWh, Peugeot iOn - 15 kWh (usable)), which is relatively small compared to other available EV (see Table 2). The average daily driven distance was 38.9 km in this trial [94].

Nevertheless, as discussed in Section 2.1.1, OEMs tend to equip vehicles with greater batteries in newer vehicle generations to create larger ranges. Apart from the qualitative survey in [95], the data allows no assumption about the users' actual charging motivation. For instance, Franke et al. provide information that charging decisions are, among others, based on a user's "comfortable range" and "battery interaction style" [46].

Building upon findings of [46], Nicolo modelled EV use and charging behaviour in a conceptual and analytical framework [50]. Based on the limited data that captures the real charging behaviour of EV users, Nicolo assumes that EV drivers base their charging decision only on the currently available energy (and derived vehicle range) and the energy required until the next charging opportunity. This automatically results in a myopic charging decision, because the decision does not entail considerations of the characteristic of all charging opportunities within a given time frame. This is a simplification if one considers the variety of charging opportunities that were available to a price-sensitive user.

Only very recently, more real-world data is available to be evaluated regarding EV owners' real-world charging behaviour. The *UK "Electric Nation" EV Smart Charger Trial* being the largest smart charging trial in the world[5], according to the conducting entity, is currently investigating EV users' willingness to participate in smart charging solutions. The trial's full findings were not available for this dissertation, however, initial findings were made available. In principle, participants of the trial accepted smart charging, that shifted their charging events based on adjusted timers, for as long as the amount of charge was provided when they needed it.

2.2.4 Discussion

The assessment of the aforementioned literature reveals that time and location play an essential role in the impact evaluation of charging EVs. However, these aspects also reveal the underlying uncertainties in previously conducted research projects since they are mostly based on different demographic data and assumptions regard-

[5]http://www.electricnation.org.uk/

ing user and charging behaviour. For instance, due to missing information, most projects expect that vehicles are either charged after every trip or after the last trip of the day. In the long term, however, these assumptions must be critically assessed. Further observations are necessary to confirm that vehicles will be connected to the grid after every trip, especially if improved EV ranges, that make frequent charging unnecessary, are taken into account. Furthermore, it needs to be taken into account, that a higher EV market penetration will increase the number of private EV owners with no access to residential charging infrastructure. Hence, for EV owners without a dedicated charging location, the assumption of frequent and regular (short) charging events is not necessarily applicable.

2.3 Smart Charging Schemes

Building upon findings and anticipated effects of EVs on power grids that are described in Subsection 2.2, research was conducted to optimise the integration of EV into the power grid which is referred to as *smart charging solutions*. The notation *smart charging* summarises a great number of different schemes that are proposed to mitigate negative and promote positive effects of EV charging. They are referred to as "smart" as they intend to organise resources in an efficient way. The following paragraphs provide some examples of works that aim toward smart charging solutions.

Optimisation regarding EV grid integration can target different aspects, such as load mitigation and loss reduction. Steen et al. [59] showed that coordinated charging strategies can reduce loads and losses in a power grid in contrast to uncoordinated charging. Their strategy schedules vehicle charging based on time of day and a vehicle's anticipated location under the assumption of hourly electricity prices at the Nordic day-ahead spot market. Vehicles future locations were anticipated from demographic data, provided by a national travel survey [96].

A comparable approach was presented in [62] in which a scheduling function for online optimal charging is proposed. The scheduling strategy optimises the charging of an EV fleet by considering load and price forecasts. The charging demand and

corresponding load were simulated based on arrival times on workdays and weekends, derived from data collected in the "Mobility in Germany 2008" travel survey.

Pointing out the future necessity of scheduled EV charging in [36], Sundstroem et al. propose two methods, one linear and one quadratic approximation of battery behaviour, to schedule EV charging concerning wind power availability, power price and an EV fleet's energy demand. In [36] it is pointed out that a vehicle's energy demand must either be set by the end-user or should be the result of predicted driving patterns. However, Sundstroem et al. exclude the prediction of driving patterns in their publication. The EV fleet's data, which has been used to validate their scheduling scheme, is not made accessible. Further, comparable, smart charging models are proposed in [54][57][62][97][16][64][98][99] and [100]. All listed smart charging proposals share systematic similarities in their design. EV energy demand is usually anticipated from some sort of statistical movement/travel data. The anticipated EV energy demand is assigned to variable time slots, which in some investigations are location variant. Charging events and/or energy demand is then arranged to avoid negative grid impacts and/or maximise RE utilisation.

Building upon a similar systematic, Daina [50] used two real-world data sets ECarSim [50] and [38] to propose a random utility model for joint EV drivers' activity-travel scheduling and charging choices. Daina's work differs from previously described researches in that an EV's energy demand is determined by a user's preference regarding the activity choices, which is expressed via a human-machine interface (HMI). More specifically, an EV user can choose between different proposals regarding the charging schedule. Daina's work is one of the first scientific contribution that focuses on a user's charging choice rather than on a charging demand that is treated as a generic input to a smart charging scheme.

Simplified, most existing smart charging solutions shift charging related loads into times when it is uncritical for the grid and/or advantageous in terms of power production or availability. This primarily serves the interest of grid operators and is, therefore, a one-sided motivation that often ignores the original purpose of electric mobility.

Summarised, smart charging strategies rely on information that is required to be provided by a user, e.g. at what time charging has to be finished and/or what is the desired SOE? From a user's perspective, it is neither practical nor convenient to provide this information for every single charging session. Sometimes it even appears to be impossible for a user to know how much energy would be required to reach the next destinations. Smart charging is likely to fail, assuming that a user would have to provide an accurate schedule for all of his planned trips.

As to date, all incentivised smart charging schemes are time and energy-dependent and rely on similar inputs, which have been summarised in [50] as:

- charging start time preference
- charging end time preference
- preference in available energy at the end of the charging operation.

For this dissertation, it will be assumed that sooner or later one or multiple models of incentives for smart charging will prevail. The assessment of existing smart charging solution reveals that they follow different strategies to pursue mutual targets.

2.3.1 Smart Charging Considerations

Smart charging aims to harmonise power demand and supply. This can be achieved by adjusting the power demand, supply or both. This goal can be achieved with different strategies, which shall be explained in the following paragraphs.

Peak Shaving/Valley Filling

As previously explained, the main motivation for coordinated charging is to reduce stress on power grid components. Standard profiles in Figure 6 show that the majority of grid load is produced in a few "peak hours" in which the demand for energy is particularly high. The concept of *peak shaving* pursues the goal of shifting loads from these peaks into "demand valleys", thus in times in which the power demand is usually lower, for instance during the night. Naturally, this is only applicable for

shiftable loads, which do not compromise users in their power shifting capability. A few examples for such loads are heat pumps, freezers and heating devices, which, due to their thermal inertia, can be operated to fulfil their tasks while reducing their loads for specific periods of the day to a minimum [101]. EVs offer similar capabilities as they can fulfil their purpose, independent from the time in which they where charged.

Delayed Charging

The multimodal shape of prevalent load curves (Figure 6) can be explained by the daily habits of a large number of individuals. A peak in the morning is being created by a large number of people waking up and getting ready to work. A peak in the afternoon is due to returning people to their home and using different electric devices, as has been described in various other sources [83]. An often discussed aspect is the assumption that the demand peak in the afternoon could grow significantly when people arrive at home and start charging immediately.

An oversimplified concept of smart charging is to delay charging events, to mitigate the aforementioned effect. However, to delay charging simplifies the overall challenge that is addressed with smart charging. To delay charging by a static time factor also neglects the possibility to use a charging event as dynamic load and loses the possibility to facilitate peak shaving or the utilisation of fluctuating renewable energies. In addition to that, Schey et al. discovered that due to a time-of-use tariff that offers financial incentives starting from midnight, a demand spike at midnight was created as a great number of users scheduled charging events at the same time [102].

Renewable Energy Utilisation

The strongest argument for the electrification of passenger vehicles is the possibility to utilise RE as a source for propulsion. This idea complements the concept of "Smart Grids" in which bi-directional communication and control signals are used to optimise decentralised power generation and grid operation.

RE generation, for instance through photovoltaic or wind energy, is subject to prevailing weather conditions and underlies fluctuations [103]. To provide a reliable power source for EV charging, RE would be required to be buffered. Buffering electric energy, however, is expensive [104] and lowers RE's positive impact as it creates losses and requires additional equipment. An efficient combination of RE generation and smart charging creates interdependence between both processes.

High costs for storing electric energy and the volatility of RE generation creates another challenge that is addressed with smart charging. In grid branches into which a large proportion of renewable energy is fed, power surplus can become a problem [105] and forces grid operators to degrade RE generation when power production surpluses the demand. Similar to other devices such as heat pumps, EVs can be used as a flexible load. This means that their load can be adapted within technical limits. Simplified, charging power could dynamically be increased to reduce sporadic RE generation surplus [103].

Cost optimal charging

Apart from different motives of existing smart charging proposals, the vast majority of scientific contributions does not consider a user's motivation to participate in smart charging or argues that monetary benefits for EV users justify the accompanying user tasks. Creating financial incentives to shift EV charging describes an indirect control mechanism (see Subsection 2.2.2). Potential monetary benefits are challenged, for instance in [103], in which it is questioned if a vehicle owner would be willing "to waiver a part of the comfort for the chance of reduced costs, offered by a flexible tariff.".

The entanglement to flexible tariffs constitutes a further shortcoming of existing smart charging solutions. Using Germany as an example, the roll-out of smart metering hardware, which is a requirement for the provision of flexible tariffs, will not be finished until 2032[6]. Accordingly, financially incentivised smart charging would be limited to regions with advanced metering equipment.

[6] § 29 Abs. 3 S.1 MsbG

Utility Controlled Charging

DLC (see Subsection 2.2.2) in the context of vehicle charging is referred to as Utility Controlled Charging (UCC). UCC describes a form of smart charging in which the planning of charging and discharging of plugged-in EVs is handed over to an electric utility or third party [47]. To anticipate the acceptance of EV users to utility controlled smart charging services, Bailey et al. conducted a survey on 1470 participants and found out that 24% of the participants agreed strongly to the statement that UCC would be an "invasion of privacy" while 39% strongly agreed or agreed to the statement that UCC "takes control away from me in a way that I would not like" [47]. Due to the little acceptance, the concept of UCC is not further analysed for this thesis.

2.3.2 Summary of Smart Charging Solutions

Charging an EV with high power can create situations where conflicts of interests arise. While utilities and grid operators are interested in optimised and secure grid operation, users of EVs wish to fulfil their mobility demand at any given time [38] [62] [106].

The development of existing smart charging solutions is mostly based on statistical data of user behaviour and does in most cases not consider *individual* behaviour or preferences. Most solutions rely on users' price sensitivity to participate in smart charging.

The impact of EVs and the effects of fluctuating renewable energy have not been critical in the past, but will become more relevant if the trends in EV market penetration and RE energy installations continues to grow. Hence, smart charging concepts aim to combine the following aspects:

- Prevention of congestion of the transmission and distribution grid
- Prevention of congestion of single branches
- Utilisation of renewable energy production
- Utilisation of power price incentives

- Respecting the EV user's mobility demand

Deduced from the listed findings on EV-grid integration, the following generic inputs are of relevance for smart charging concepts:

- Plug-in time (for conductive charging) [d:hh:mm] (Details in Section 2.3.2.1)
- Plug-off/departure time (for conductive charging) [d:hh:mm] (Details in Section 2.3.2.1)
- Required energy [kWh]
- Available power as function of time [kW]

Further data is optional to optimise charging (Details in Section 2.3.2.2):

- Price per unit energy [-]
- Price per unit power [-]
- Percentage of renewable energy [%]
- Percentage of self-generated energy [%]

2.3.2.1 Plug-in time and plug-off time

Plug-in and -off-time define the period in which charging of a vehicle can be conducted. This period can be longer than the necessary charging time, which creates "flexibility". This flexibility allows charging the vehicle preferably in times of excessive power availability or in times of cheap energy/power availability.

"Plug-in" and "plug-off" events define a period in which a vehicle is connected to the grid and could potentially be charged. In an uncontrolled charging scenario, a vehicle starts charging immediately after being connected to the grid. After reaching the target SOC the vehicle remains idle until it is plugged off. Charging immediately after plugging-in reduces flexibility. Once fully charged, the battery offers no buffer capability for RE or cheaper energy.

"Flexibility" is only available, if the charging time with full charging power is shorter then the period in which the vehicle is plugged in. Hence, for smart

charging it is mandatory to have information about the planed unplugging time and the desired energy since a fall-short of the charging target could compromise the user's mobility. The availability of power can change dynamically, for instance due to other loads in the grid branch or fluctuating power production. Thus, postponing charging is always associated to a risk of not reaching an EV user's energy demand.

2.3.2.2 Charging Strategies

Smart charging is conducted by following different strategies to achieve specific optimisation goals. These goals may be defined as minimising the cost of charging or minimising a vehicle's charging impact on a power grid or to maximise the RE utilisation. Depending on the optimisation goal, different signals are required.

Figure 9 depicts an overview of some of the factors that influence smart charging strategies. A holistic smart charging strategy requires to take both vehicle and grid-related aspects into account to create a charging plan that fulfils both party's requirements.

2.3.3 Challenges and Discussion

The assessment of current smart charging solutions exhibits that existing concepts are mainly derived from findings regarding EV charging impact on the power grid.

As a result, these solutions postulate a demographic rather than individual user behaviour. By using demographic behaviour as the basis for the development of smart charging solutions, the effectiveness of proposed systems is sensitive to individual user behaviour deviations.

Previous studies, that are based on user surveys and trials, expect a myopic charging behaviour [50]. Short term charging considerations, however, stand in conflict with the objectives of smart charging. This is because they create spontaneous power demand peaks which can not be postponed in more sensible periods.

Fundamentally, smart charging can be described as a technical concept that is motivated by the objective of a stable grid operation. Rationally, an EV user does not benefit from smart charging, when instant charging without any scheduling

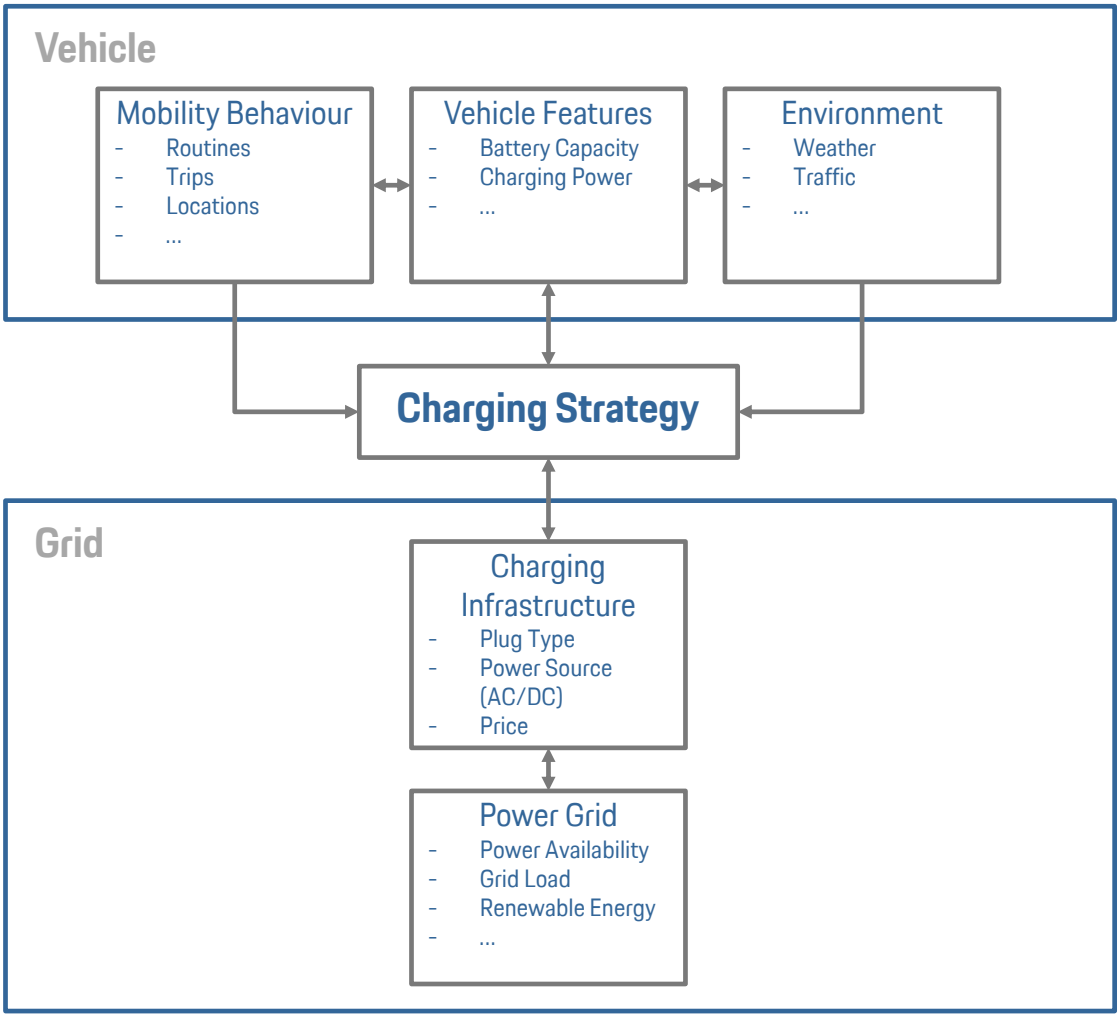

Figure 9: Overview of factors that are involved in the process and application of smart charging.

is considered as an alternative. Hence, existing smart charging concepts propose incentives to utilise EV users' price sensitivity for smart charging participation.

Some findings of EV charging trials suggest that distinctive user groups are in general susceptible to incentives [50]. Despite limited representativeness of the conducted studies, the investigated applications of smart charging require manual input from the EV user regarding charging preferences, e.g. required energy and time at which charging must be completed, to be functional. Ideally, charging needs should be communicated as early as possible, to utilise the time between the moment in which the need is determined and the time the energy should be provided.

Based on the previous summary, smart charging is an integral part of a smart grid, which is required to harmonise power demand and supply. A smart charg-

ing framework's task can be formulated to answer the following (vehicle-related) questions:

- Until *when* has the vehicle to be charged?
- *How much* energy will be needed?
- *Where* will the vehicle be charged?

All of the aforementioned factors are dependant of a vehicle user's *individual* mobility behaviour. Mobility behaviour, as will be demonstrated in the following section, is often characterised by repetitive patterns. Therefore a framework that is capable of providing the required information for smart charging needs to be able to learn and predict individual mobility behaviour.

While the framework focuses on learning *individual* mobility behaviour, the collective knowledge of many users can be utilised for the higher purpose of smart charging EV fleets. Based on previously described findings, a smart charging solution should either be aware of the time-varying grid load and schedules charging in periods of little residual loads or contribute to the determination of a reliable load profile for efficient time-dependent resource allocation. The identification of relevant input parameters provides the groundwork for the development of an adequate smart charging framework. Other than previous works, e.g. [50], this project aims to relieve an EV user from considerations such as "charging decisions once they arrive at a location where charging is available" or "decisions when to depart jointly with the charging decision". This includes that a user is not required to choose between different options for smart charging, which is offered to him after every single trip.

A key advantage of an automated smart charging scheme is that grid resource allocations based on individual charging schedules could be conducted earlier than with manual inputs. Individual and time-dependent energy demand could be updated every time a new charging schedule is created, which could be done in real-time. Up to date charging demand in the form of individual charging schedules could help to identify situations of potential grid congestion or missing RE availability early in advance.

2.4 Travel Pattern Analysis and Mobility Prediction

Travel patterns of humans have been in the focus of scientific investigations since multiple decades. In 1984 Recker et al. [107] described activity patterns "as a set of measurements that define human movement and the output is the classification of this movement into a set of either 'natural' or predetermined categories.". Challenging, however, is "the reduction of the complexity of the measurement vector while maintaining the corresponding information content for pattern comparison [...]". A deeper analysis of corresponding literature shows that travel patterns are often used to describe frequently observable trajectories.

Mazimpaka et al. give a comprehensive overview of methods and applications of trajectory mining. Based on [108], this thesis follows the conceptual approach of *describing* individual vehicle related spatio-temporal patterns, which intends to find human-interpretable structures describing the data. To this end, Chapter 3 analyses and illustrates vehicle-related movement patterns, that have been collected specifically for this project.

The description of movement patterns sets the basis for the subsequent *prediction* of corresponding patterns, aiming for an accurate *individual* and vehicle-related spatio-temporal energy demand schedule.

Out of three different pattern mining categories, that are *Frequent Pattern Mining, Group Pattern Mining* and *Repetitive Pattern Mining*, the latter is of interest for individual mobility prediction. It is used to describe regular movement patterns such as the movement of a commuter [108]. Regularity in this context encompasses some kind of *periodicity*, which promotes the object's *predictability* [109].

2.4.1 Travel Patterns

A review of pertinent literature shows that the term "mobility" is used in different descriptive contexts. Hence the interpretation of "mobility prediction" is context related and therefore used for different application problems [110]. By definition, the term is applied to describe an object's movement within a predefined space.

Relating to human mobility, this can describe mobility within an apartment, a

house or a building where a "relevant place" can be a single room or even a part of one specific room [111] [112]. In a greater scale, covering areas of, for instance, a University Campus [113], some sources refer to mobility within greater areas. Qin et al. simply define mobility as spatio-temporal tracks of individuals [114].

To this end, mobility in the context of this research refers to mobility that is not limited by a specific spatial or temporal restriction. However, the focus is set on a spatial and temporal scale, that is relevant for a framework that schedules charging events for EVs.

2.4.2 Human Mobility

Inherent in the historical development of human societies, human mobility behaviour covers different domains. Independent from its domain, human mobility can be described as an alternating process that consists of "jumps" (between locations) of length Δr and waiting times (time spent at the location) of duration Δt. Findings of [115] indicate that the distributions P of Δr and Δt are both fat-tailed and can be expressed with

$$P(\Delta r) \sim |\Delta r|^{-1-\alpha} \tag{1}$$

with $0 < \alpha < 2$ and

$$P(\Delta t) \sim |\Delta t|^{-1-\beta} \tag{2}$$

with $0 < \beta \leq 1$ [116]. Figure 10 illustrates Δt which has been observed in [114].

The characteristic fat-tailed shape of these distributions suggests describing human travel behaviour as Lévy flights or Continuous-Time Random Walks (CTRW). Both Lévy flights and CTRW have well studied modelling frameworks, as has been pointed out in [116], and propose a simple framework implementation for human mobility prediction. However, Song et al. demonstrate that both models do not explain and sometimes even stand in conflict with reproducible scaling laws regarding human trajectories, which they derived from two large mobility data sets.

Using among others [116] as a baseline, Schneider et al. broke down human mobility patterns to three key indicators [117]:

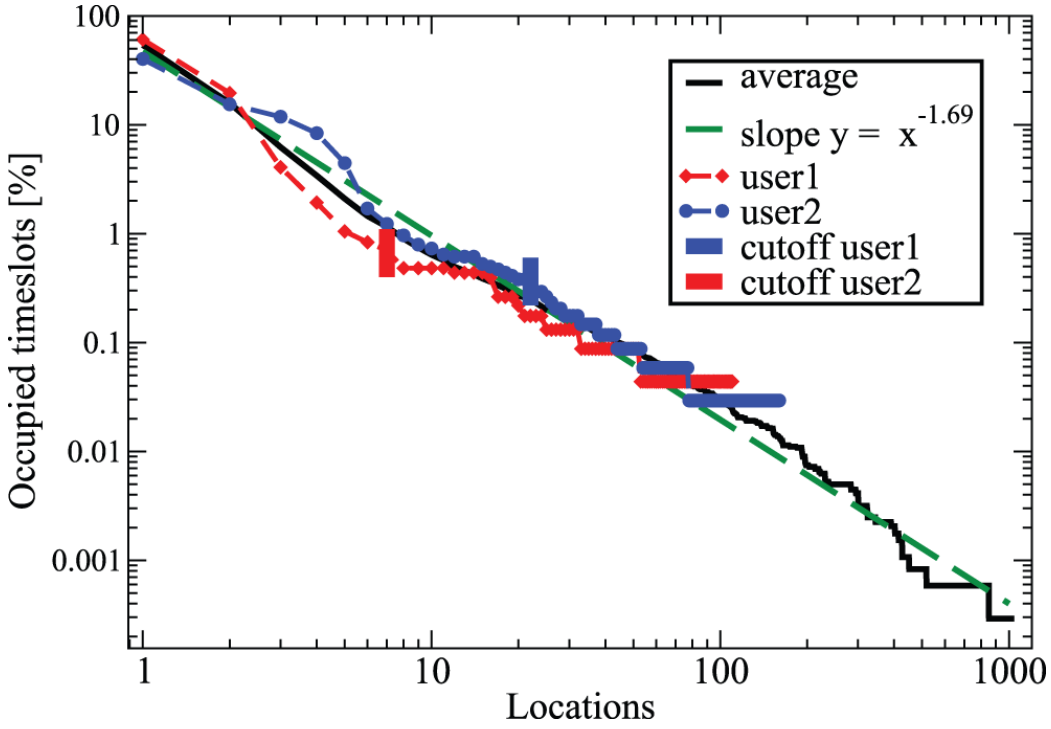

Figure 10: Residence time at most relevant locations [114].

- the trip distance distribution $p(d)$
- the radius of gyration $r_g(t)$
- and the number of visited locations $S(t)$ over time.

Several researchers dedicated their work to finding statistical models which can be used to describe these three key indicators. Brockmann et al. found out, that when $P(d)$ is interpreted as the probability of finding a displacement of length d the trip distance distribution can be approximated with

$$P(d) \sim d^{-(1+\beta)} \tag{3}$$

where $\beta = 0.59 \pm 0.2$ [118]. Gonzales et al. [115] concludes that the radius of gyration distribution $P(r_g)$ can be approximated with

$$P(r_g) = (r_g + r_g^0)^{-\beta_r} exp(-r_g/\kappa) \tag{4}$$

with $r_g^0 = 5.8$ km, $\beta_r = 1.65 \pm 0.15$ and $\kappa = 350$ km. Furthermore, in [116] it has

been found out that the number of distinct locations $S(t)$ visited by a randomly moving human can be approximated with

$$S(t) \sim t^{\mu} \tag{5}$$

with $\mu = 0.6 \pm 0.02$.

Three aspects of the aforementioned findings should be critically assessed. One is that the data sets that were used for the formulation of the aforementioned equations do not consist of ground truth data. Instead, the location data is derived from mobile phone records that were either captured when a person received a text message/call or periodically once per hour. The individual's location was then assumed to be in the vicinity of the closest telephone tower. Similar approaches can be found in [119] [115] [120] [121].

Hence the second aspect: The data sets that were used to derive (3) (4) and (5) are rather coarse-grained. An individual's movement within the range of one single tower is not being reflected. In their data set, consisting of mobile phone records from the area of Seoul, Chon et al. detected 11±2 significant places in the range of one telephone tower [122].

The third aspect is that the proposed methods were tested on long-term mobility behaviour, usually covering periods of more than eight weeks. As has been pointed out in [116] and [117], $S(t)$ does not show a robust scaling exponent μ for $t < 24$h. Furthermore, it has been demonstrated in [115] that r_g stabilises only after a few months.

Referring to a smart charging framework, empirically observed scaling laws for human mobility do not suffice to predict an individual's mobility for charging purposes. This is due to individual deviations and the difference in prediction periods. However, these scaling laws help to identify relevant parameters, which are the locations, the step length and waiting times (dwell times) at specific locations.

2.4.3 Movement Clustering

Clustering of movement has been conducted for different purposes. Lv et al. [123] clustered movement patterns according to the hourly movement data entropy to identify four different user types.

Qin et al. [114] propose two different clustering methods to identify similarities in spatio-temporal movement data. One method uses k-means clustering and the hamming distance to measure the distance between two day vectors. The second method they propose is based on a community network detection [124]. With this method, user mobility records create an individual weighted network. Similarities of day vectors are expressed as weight, where days with similar vectors have a weight of one and day vectors with little similarity have a weight close to zero.

A benefit of this approach is that it is not necessary to adjust the number of clusters a priori. More specifically, Qin et al. use a variant of the algorithm proposed by Duch et al. which is based on an extremal optimisation (EO) of the value of modularity and is feasible for the accurate identification of community structure in large complex networks [124].

The corresponding clusters were then used to create an "average day" from all days of one cluster, under the assumption that this average is a good representation of the created cluster. An important finding is that with data clustering, Qin et al. is able to reduce the uncertainty, measured as entropy in movement data. Entropy in context of mobility data is used to quantify the randomness in mobility data and is discussed in more detail in Subsection 2.4.9. Reducing the uncertainty implies an increase in predictability, hence an opportunity to enhance the performance of a prediction algorithm. Figure 11 illustrates the number of different clusters, the number of frequently visited locations and the user profile specific entropy before and after clustering. All data profiles consist of smartphone location data.

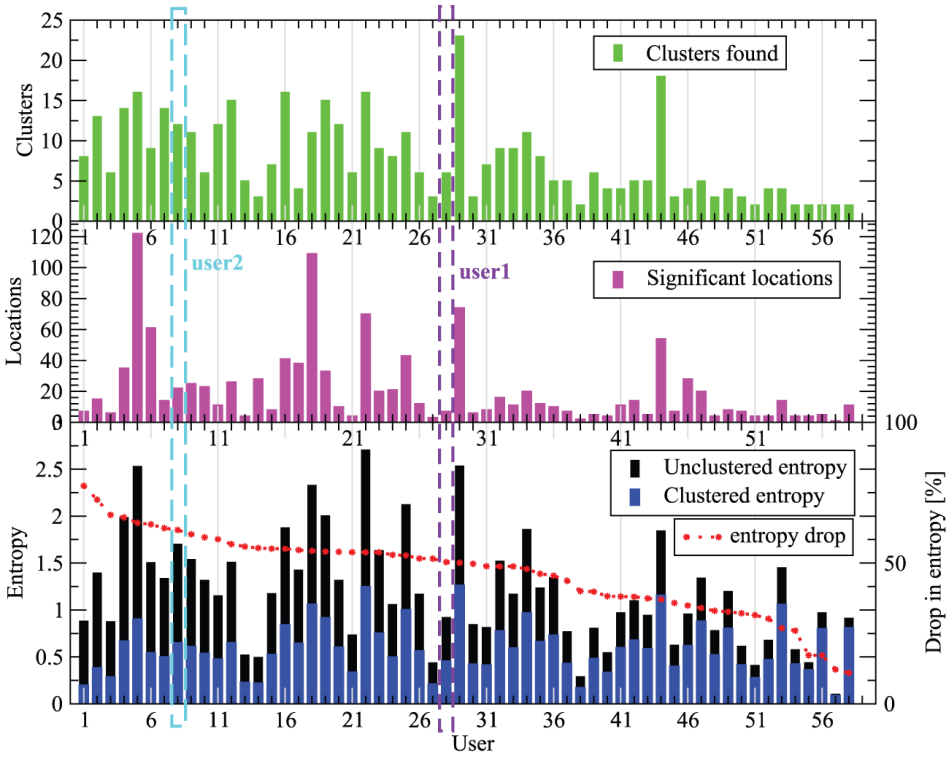

Figure 11: Difference in entropy before and after clustering mobility profiles. The clustering was done with help of an extremal optimisation (EO) algorithm [114].

2.4.4 Mobility Prediction Applications

Motivations that are often presented for research in the context of mobility prediction and travel pattern analysis are: urban planning and traffic forecasting [125] [126] as well as migratory flows [110] and epidemic modelling [127]. More recent work can be found in the context of network performance improvements [128] [129], data pre-fetching [130] [131] and energy consumption of smartphones [132]. Economic motivation is presented by Barbosa-Filho et al. [110], in which a better understanding of human mobility behaviour is motivated by findings of studies in Europe and the USA, which state that households spend 15-20% of their expenditures on transportation, making it the second-largest expenditure category after housing. In addition to that, [110] also emphasise, that transportation is the second-largest source of GHG and therefore has an enormous impact on human societies.

A technology-driven indication for the relevance of user mobility/location data is demonstrated in "Google data collection" by Douglas C. Schmidt [133]. Schmidt

found out that a device with Google's browser, Chrome, installed, sends around 340 location updates per day to Google's servers, even if the device is dormant and stationary. This accounts for 35% of all data samples sent to Google.

2.4.4.1 Location Based Services

Location-based services (LBS) describe information technology (IT) services that utilise an individual's or object's location to provide specific functionalities or services [134]. To provide this service, specific parameters need to be known to the corresponding IT system. This includes an individual's current position and the assignment of a service to a location. A location, in this context, is defined as a spatial region of any size or form. Both an individual's current position and the assignment of a location are the fundamentals of human mobility prediction, which is why mobility prediction could be described as an extension to LBS.

An example for the close relationship of LBS and human mobility prediction is given in [135]. Krumm et. al. used GPS-data of vehicles to create a probabilistic map of location dependant destinations. Extending the probable destinations with route guidance and traffic information provides a useful LBS to drivers. The proposed solution must not be considered as a genuine prediction mechanism. Relevant aspects, such as temporal correlations and departure times were excluded from the research. However, the proposed model in [135] aimed to predict destination while the vehicle was being on a trip and used LBS data to anticipated a vehicle's future whereabouts. Further examples for LBS are given in [136][131] [137] [138] [139] [140] [141] [142] [143] [144] [145] [146] [147] [148] and [149].

2.4.4.2 Network Performance Improvement

More recent applications use mobility prediction in wireless networks for network performance improvements and handover events [150]. Baumann [130], for instance, investigated different variants of Markov Model-based prediction methods to predict a user's location within a wireless network to pre-fetch relevant data for smartphone applications. Another example of smartphone-related mobility prediction is [149]. To predict a smartphone user's mobility, kernel density estimation is used on multiple

temporal and spatial variables for location prediction. While these are just some examples for potential network improvements, smartphone related applications have been one of the biggest drivers in the realm of user mobility prediction. To this end, researchers often use smartphone sensor data for prediction applications. However, similar to most prediction tasks in wireless networks, smartphone application-related prediction often focuses on *short term* predictions for periods of seconds to minutes, which describes "next step" prediction tasks [130].

2.4.5 Prediction Methods

At the beginning of mobility research, Origin-Destination (OD) matrices (T) were used to capture the number of individuals T_{ij} which travel between predefined origin zone i and destination zone j. While in the past T_{ij} was based on travel surveys or traffic counts and used to describe mobility on a population level, rather than individual level [110], individual GPS data allows to adapt the OD-matrix concept to predict mobility behaviour on an individual level (see Section 2.4.5.1 for a more detailed discussion).

An assessment of different data representations helps to assess various prediction methods, that are presented in recent literature. Depending on the prediction task, the literature proposes different forms of representation for mobility data. An overview of different travel data representations is given in [151] of which some are illustrated in Figure 12.

In its simplest form, location prediction is location independent (LI). This means, that a *naive* predictor chooses the most observed location in an individual's location sequence as the individual's future location. While this may look like an oversimplification of the prediction task, [115] demonstrated that in a ranked list of locations, where the highest ranked location is the location at which an individual was observed most often, the probability to find a person at a location with rank L is:

$$P(L) \sim 1/L \tag{6}$$

which describes the Zipf law [152]. However, a naive predictor is of little help for

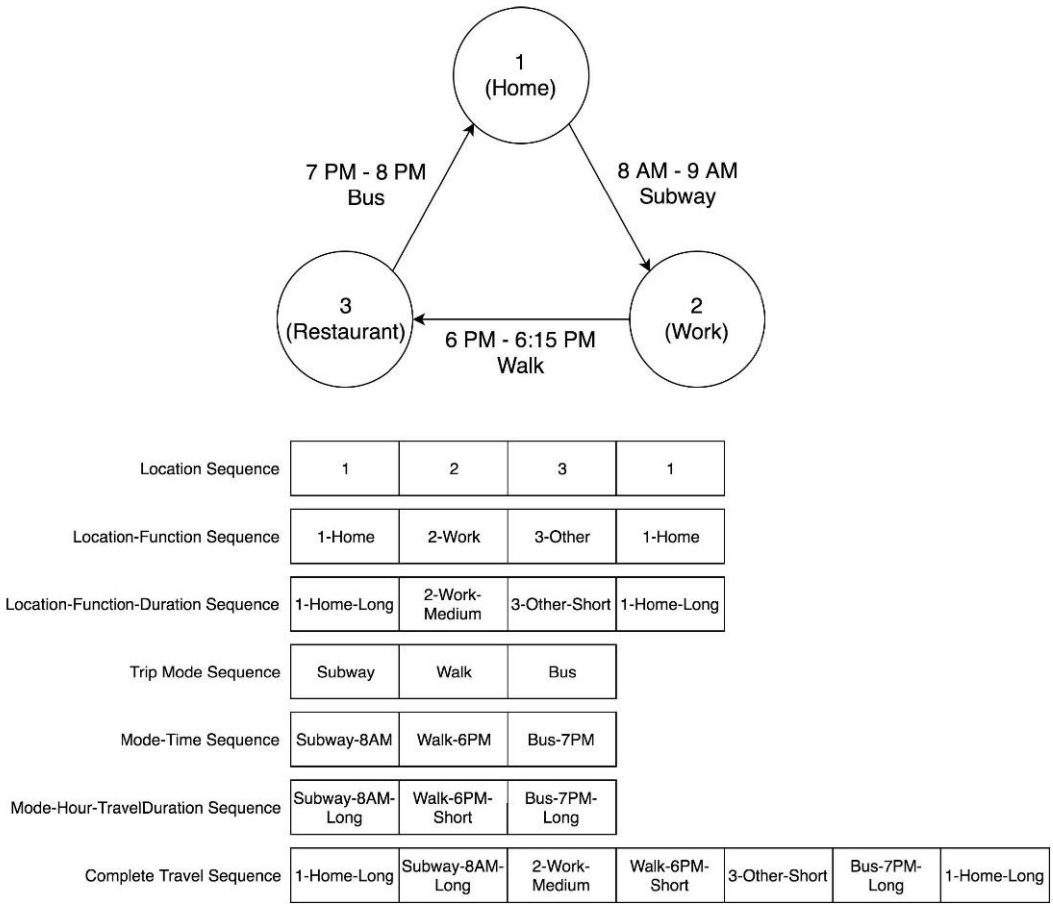

Figure 12: Different travel sequence representations [151].

applications that require spatio-temporal predictions of human travel behaviour as it predicts an individual to always be at the same location.

Other systems use visitation sequences, as illustrated in Figure 12, to compute transition probabilities between locations. These systems are described as location dependant (LD) systems, as an individual's location is considered as input for the prediction task. Temporal parameters increase a prediction task's complexity [153]. To limit the complexity of time dependant location predictions, a popular method is to discretise time intervals (see Figure 12) to limit the number of possible prediction outcomes. However, this step reduces the achievable temporal accuracy of a prediction (see Section 4.6 for a more detailed discussion). Further overviews about different mobility prediction methods are given in [149] [154] [130] [108] and [110]. The following subsections discuss different mobility predictions approaches, presented in recent literature. Note that due to the growing scientific interest in

human travel patterns, there is a great number of different iterations of prediction mechanisms. The following subsections discuss the conceptual approaches behind these mechanisms and will highlight transferable aspects, which are of specific interest for the investigation of EV related mobility prediction, focusing on smart charging use cases.

2.4.5.1 Discrete-time Markov Models

Markov models are one main type of human mobility prediction methods [154]. Referring to [155], a Markov model describes a stochastic process or a sequence of random observations, where an observation is independent of all other observations except the antecedent. Observations also referred to as *system states*, can be used to describe a person's presence at a defined location (L). Transferring a first order Markov model to mobility behaviour, the sequence of a person's visited locations (system states) allows calculating the transition probabilities from one location to another. Figure 13 illustrates a simple Markov process, in which a systems transitions from state l_1 to l_2 to l_3 and so on.

Figure 13: First order Markov illustration

According to [155], the conditional distribution for observing l_n, given all previous observations up to time n, is given by

$$p(l_n|l_1, ..., l_{n-1}) = p(l_n|l_{n-1}). \tag{7}$$

Assuming that only a person's current location is relevant for the transition probability to the next location, describes a Markov model of first order. Likewise, if a person's current and previous location is used to compute the transition probability to the next location, a Markov model of second order is being obtained, where the

joint distribution is given by

$$p(l_1, ..., l_N) = p(l_1)p(l_2|l_1) \prod_{n=3}^{N} p(l_n|l_{n-1}, l_{n-2}). \tag{8}$$

It is possible to create a transition matrix that contains probabilities from a set of locations to all attainable locations. The parameters of a Markov process can be expressed by a transition matrix, written as

$$P = \begin{bmatrix} P(l_1, l_1) & P(l_1, l_2) & \dots & P(l_1, l_n) \\ P(l_2, l_1) & P(l_2, l_2) & \dots & P(l_2, l_n) \\ \vdots & \vdots & \ddots & \vdots \\ P(l_n, l_1) & P(l_n, l_2) & \dots & P(l_n, l_n) \end{bmatrix}. \tag{9}$$

Based on a traditional Markov model, future states can be predicted by choosing the state that is, based on the transition probability, most probable to occur for the next step. This approach shows similarities with the previously described OD-matrices as it is based on a $n \times m$ matrix that is created by origin-destination couples but replaces the number of individuals that travel from i to j (T_{ij}) with the probability of an individual to travel from i to j (P_{ij}).

Markov models provide the basis for many location prediction applications. In these applications, Markov models with little complexity (first order with fallback solutions) performed best for "next step" predictions [130] [153]. A fallback solution, in this occasion, describes a mechanism that allows the algorithm to "escape" into a different state [153].

2.4.5.2 Neural Networks

Neural Networks (NN) are often used for clustering, classification, pattern recognition, forecasting and association tasks [156]. Their strength, characterised by their ability to recognise patterns [157], proposes their applicability for travel pattern analysis and prediction.

Based on [157], the fundamental concept of NN for classification and regression problems will be summarised in the following. Consider a classification problem

in which an input is to be assigned to a correct class in a set of classes $\mathscr{C}_k$ where $k = 1, ..., n$. Let a set of input variables for the classification be denoted as $x_1, ..., x_d$ and a set of output variables as y_k where $k = 1, ..., c$. The intention of using a NN is to use some mathematical equations with adjustable parameters whose values are determined with the help of example data to solve this classification task correctly. This task can be written in the form

$$y_k = y_k(x; w) \tag{10}$$

where w is a vector of parameters. *Learning* and *training* in the context of NN refers to the process of finding values for the vector's parameters which fulfil the classification task most accurate on an example data set.

When categorical data is used to train a NN, the data must be provided in a form, that presents features in a processable integer format. A simple method for this processing step is an *one-hot encoder* to perform "binarisation" of categorical data and to include it as a feature to train a model. Table 3 illustrates how categorical data can be encoded to train a NN.

Table 3: Example of *one hot encoded* categorical data

Category		**Category 1**	**Category 2**	**Category 3**
1	→	1	0	0
2		0	1	0
3		0	0	1

To create interpretable results for mobility prediction applications with NN, *softmax* functions are applied to obtain probability distributions of the generated output [155]. This could be necessary to assign probabilities to a set of locations, comparable to the output of a MM based mobility prediction.

An example of mobility prediction with the help of NN is given in [158], in which an individual's future trajectory is predicted to identify relevant base stations in a

5G network cell. For a similar use case, reference [159] used NN to predict handover events in wireless networks to improve a user's service quality and network resource allocations.

As the mobility prediction domain is dominated by MM based prediction methods, only very few scientific investigations provide a direct comparison with NN based prediction methods. An example is [160] in which three different prediction methods, including a NN, are compared to a naive predictor and a first order MM. On the used data set, the introduced NN outperformed the MM by around 8% on average for "next place" predictions. However, with 44% accuracy for the MM implementation in [160], the indicated performance is significantly lower than what has been reported in several other pieces of research that utilised MM based prediction methods for mobility prediction [130] [153]. Since Etter et al. left out a detailed explanation for the applied input parameters for their MM implementation, the presented results can not be compared to other implementations.

2.4.5.3 Probabilistic Kernel Method

In cases in which the probability distribution for a process or event is unknown *Probability Density Estimation (PDE)* can be employed. In the case of mobility prediction, PDE has been applied to estimate various spatio-temporal parameters. Do et al. [149], for instance, used PDE to estimate the time dependant probability to find an individual in a set of known locations. For this purpose, location specific data points were created in a five minute interval, when a user was registered to be in a known location via a smartphone's GPS. New locations were added with an incremental identifier to an individual's set of locations. "Locations" were declared as GPS points with a 100 meter radius. By overlaying 24-hour intervals, Do et al. used different kernels to create a probability distribution for the aforementioned location identifiers. Intuitively, a more frequently occurring identifier (often visited locations) creates a time dependant higher density, hence a higher probability in contrast to a less occurring identifier (less visited location).

The introduced model was validated with a data set of 133 smartphone records,

collected in a period of at least three months. The prediction accuracy was reported to be 84% on average for one-hour predictions and 77% on average for three-hour predictions, starting from a user's current location. With their model, Do et. al. presented remarkable results regarding the prediction accuracy for one and three hours. Referring to a smart charging scheme however, one to three hours of prediction horizon is too short to create a reliable charging schedule. Nevertheless, the concept of PDE has been demonstrated to be a useful tool for the estimation of transitions times (see Section 4.6 for a more detailed discussion).

2.4.6 Mobility Prediction Challenges

Mobility prediction in the context of human mobility is subject to some degree of uncertainty, due to the randomness in human mobility behaviour [119]. Hence, challenges in human mobility prediction are a) to capture the uncertainty of an individual's travel behaviour and b) to adapt schemes that use mobility prediction according to the degree of uncertainty. The following subsections give an overview of relevant findings in the field of human travel patterns, which should be considered in the design of a smart charging framework.

2.4.7 Atypical Travel Behaviour

So far the reader has been introduced to different machine learning techniques together with different fields of applications. What most of the introduced prediction frameworks have in common is a static distinction between mobility behaviour on different days of the week. While some researches further distinguish between working days and weekends [130] [161], this simplification assumes periodicity-based travel behaviour. Hence the prediction of events on a Monday is based and limited on historic data of all Mondays (or all working days). A periodicity-based approach neglects a phenomenon that has been described as *atypical travel pattern* in [151]. With help of a large sample of transit smart card records from London, Goulet-Langlois et al. were able to demonstrate that regularity in travel behaviour is not tied to the periodicity of fixed time intervals (weekdays or week). How the proposed smart charging framework will take into account atypical travel behaviour will be

explained in Subsection 4.4.

2.4.8 Predictability

Independent of the field of application, human mobility is subject to some degree of randomness in human behaviour. One of the most cited work in the field regarding randomness in mobility prediction is [119] in which the theoretical limits of human mobility predictions have been investigated. The work described in [119] was the starting point for several researchers to investigate the correlation between spatial and temporal features that enabled prediction schemes to reach the in [119] claimed upper limit of human mobility predictability of 93%.

Predictability can be defined as the mean probability to predict a person's next location correctly [162]. Based on this definition Song et al. presented a method that aims to determine the limits of human mobility prediction mathematically [119].

Different aspects of mobility, such as arrival time and dwell time, show differing degrees of predictability, based on entropy calculation. Baumann used the Mobility Data Challenge (MDC) data set[7] to calculate the predictability of residence time and arrival time of individuals' three most visited locations and showed that residence time is characterised by higher predictability than arrival times. Figure 14 depicts Baumann's results.

The results reveal that it is generally easier to predict where somebody will be than the corresponding arrival times, which coincides with findings of [153].

2.4.9 Entropy

In information theory, *Entropy* measures the average number of bits that are required to code a given message with a set of symbols, for which their probability of occurrence is known [163].

In the context of mobility prediction, *Entropy* can be used to measure the irregularity in behaviour, which is an indicator for a person's predictability. A pertinent work in this regard is [119], in which *the limits on the predictability of human mobility* have been investigated. Song et al. used entropy of mobility records to describe

[7] https://www.idiap.ch/dataset/mdc

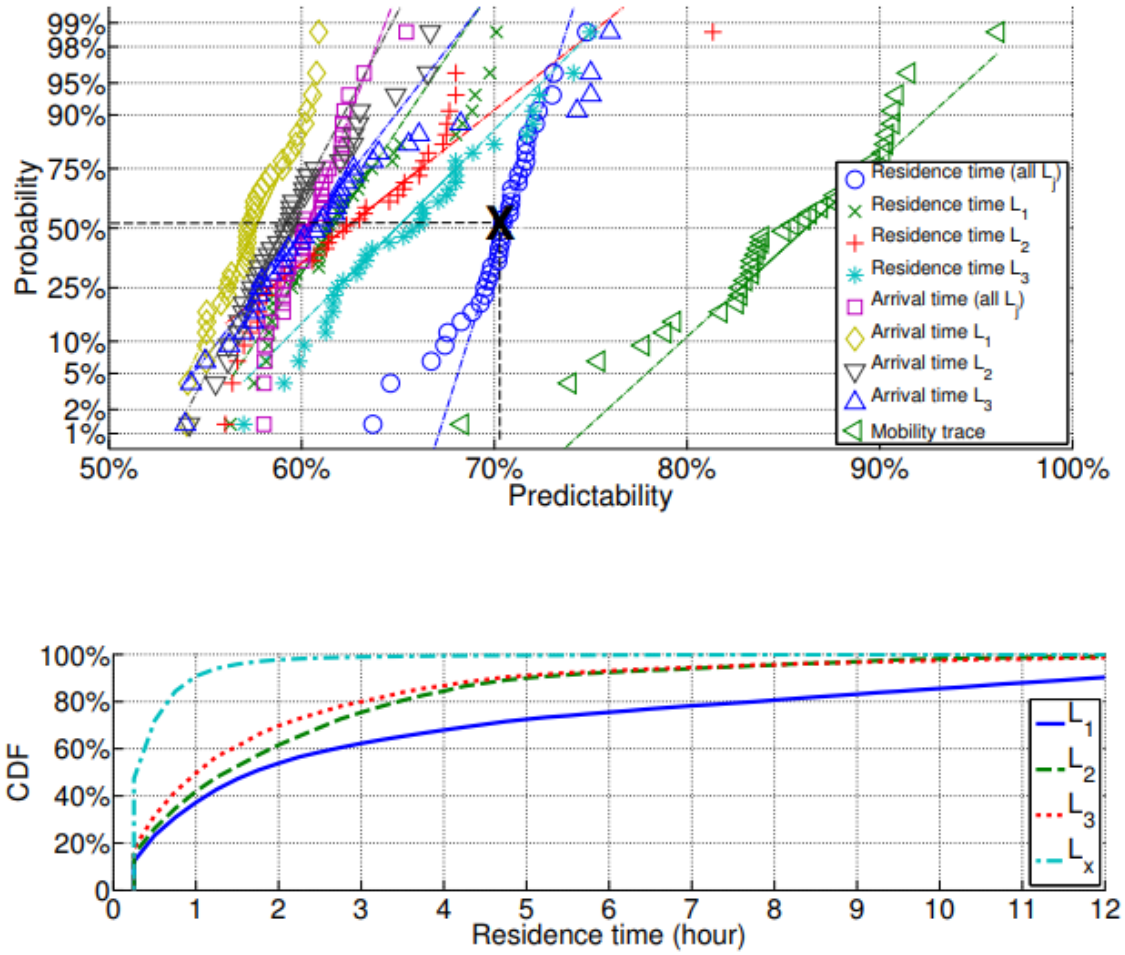

Figure 14: Findings of Baumann in the MDC data set. Correlation of probability and predictability for residence time and arrival time and cummulative distribution function of residence time for L_1= most visited location, L_2= second most visited location, etc.[130].

the interplay of regular and therefore predictable behaviour and behaviour that occurs randomly, hence being unpredictable. Based on the mobility data of 45000 individuals, Song et al. claimed an upper bound of 93% predictability.

Song et al. introduce three entropy measures, that have been applied on mobility data consisting of individual, slotted sequences of cell phone tower symbols: the random entropy, the temporal uncorrelated entropy and the "actual entropy". The random entropy is defined as

$$S_i^{rand} \equiv log_2 N_i \tag{11}$$

where N_i is the number of individual locations visited by user i, assuming an even distribution of probability per location. This value is considered as indicator about a user's predictability as, under this assumption, the probability to predict a user's

location correctly is $1/N$ and S increases with N. In reverse, assuming an individual is completely predictable (for instance because it is always at one location) S equals 0. However, this is obviously not the case, as humans tend to visit a limited number of locations with distinctive probabilities. To account for the difference in popularity of all user specific destination, the temporal-uncorrelated entropy is introduced as

$$S_i^{unc} \equiv -\sum_{j=1}^{N_i} p_i(j) log_2 p_i(j) \tag{12}$$

where $p_j(j)$ is the probability that location j was visited by the user i. As S_i^{unc} does not capture the temporal aspect of the location sequence, the "actual entropy" is defined as

$$S_i \equiv -\sum_{T' \subset T_i} P(T') log_2[P(T_i')] \tag{13}$$

where $P(T_i')$ is the probability of finding a particular time-ordered subsequence T_i' in the sequence T_i. In (13) S_i depends not only on the frequency of visitations but also on the order in which the nodes were visited and the time spent at each location, "thus capturing a spatio-temporal order presented in the individual's mobility pattern".

However, in [119] data was divided in hourly intervals. As Burbey illustrated in [164], the form of representation of mobility data has an impact on the prediction outcome. This is related to findings of [165], which show that the spatial and temporal resolution of data influences the maximum predictability of movement data. The stated maximum predictability of $> 90\%$ was also discussed, among others, in [151], [162] and [166] to refine the aforementioned upper limit.

Ikanovic et al. show in [165] that the maximum achievable predictability increases with a lower temporal and spatial resolution of the same data. Similar findings were presented in [151] in which it is argued that, due to the hourly resolution of cell phone data in [119] in conjunction with the entropy measure described in Equation (13), their findings merely reflect the tendency of an individual to stay in a location for multiple hours. In [151] in particular, it was made transparent, that the predictability for a "time-bin location" is higher than for a "next place"

prediction.

Equally Zhao et al. pointed out that for travel behaviour prediction, the few hours when people travel to different locations are much more important than the majority of hours, in which they do not [167]. Thus, a user's location will more often than not, stay the same, which explains the high theoretical limit of 93% predictability in [119].

The different interpretation of [119] and [162] regarding mobility data entropy estimation illustrates that there is not *one* general rule for computing mobility data entropy. To account for the number of time slots in the investigated data, user mobility entropy S in the remainder of this project is, similar to [162], estimated with:

$$S = -\frac{\sum_{j=1}^{N} \sum_{i \in I} \frac{l_{ij}}{D_{tot}} \cdot \log\left(\frac{l_{ij}}{D_{tot}}\right)}{T_{tot}} \tag{14}$$

where the number of time slots in one day is T_{tot}, the number of days is D_{tot}, I is the set of all visited locations and l_{ij} is the number of times location i dominates time slot j.

2.5 Literature Summary and Discussion

EVs offer great potential to reduce transportation related pollution. The integration of EV into power grids is challenging, as the magnitude of effects that are caused by charging vehicles are the product of many dynamic factors. Simultaneously, EVs create possibilities to be used as flexible loads, which can be used to utilise fluctuating RE.

For the integration of EVs into smart grids, that organise grid resources to harmonise power demand and supply, smart charging solutions are proposed. Smart charging requires the provision of information about the time and location dependent energy demand of EVs. The time and location dependent energy demand is a function of an EV user's mobility. Hence, existing smart charging schemes are dependant on a user's charging decision and the willingness to provide the necessary information.

Studies that investigated the charging decision process of EV owners assume a

joint charging and travel decision. Based on considerations of the currently available energy and the energy required until the next charging opportunity is available, charging decisions are myopic.

Myopic charging behaviour, however, stands in conflict with the fundamental concept of smart charging. Smart charging, which requires bi-directional communication, works best when individual charging needs are communicated as early as possible to be able to organise grid resources and schedule charging loads into sensible periods.

Existing smart charging frameworks prioritise a grid-centric approach for scheduling schemes. Existing user-centric approaches discuss the aspects of charging EVs, but lack an investigation of the *smart* charging principle. Apart from monetary benefits, that are claimed to motivate users to conduct smart charging, little attention is set on a user's motivation and benefit of using smart charging technology [168].

As has been pointed out, a vehicle's energy demand is a function of a user's vehicle-related mobility. Humans tend to follow circadian rhythms in their mobility which can be used to make reasonable assumptions about their future whereabouts. Travel behaviour also allows making predictions about the type of transportation and the taken routes.

Insights into human travel patterns, progress in the field of mobility prediction and findings of user mobility entropy allow the application and adaption of various prediction methods which can be used to derive individual charging parameters.

Existing smart charging schemes can be improved by a smart charging framework that takes an individual's mobility into account and provides vehicle-related energy demands automatically to the grid instances to relieve the user from being involved in charging decisions and the burden of providing charging parameters manually.

This dissertation introduces a joint framework for automated user mobility prediction and smart charging. Empirical implementations of the joint framework are carried out with mobility data of smartphones and vehicle data that has been specifically collected for this research.

The applicability of such framework on real world data is used to demonstrate that a smart charging framework can avoid EV charging related disutility and that a user is not required to adapt his/her mobility behaviour due to EV related constraints. The resulting framework should not only contribute to the wider adoption of smart charging but also to an improved EV acceptance.

Chapter 3: Data Collection and Augmentation

Due to data scarcity, researches often make use of mathematical models for an impact evaluation of EVs on the power grid. This can be attributed to the relatively low EV adoption at the time of writing and due to the challenges that researchers encounter when personal vehicle data needs to be collected [50].

Nonetheless, research in *mobility prediction* generated a number of different mobility data sets and surveys that were made available in recent years [49] [169]. Processing real-world data avoids to make assumptions about the stochastic nature of human mobility and reduces corresponding uncertainties [38].

Human travel behaviour prediction for automated smart charging purposes creates specific requirements which suspends the usability of most available data sets. The prediction of specific trajectories requires detailed data to identify similar trips and their characteristics to derive their significance and energy related context. More specifically, the mobility data must contain features which allow the computation of route specific energy demands.

To this end, Chapter 3 describes a mobility data set trial, in which vehicle data has been collected specifically for this project.

To account for the specific requirements of a smart charging framework, several requirements regarding the data features must be satisfied. For example, the mobility data must provide details about the driving trajectories to assess route-specific energy demand. Hence, it is insufficient to use mobility survey data, which is usually limited to the number and/or length of trips per day (e.g. [49] and [169]). Facing similar challenges as other researches, the lack of both public data and an EV fleet requires this project to rely on vehicle data that has been collected with conventional (internal combustion engine) vehicles [170]. Conventional vehicle data can lack representation due to EV related aspects, for instance, range anxiety, charging infrastructure scarcity and biases. However, simulation results in this thesis demonstrate that mobility demand recorded with conventional vehicles could be satisfied with EV, without any trade-offs. Hence, it is valid to state that the aforementioned

preconceptions are unfounded and that users can eventually drive EVs with similar requirements as ICEV [170].

Based on the aforementioned challenges and preconceptions of electric mobility, a framework that predicts and simulates charging demand based on data collected with ICEV proves that corresponding mobility demand could be satisfied with EV. At the same time, "ICEV-mobility data" is unbiased in the sense that the observed individuals did not adapt their mobility due to range anxiety or other EV-related aspects.

The illustration of data that has been collected in the context of this work will show that it exhibits characteristics similar to those used by other research projects [130] [149] [169] [170] [171]. Based on the similarity of specific data features, it is valid to state that the majority of data collected and used in this thesis appears to be representative for typical travel behaviour. The capability of the proposed framework to predict behaviour learned based on the collected data is thus transferable to other data of similar features and provides an original contribution. However, the reader should recall that, as in any empirical analysis of travel behaviour, the data is affected by geographical, cultural and temporal aspects. Furthermore, exceptions within the used data sets, for instance, atypical travel behaviour, will be discussed and examined separately in Section 4.4.

Chapter 3 discusses some general features of the collected data sets. However, due to limitations in space, only some user profiles will be illustrated in detail to visualise distinctive travel behaviour characteristics. These characteristics are, if not stated differently, shared by most individuals in the data set and hence are not necessary to be illustrated individually.

3.1 Introduction

The prediction of individual behaviour requires historical data of the relevant individual regarding visited locations. Such data has significant privacy implications and therefore must be protected. In most cases, even low-resolution data reveals an individual's home location and allows conclusions about behaviour patterns and

lifestyle preferences.

This chapter provides details about the collection method and processing of corresponding data to *user mobility profiles*. Data Source 1 (DS1) refers to a purposely collected data set which consists of private passenger vehicle data, collected with in-vehicle GPS receivers. Based on definitions given in [167], DS1 is transportation mode-specific and can be described as *intrinsic mobility data*. Trip start and end times can be set into a direct context of a trip start and end with a specific type of transportation.

The data set for the validation of the prediction framework concept is enlarged by Data Source 2 (DS2), which utilises smartphone movement data. The smartphone data consists of multiple samples of a user's time stamped location data. This form of data is described as *extrinsic mobility data* [167]. Unlike intrinsic mobility data, extrinsic data is not assigned to a specific type of transportation. A trait of DS2 is that it is not necessarily associated with a transportation activity. More specifically, location records were only recorded when a location based service application was running and requesting the location from the smartphone's operating system. An extrinsic data collection method requires a mapping of the data records and the travel behaviour by utilising the time and distance between location samples [167].

The combination of both intrinsic and extrinsic data collection methods is used to investigate the data source's impact on the framework's output. To the author's knowledge, this work is the first that uses intrinsic and extrinsic data for smart charging purposes. Inherent to their collection method, DS1 and DS2 show different sources of error which have a measurable impact on their prediction accuracy outcome, as will be demonstrated in Section 4.8. Based on the definition given in [110], similar prediction methods are applied to data of different domains. While vehicle data is considered as a single-scale domain, smartphone data must be considered as a multi-scale domain, as it contains multi-modal movement data.

Further details about the additional processing of movement data will be given in Section 3.2.

3.2 Data Collection

An EV's energy demand is a function of its utilisation. To this end 44 privately owned vehicles, that are driven regularly, are equipped with GPS-trackers[8], to record trip specific parameters:

Table 4: Data collection parameters

Parameter
Latitude
Longitude
Altitude
Speed
Unix time
GPS-Accuracy

Trackers are connected to the vehicle's On-Board-Diagnostics-2 (OBD2) Port for power supply. For as long as the vehicle is moving, GPS positions are sent to a dedicated server via GSM.

3.2.1 Equipment

The tracking devices were calibrated to be activated when a vehicle was started and to be deactivated when the vehicle was shut off. The selected tracking devices, illustrated in Figure 15, were equipped with internal storage of 160 Byte to buffer data when no signal service was available.

[8]GV500 Queclink, http://www.queclink.com/GV500

Figure 15: Tracking device with two GPS antennas, internal storage of 160 Byte, backup battery and GSM module.

3.2.2 Experiments Setup

Participants were asked to keep the tracking device installed for at least eight consecutive weeks. There were no additional requirements set, apart from that the vehicle should be used on more than three days per week, to provide a minimum data input for simulated charging needs.

Table 5: Collected demographic data

Description	**Participants**	**Percent**
Female	9	20.5
Male	35	79.5

It is recognised that the acquired sample size should not be considered as representative for any EV user group. However, as will be illustrated in the remainder of this chapter, the collected data is a good representation of mobility patterns, that were reported in other mobility studies. Therefore it is reasonable to assume that results that will be extracted from the acquired data will provide a scientific contribution and that later derived prediction schemes are applicable for other individuals.

Table 5 gives an overview of the basic demographics of the trial's participants. The influence of demographics on a mobility predictor's performance has been reported as negligible [130].

Due to the sensitive nature of the collected data, participants received a privacy policy information sheet before the tracker installation to inform about the data collection scope and handling process. At no time tracker data and personal data were stored on similar devices or in the same network. The server that hosted the database stored tracker data linked to the tracker device's International Mobile Equipment Identity (IMEI) number.

The web front end which allowed access to the database was secured by a Flask[9] reference module [172]. To secure the transmission of a user name/password combination, communication between client and server was carried out exclusively via Hypertext Transfer Protocol Secure (HTTPS). To access data via an Application-Programming-Interface (API), a predefined API-key was required. Requests without the API-key were denied. The server that stored the data was located in a locked server room at the Stuttgart Media University and secured through a Firewall. The data handling throughout the experiment was in compliance with the General Data Protection Regulation (GDPR).

3.2.3 Route Matching

Location prediction methods require input about the sequence of visited places. However, for energy related queries information about trajectories between these places are necessary. To identify repetitive driven routes, a *route matching* scheme is employed. Route matching refers to the process of assigning a degree of similarity to a set of trajectories [173]. Note that route matching is done for every user, more specifically for user specific mobility record, individually.

Calculating the geographical distance between GPS coordinates can be done, among other methods, by calculating the Euclidean distance or great-circle distance depending on the desired accuracy [173]. For this thesis, a Eucleadian distance based method is used to compare the similarity of trajectories. The conducted trial uses GPS latitude/longitude/altitude records which allows an object's localisation in a three-dimensional space. Hence trajectories are not required to be compared according to their shape solely. A shaped based comparison would create high

[9]https://flask.palletsprojects.com/en/1.0.x/

computational costs since a new route record would have to be compared to the set of all existing user specific routes. The computation costs can be reduced by an initial comparison of the start and end points of two to be compared trajectories. When corresponding start and end point are outside of a to be defined space (which define visited places), they can be excluded from the comparison, as these trajectories cannot be similar.

Raw coordinate values are not sufficient to be compared with each other to determine route similarity in the conducted trial. This is because the number of captured coordinates, even on similar paths, can vary depending on the tracker calibration (time or distance dependant records, filters that optimise storage and performance, etc.). Hence, the route matching method is adapted accordingly.

First, a trajectory T is defined as in [173]:

$$T : ((p_1, t_1), ..., (p_n, t_n)) \tag{15}$$

where $p_k \in \mathbb{R}^2$, $p_k \in \mathbb{R}\ \forall k \in [1...n], \forall n \in N$ and n is the length of the trajectory. The real location between t_i and t_{i+1} is unknown. A line segment between p_i and p_{i+1} is defined as s_i.

The Euclidean distance between two trajectories can then be expressed with the *Hausdorff* distance. To compute the Hausdorff distance the infimum distance between a point of set 1 (Route A) to all points of set 2 (Route B) is determined. The supremum (longest of all shortest) of this set of distances defines the *Hausdorff* distance. It is defined as:

$$d_{\mathrm{H}ausdorff}(A, B) = \max\{ \sup_{a \in A} \inf_{b \in B} d(a, b), \sup_{b \in B} \inf_{a \in A} d(a, b) \}. \tag{16}$$

Because the shortest distance from one point set to the other is not symmetric, it is required to compute the geographical distance from Route A to Route B and from Route B to Route A. This method is non-directional as it does only compare the shapes of two routes and does not take the route's direction into account. A route from Location A to Location B and a route from Location B to Location A

would be considered as similar when the same paths were taken [174]. However, this method is robust against an unequal quantity of coordinates that represent the respective routes as it does not compare them consecutively.

The method, as described in (16), is a point-to-point based distance calculation and thus prone to GPS outliers. The effect can be mitigated by using a point-to-segment comparison [173]. A point-to-segment based approach considers the entire route for the distance calculation instead of just the recorded coordinates.

The method is still Hausdorff distance based but instead of determining the maximum distance between two routes, the average distance is calculated. More specifically, the degree of route similarity is determined by the average value of all straight line distances between each coordinate and its closest segment of the opposing route. Calculating the average deviation has the advantage of being robust against outliers.

Informally, the process is summarised with the following steps:

1. For each coordinate in Route A, calculate the straight line distance to all segments of Route B.

2. Select the minimum of all these calculated distances for each coordinate.

3. Add together all previously determined minimum point to segment distances to get a total of all distances.

4. Repeat the previous steps 1-3 for each coordinate of Route B to Route A.

5. Similar to the approach of calculating the Hausdorff distance, this leads to two values: The sum of all minimum point to segment distances from Route A to Route B and the sum of all distances from Route B to Route A. Add both of these values together and divide the result by the total amount of recorded coordinates.

Based on the Hausdorff distance approach, this algorithm compares the shape of two routes without taking their direction into account. Since the direction of a route may have implications on the energy demand, the start- and endpoints of two

routes are compared. Only if the geographical distance between the start coordinates and the distance between the end coordinates of both routes are within a radius of empirically determined 800 m [175], routes are being compared with each other.

The threshold was determined to be big enough so that route deviation originating from parking the vehicle at different locations are ignored but small enough to consider short trips between close locations (the trip would be ignored if the length of the trip is below the threshold).

3.2.4 Preprocessing

Matching trajectories is a pre-processing step to assign distinctive trajectory identification numbers (trip IDs) to recorded trajectories. Once a new trip is successfully compared and assigned to a previously driven trip, it is labelled with the same ID that has been given at the first trips appearance. The computational cost for this process is justifiable as it reduces the input for a learning algorithm significantly. Transitions between locations can thus be expressed by a single trajectory identifier only.

Recall that prediction methods such as MM are based on a system's "state changes". In the case of mobility prediction, these states are defined as a presence at specific locations. This mechanism requires to identify significant locations, which are referred to as personal points of interests (POI).

Assigning POIs is comparable with the assignemtn of trip-IDs. Data records at a relevant location will be distributed around the actual location. This is because a user could park a vehicle at different locations around a distinctive destination. Also, GPS-errors could falsify the determination of a POI, for instance in a parking garage.

The clustering method selected for this thesis is based on a method proposed by Ashbrook et al. [139]. The concept behind this proposal is adapted by assigning a radius to the last coordinate of every trip, which then defines a POI. Every trip end that lies within the radius of a previously defined POI is assigned to the corresponding POI. Since endpoints may be distributed around a POI centre, for instance, due

to different parking spots, k-means is used to continuously adapt a POI's centre point. Recording trips as described in Section 3.2.3 allows defining route-specific POIs as they are start and endpoints of a trajectory. The duration between two consecutive trips can be defined as parking time. The time that a vehicle remains at a POI together with trip sequences allows drawing a contentious timeline that can be used as input for predicting a vehicle's prospective energy requirements.

3.2.5 Observation and Analysis

Different data features can be characterised for distinctive properties of collected user profiles. The identification of distinctive user characteristics is useful for multiple reasons. Being able to classify users in groups of similar movement behaviour helps to adjust the prediction framework accordingly to subsequently improve the individual prediction performance.

Data of 27 participants met the requirements that were set to be eligible for the prediction framework. Data from the remaining users had to be neglected from the evaluation since their records were inconsistent or incomplete.

Table 6 gives an overview of the collected data of DS1. Key indicators such as the average number of trips per day and the average distance per trip are comparable to data of [49], which is illustrated in Figure 16.

Figure 17 illustrates all driven trip distance of the analysed data. Note that 90% of all trips are shorter than 48 km. Assuming an average power demand of 22 kWh/100km for an EV, which is a typical value for medium size EVs [43], means that 90% of all trips require less than 10.5 kWh per trip. Furthermore, it was found out that trips that account for the longest 10% have a repetitive factor of 1.4. This shows that these trips are most of the time, not part of routines. Figure 18 and Figure 19 illustrate the trip distance distribution of User 2 and User 6. Plateaus at 30 km (User 2) and 38 km (User 6) illustrate that a great proportion of all driven trips for these individuals are comparable in length. By clustering similar routes with unique identifiers, the analysis of trip IDs revealed that for both users the plateaus are mainly created by the daily commute between home and work. Apart

Table 6: User data overview DS1

User	**Days of observation**	$\sum$ **Trips**	**Av. Trips/ Day**	**Mean trip [km]**	**Median trip [km]**	**total Dist. [km]**	**90th percentile [km]**
1	71	116	1.6	16.48	9.08	1108	32.49
2	57	77	1.4	12.54	8.65	1727	30.73
3	70	188	2.7	14.72	5.95	4961	52.00
4	54	187	3.5	22.92	13.11	3444	33.82
5	58	183	3.2	19.58	5.04	1700	49.38
6	69	162	2.3	18.85	12.75	4416	38.91
7	111	311	2.8	27.17	13.24	5586	37.98
8	160	392	2.5	30.04	4.25	7301	29.29
9	139	389	2.8	27.44	8.43	6309	61.01
10	114	264	2.3	29.24	9.65	6430	40.44
12	82	261	3.2	22.21	7.40	4505	29.84
13	111	299	2.7	22.35	8.43	6821	54.34
14	172	229	1.3	11.59	6.17	1815	12.56
15	134	291	2.2	36.98	17.00	8440	67.94
16	113	180	1.6	24.62	17.70	4477	49.34
17	98	453	4.6	15.20	6.48	6748	31.55
18	94	333	3.5	14.24	5.09	3999	22.52
19	384	784	2.0	11.29	5.00	6545	29.79
20	394	699	1.8	21.86	9.17	8239	19.79
21	74	304	4.1	12.34	5.62	2797	18.94
22	132	480	3.6	10.17	5.20	3598	12.75
23	131	401	3.1	11.89	8.74	4343	20.30
24	132	501	3.8	13.89	7.72	6305	32.36
25	368	302	0.8	25.33	6.72	4781	38.92
26	390	672	1.7	8.70	6.46	2837	8.53
27	86	315	3.7	15.03	5.73	3811	20.00
28	133	258	1.9	37.65	20.20	8310	48.14
Total	**3931**	**9031**				**133527**	
Av.	**140**	**343**	**2.6**	**21.59**	**9.32**	**4945**	**34.21**

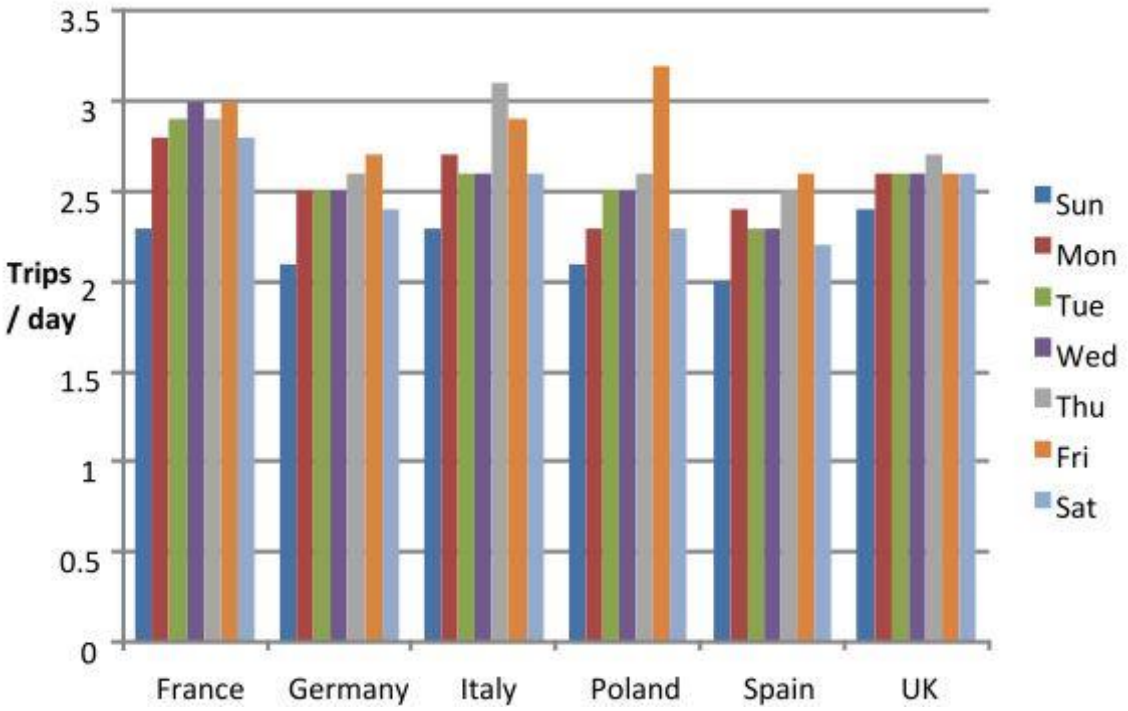

Figure 16: Average number of trips per day by country [49].

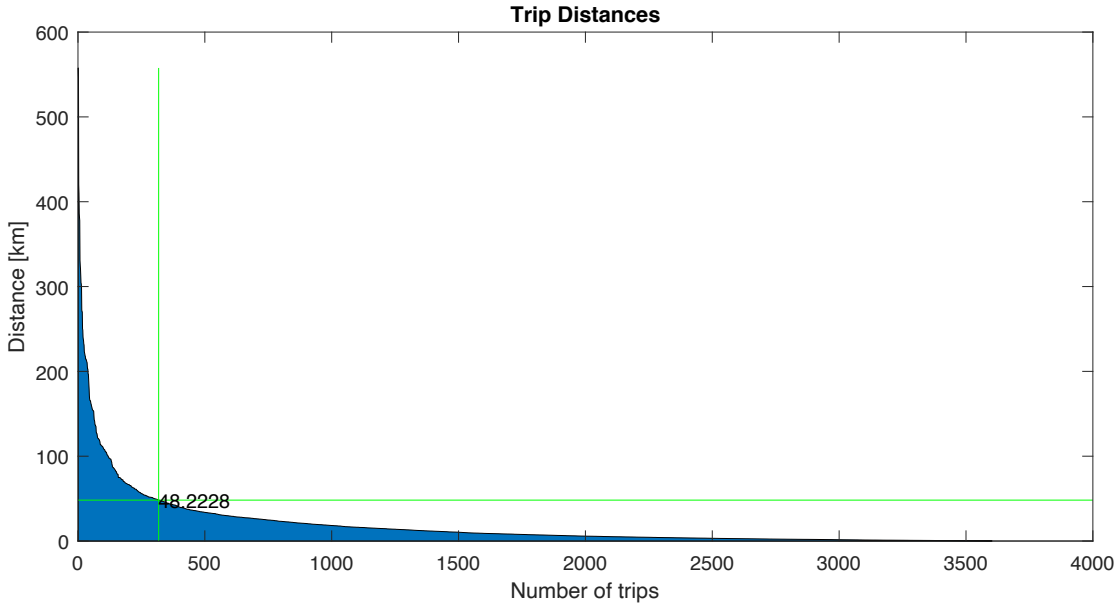

Figure 17: Trip distance distribution of all users of DS1. Trips shorter than 1 km are excluded from the illustration. The green lines mark the 90th percentile.

from the similarity in length, these trips also show a high degree of regularity in terms of their appearance frequency.

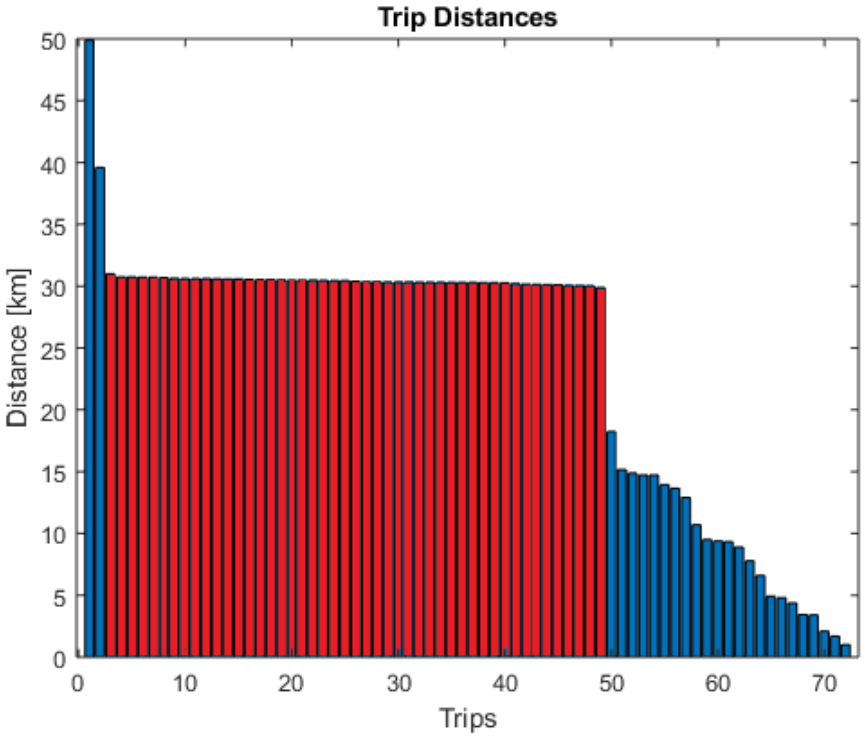

Figure 18: Trip distance distribution of User 2. Commute is coloured in red. For scaling trips shorter than 1 km are excluded from the illustration.

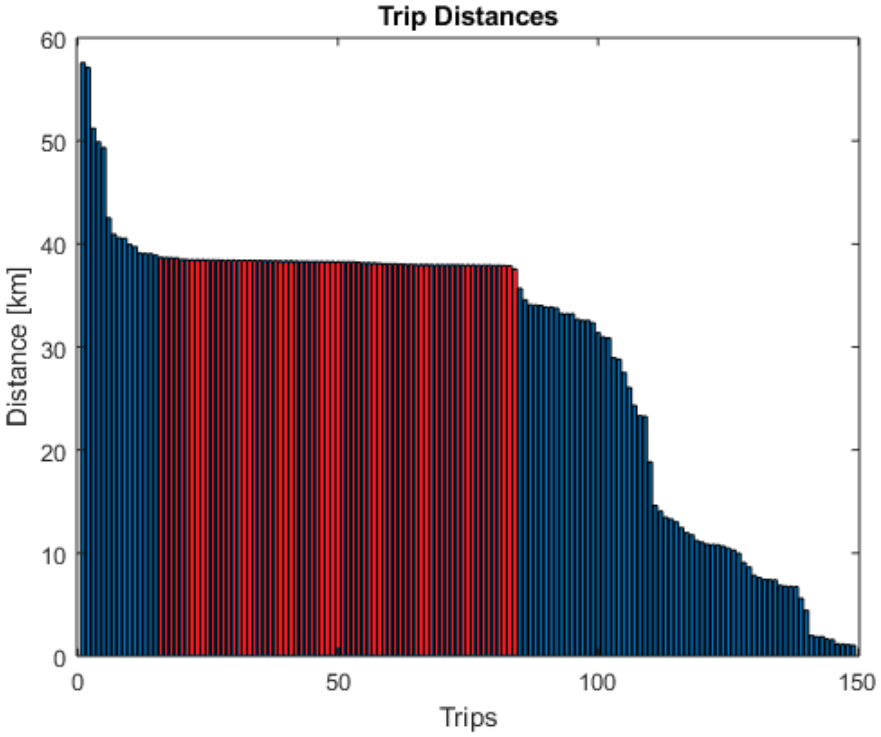

Figure 19: Trip distance distribution of User 6. Commute is coloured in red. For scaling trips shorter than 1 km are excluded from the illustration.

Several sources report observations that indicate that humans tend to travel between few significant locations [115] [116] [118]. DS1 confirms these observations. 89% of the total observation time, participants spent at one of the three most visited locations. This is reflected by the visit count as well as the dwell time per relevant POI, as illustrated in Figure 20. Vehicles remained parked for around 61% on average at their most visited location while location data of smartphones indicate an average of 54% of dwell time for their most visited location. The lower value for smartphones can be explained by the comparatively higher number of locations that were recorded in DS2 compared to DS1 (e.g. a person might visit two stores while the person's vehicle was parked at a single location).

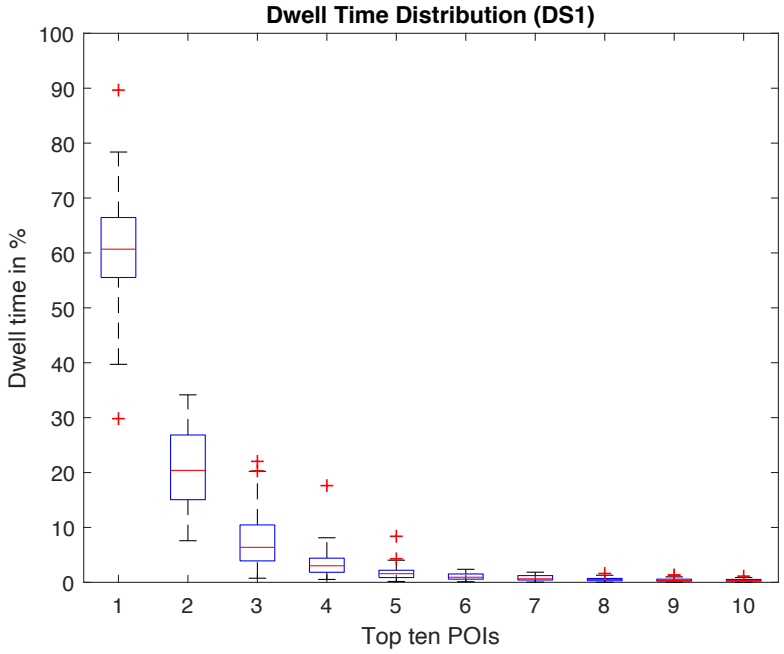

Figure 20: Dwell time in percentage per top ten locations for vehicle data (DS 1, 27 data samples)

Due to their high frequency and long dwell times, frequently visited locations, such as home or workplaces, offer great potential for optimised charging events. To this end, the individual dwell time distributions on these locations are of specific interest. Figure 21 and Figure 22 illustrate dwell-time distributions of User 2 and User 6 at their two most visited POIs. In both cases, a great proportion of stopovers show a similar duration which suggests good predictability of dwell times at these locations. Only on a few occasions, the dwell time is significantly higher than usual,

which could illustrate weekends at which the vehicle was not used, holiday's or times in which another vehicle was used.

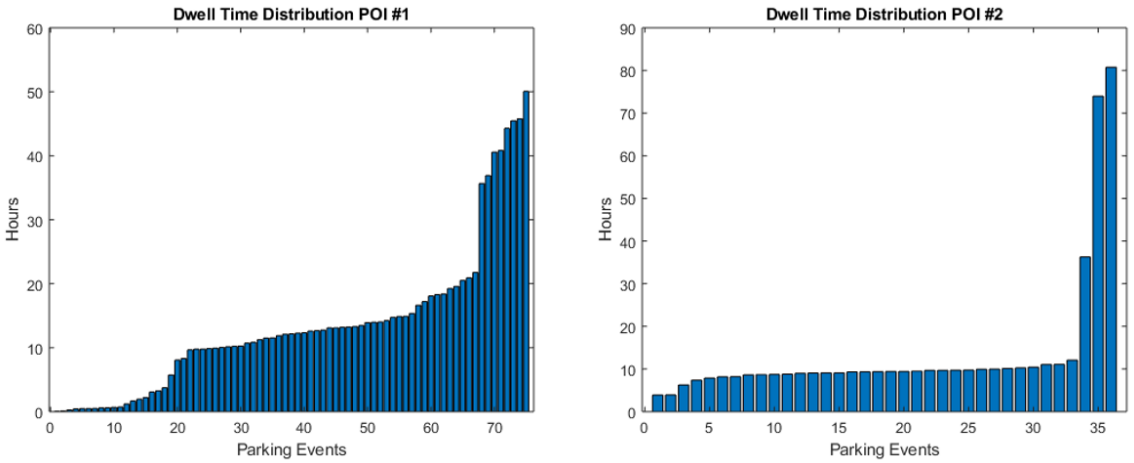

Figure 21: Dwell times on the two most visited locations of User 2

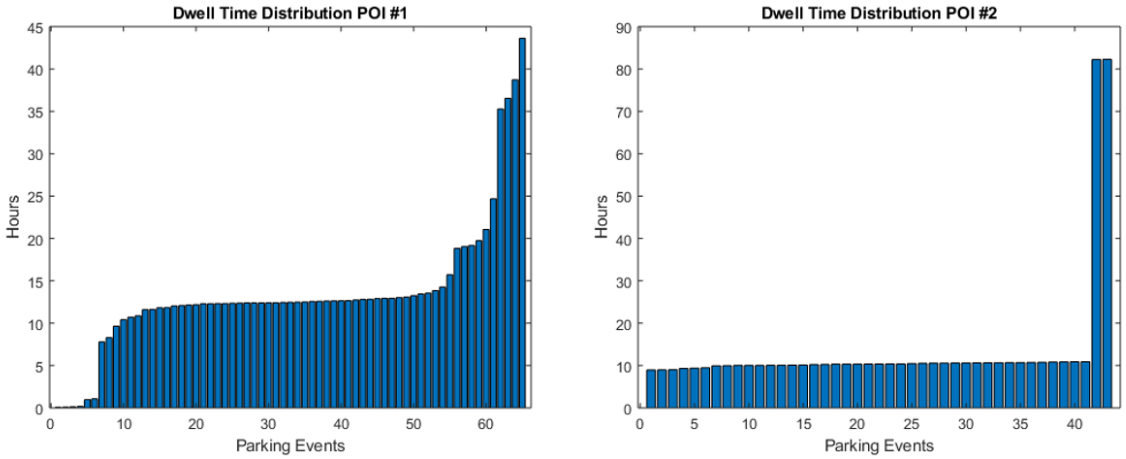

Figure 22: Dwell times on the two most visited locations of User 6

User 2 and User 6 are examples of characteristic mobility behaviour in DS1, which is distinguished by a great degree of regularity. Their mobility behaviour is also following findings of other researchers, such as [113] in which 69% (+-7%) of transitions are towards a location that is visited at least three times in a period of two months.

All location records of User 6 are presented as colourmap in Figure 23. The travel records show that the person travels regularly from its home location to the working place in the morning and back home in the evening. A regular visit is also observable on the last working day of the week (Fridays). The travel behaviour at weekends is rather irregular. The user's average profile entropy is 0.68. Just by visualising

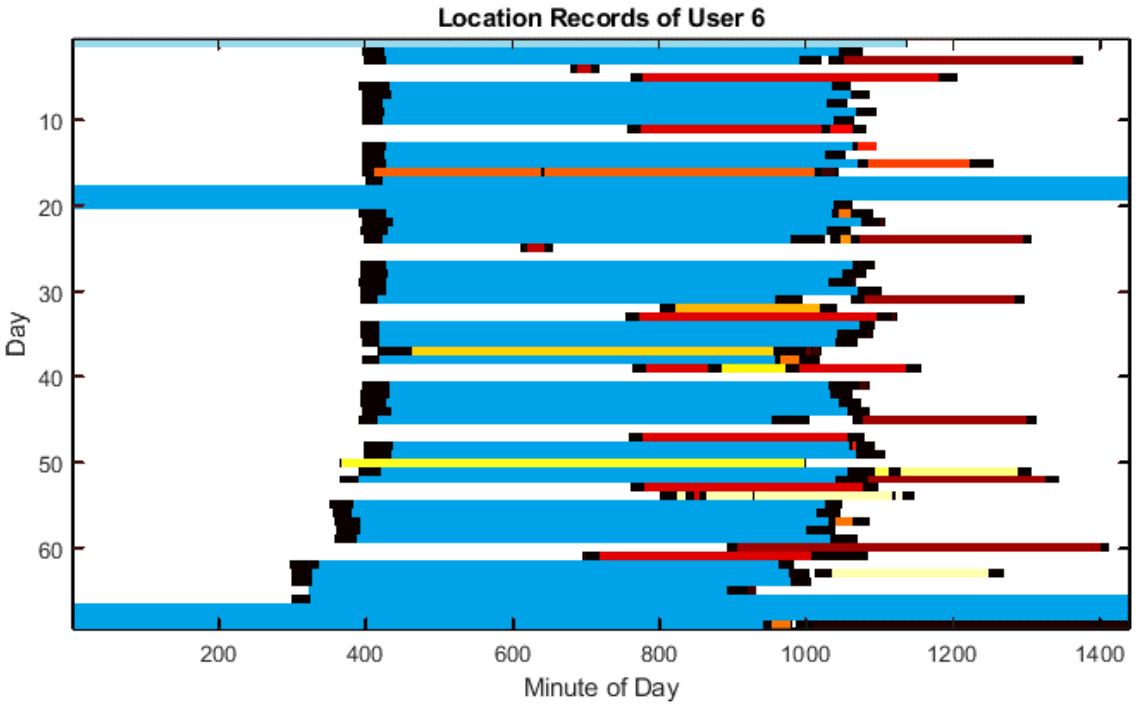

Figure 23: Colourmap of all location records of User 6 (69 days). The first recorded day is a Wednesday. Different colours indicate presence at different POIs. Black entries indicates periods of driving. Note that departure time on the last weeks of record are shifted to the left, due to clock change (daylight saving).

the data, it is possible to identify a high degree of regularity for departure times in the morning. Furthermore, it becomes apparent, that departure times from work to home in the afternoon underlie more deviations. The distribution of departure times in the morning and evening respectively are illustrated in Figure 24. In the morning User 6 leaves most of the time in a period between minute 386 and 400. A few times he left earlier between minute 351 and 365. Departure times from work to home are wider distributed, creating a "leaving period" of roughly 100 minutes. Note that the distributions in Figure 24 only depict departures from home to work and vise versa. Departures to other destinations are excluded. Departure time distribution, trip length distribution as well as the dwell time distribution of Users 2 and User 6 show characteristic shapes, which can be observed for most user profiles in the data collection trial.

Naturally, there are users with less characteristic travel behaviour. In that regard, an interesting observation was made on data of User 16. The shape of trip distance distribution (Figure 25) is comparable to Users 2 and 6 (see Figure 18 and 19), however, the mobility pattern illustrates a distinctive difference to other users.

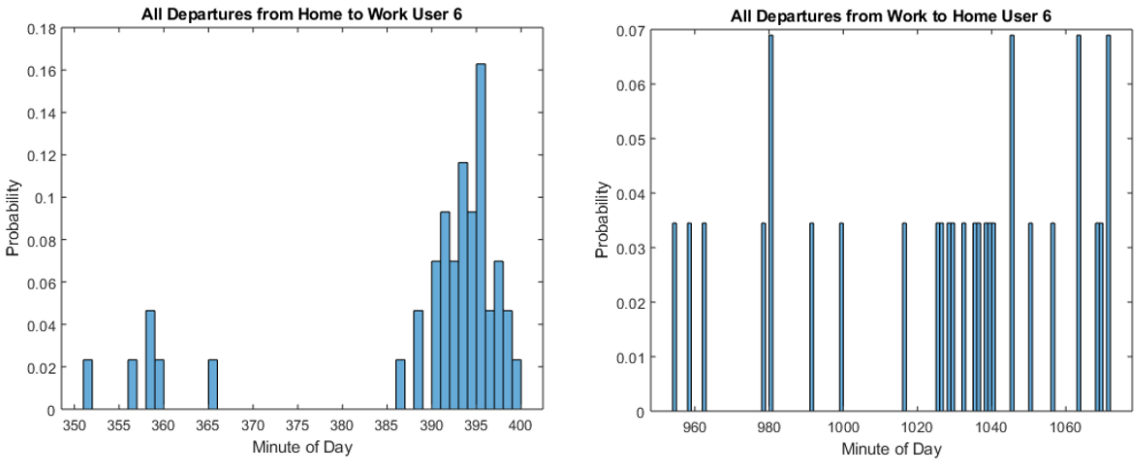

Figure 24: Departure times in the morning and in the evening (with corrected day time saving offset).

Figure 28 shows that User 16 follows a travel behaviour, that can be described as

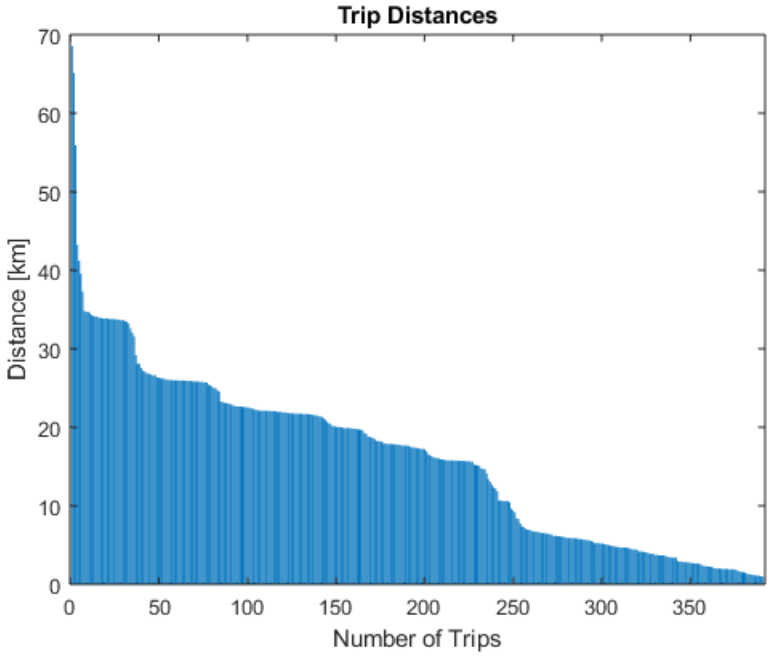

Figure 25: Trip distance distribution of User 16. For scaling trips shorter than 1 km are excluded from the illustration.

atypical [151]. Trips from and to work, which usually underlie great regularity and weekly periodicity, change in terms of departure time by increments of eight hours with a periodicity of three weeks. As User 16 works in a three-shift operation, the mobility behaviour contains a three-week periodicity, which consequently affects the commute times.

Other than the commute of User 6, that starts in one period with a length

of roughly ten minutes (Figure 24) , departure times of User 16 gather in three periods that are distributed over the entire day, as illustrated in Figure 26. Wider distributed events are more challenging to predict. For User 16 an average entropy of 1.18 was determined.

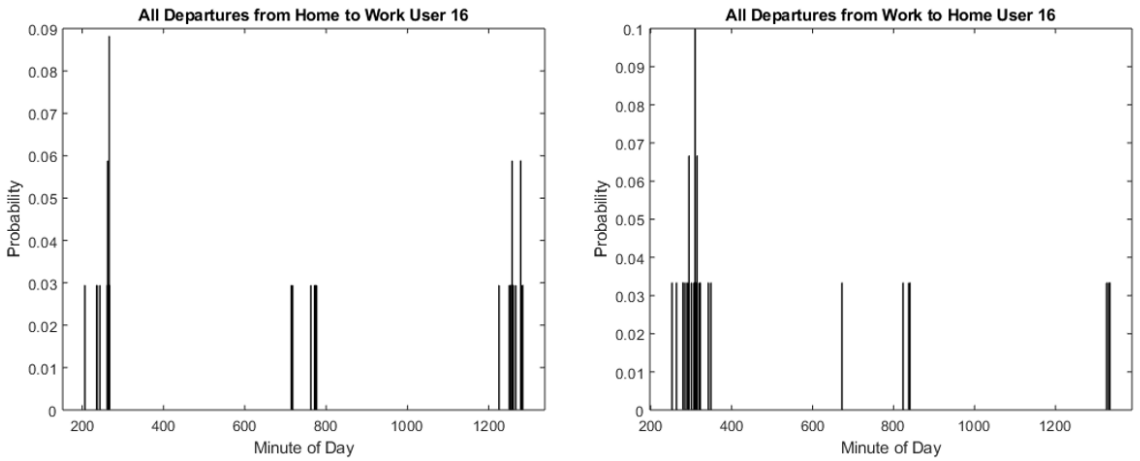

Figure 26: Departure time distribution for commute of User 16.

In Figure 26 departure events to the working place are grouped in three periods of roughly 40 minutes. The three periods are separated by eight hour increments. Departure events from work to home show similar characteristics. It is recognisable that departure times towards home in the night (around minute 100) are more pronounced. This could indicate that the person developed the habit to always drive home after leaving work in the night but to visit other locations after work if the shift ended during the day.

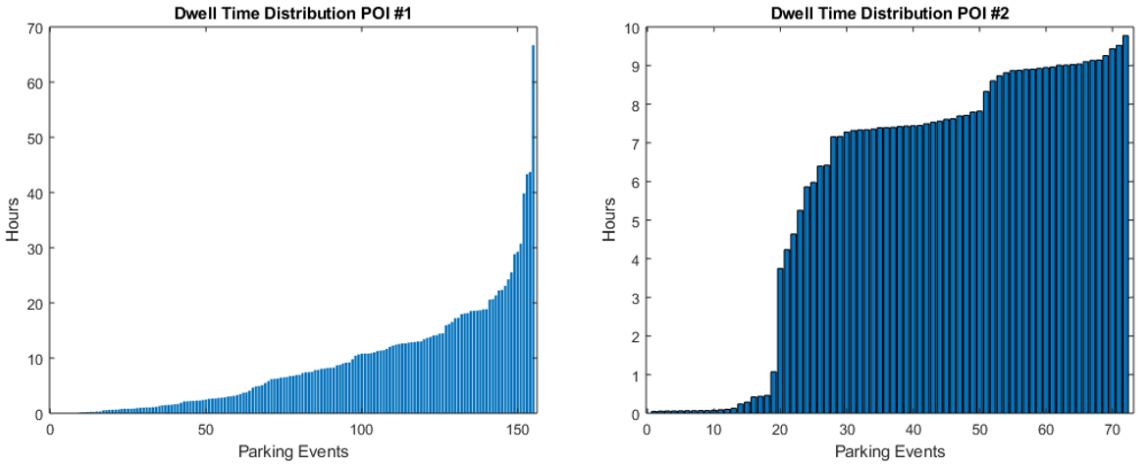

Figure 27: Dwell times on the two most visited locations of User 16.

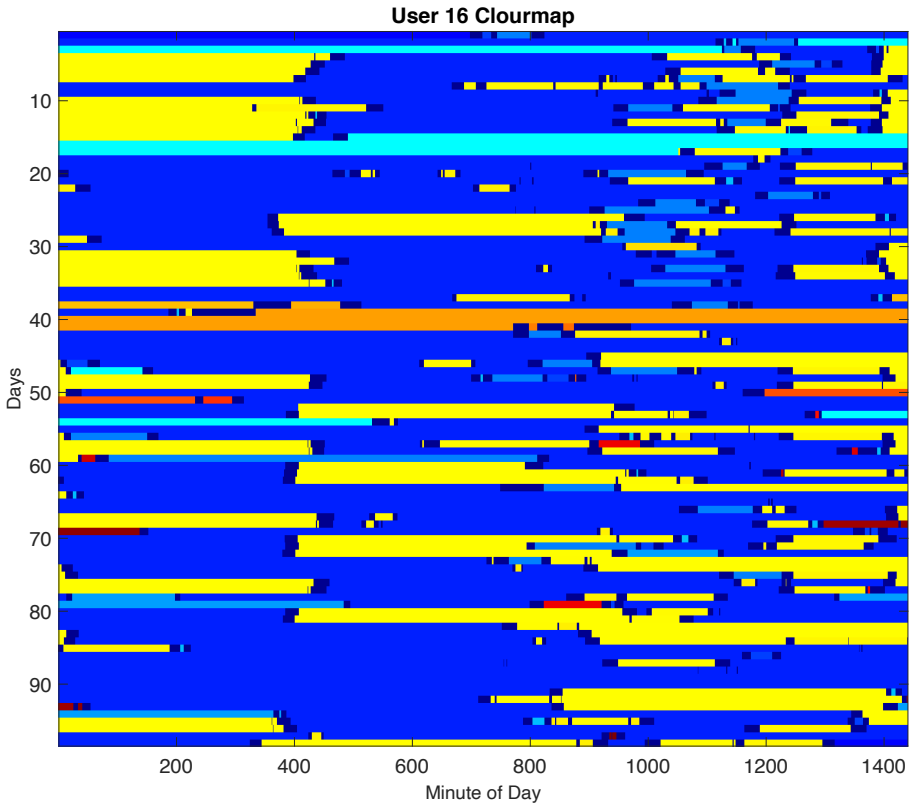

Figure 28: Colourmap of all location records of User 16. 60 minute offset due to UTC time shift.

3.2.6 Mobility Patterns from Mobile Phone Data

For the smartphone data, more than 80% of total record time is spent at one of the three most visited locations. Accounting for 89% of record time it is 9% more likely to find a vehicle at one of the three most visited parking locations. These numbers match with findings of [115] and [176] which issue similar numbers in their investigation of large mobility data sets. It can also be highlighted that for all user profiles of DS2 the following statement is true: the location that overall has been visited for the longest period is the location at which the majority of nights (11:00 p.m. - 5:00 a.m.) is spent. This permits the assumption that the longest visited location is also the individual's home location, which is of interest for charging matters and will be discussed in more detail in Chapter 4.

Figure 30 illustrates the trip distance distribution of 56815 trips in DS2, consisting of 251 user Profiles. The longest 10% of trips are between 406 km and 21.6 km in length. The 90th percentile is around 50% shorter than in DS1. The mean and median trip distance is 8.85 km and 3.65 km respectively. The total recorded

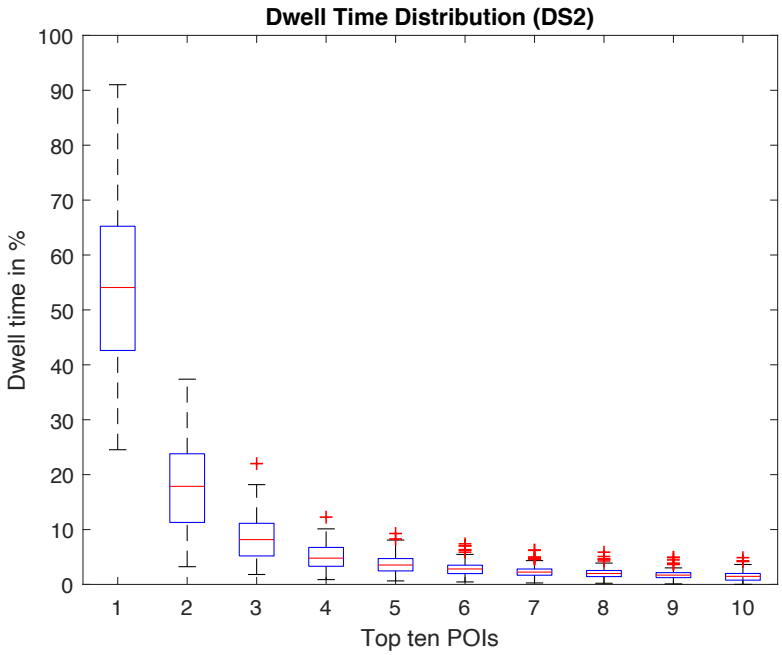

Figure 29: Dwell time in percent per top ten location for smartphone data (DS2, 96 data samples)

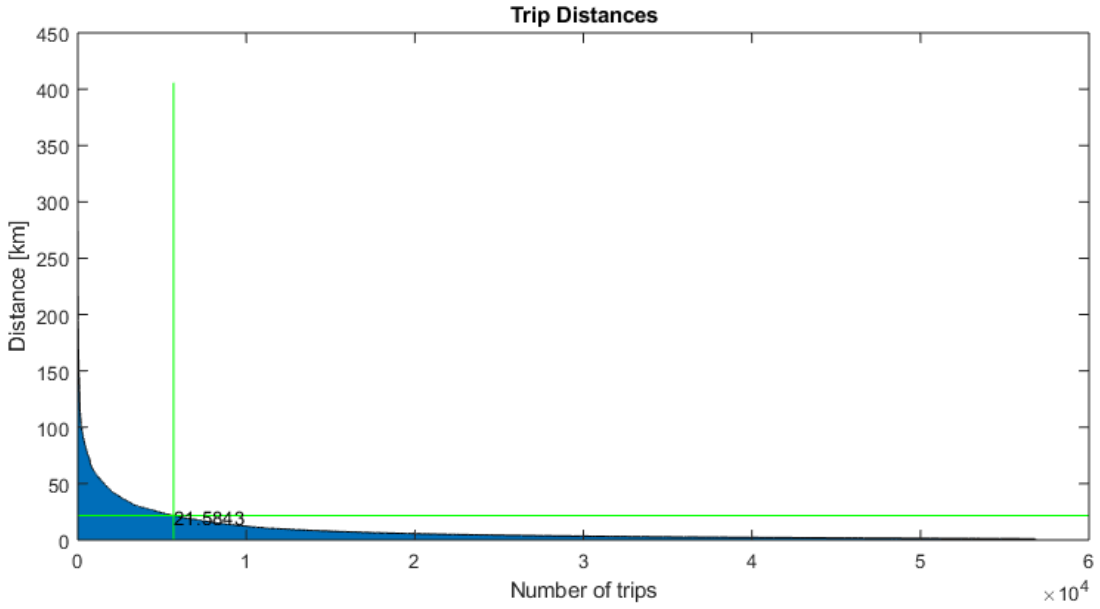

Figure 30: Trip distance distribution smartphone data (DS2, 251 User). The green lines mark the 90th percentile.

driving distance in DS2 is 503630 km.

These values indicate different characteristics than illustrated for DS1 which can be accounted to different factors. The data sets were collected with different methods. DS2 does not allow to differentiate between personal vehicle trips, passenger rides or other means of transportation such as bus or train rides. Furthermore, GPS

signal is usually not available in indoor or urban environments, where according to [113] people spend approximately 87% of their time.

State of the art smartphones use *Assisted* Global Positioning System (AGPS) to assist the satellite-based positioning system. AGPS uses cellular location data and wireless network signals to assist localisation [177]. However, DS2 is anonymised and allows no assumption about the type of smartphone or software that has been used to collect the data, hence, no indication about the data accuracy is given.

Finally, the DS2 does not indicate whether a smartphone was switched off or if a smartphone paused the location tracking for energy-saving etc. In the data, a period in which the smartphone's positioning system was switched off appears as visit at the location at which the system was switched off.

Other than DS1 which, apart from few exceptions, has been recorded in Germany, DS2 consists solely of data recorded in the USA, California.

3.2.7 Data Access

Assigning trip and POI IDs is the first step in a multi-step process to predict vehicle-related mobility behaviour. By collecting GPS data and storing it in a database allows making specific requests, independent from the applied prediction algorithm. For instance, an algorithm could request an individual's visited POI-sequence for specific periods, departure times from specific POIs or trip lengths between POIs.

A generic database sets the groundwork for the subsequent prediction task. Chapter 4 illustrates how the introduced framework builds upon the described pre-processed data structure.

3.2.8 Discussion

The vehicle data is less complex compared with the smartphone data as it features a unimodal movement record. The data shows fewer locations that are considered as relevant for the user and trajectories are in general limited to space that is accessible to vehicles. False data was observed when GPS signal strength was too weak or not existing, for instance in parking garages or tunnels.

Smartphone data is more complex compared to vehicle data as it consists of multimodal travel records and covers a greater space dimension. The separation of "travel" and "movement" data is prone to false classification and the identification of the particular transportation mode is a nontrivial task [178] [179]. Besides, DS2 consists of time-stamped GPS points without any indication of transportation mode and was collected without any temporal consistency. To this end, the data set has been re-sampled to create profiles with one GPS point per minute.

DS2 requires additional processing to be usable for this analysis. Hence GPS records were separated into *movement* data, for instance, when a person travels and *non-movement* data when a person remains stationary. A trip is assigned when the data indicates an average speed of $\geq$ 2.7 m/s for at least 180 seconds. Due to the varying data sampling frequency, it must be expected that DS2 contains noise. Departure times, in particular, might be affected by a delayed detection of movement. However, the data collection method of DS2 is comparable to data collection methods of other research projects, which investigated human mobility and travel behaviour. In [119] and [165] for instance, travel behaviour was deduced from cellphone data, consisting of cell identification numbers which were assigned according to a user's presence in the vicinity of a cell phone tower. These data sets do neither contain information about the mode of transportation but provided insights into human travel behaviour in general.

Nevertheless, findings derived from DS2 will be influenced by noise and the aforementioned re-sampling process. For instance, the analysis of DS2 neglects "trips" within a radius of around 500 metres (2.7 m/s $\times$ 180 s). Since this investigation aims to capture mobility that is conducted by a (personal) vehicle, movement that takes place within such a small radius can be neglected, as it creates no significant energy demand. On the other hand, the data set's limitation regarding the detection of transportation mode can lead to the assignment of a vehicle trip even tough the true mode of transportation was different, e.g. train, bus, etc. Thus an overestimation of required energy as a result of mobility in DS2 must be expected.

Both DS1 and DS2, as any empirical analysis of travel behaviour, is influenced

by a person's "lifestyle", "perceptions", "attitudes" and "preferences" [180]. To this end, it is recognised that not all travel choices and motivations can be captured in this work. Thus the subsequently introduced prediction framework is designed to be independent of "locational behaviour" and "activity behaviour" [180], which would involve location features and/or location-specific activities into the prediction task. Instead, the framework is designed to rely on acknowledged findings of human travel behaviour, which state that humans tend to revisit a few significant locations and follow repetitive mobility behaviour on a daily periodicity.

3.3 EV Energy Demand Model

For this study, no real-world ground truth data of EVs was accessible for evaluation. Hence mobility data of ICEVs has been collected to test the prediction of travel patterns and subsequent scheduling schemes. To create a reasonable energy demand, two different options are available:

- Calculating the energy demand based on an average energy demand per distance unit and applying it to the recorded driving distances.
- Applying a dynamic vehicle model on the recorded driving data to calculate an energy demand based on the vehicle dynamics.

The simulation of an energy demand via a vehicle dynamic model is a more complex task then assuming average energy demands. A simulation can be implemented with respect to parameters such as the vehicle's acceleration, ambient- and component temperatures, etc. Thus, simulated energy demands will account for personal driving styles and environmental conditions, which should reflect in more accurate assumptions about the individual real-world energy demand. However, a simulation's accuracy depends on the availability of such external data. If data is used, which does not contain information about acceleration, vehicle mass, temperature, etc. the complexity of simulation might not be justified. The following section describes an EV energy demand model that uses vehicle dynamic data and ambient temperature data to compute an individual's EV-related energy demand.

The assessment of sensible input parameters and the simulation model's accuracy is discussed in [172].

3.3.1 Vehicle Energy Demand Estimation and Measurement

Different studies have been conducted to evaluate passenger vehicle energy consumption. Figure 31 illustrates distributions for energy consumption for different classes of passenger vehicles including energy for auxiliaries [181]. The data[10] is derived from a dataset recorded by 522 BEVs for a period of three weeks. Table 7 summarises the results of the study for small, medium and large passenger vehicles as well as for light commercial vehicles (LCV). The results were derived from the maximum probability of vehicle class-specific energy demand distributions, as illustrated in Figure 31.

Table 7: Estimated energy consumption per 100 km

Vehicle class	**Mean [kWh]**	**Median [kWh]**
Small	14.8	14.5
Medium	20.5	20.2
Large	24.3	22.9
LCV	25.7	25.0

Further investigation concerning energy demand of EV were conducted in [43]. The illustrated values in Table 8 were determined under test bench conditions and include auxiliary consumers.

Table 8: Measured energy consumption in [43]

Vehicle	**kWh/100km**
Mitsubishi i-MiEV	14.8
Mercedes-Benz A-Klasse E-Cell	33.2
Smart Fortwo Electric Drive	17.2
Nissan Leaf	18.8
Citroën Berlingo	16.5

[10]The actual vehicle trajectories were not made available in this study.

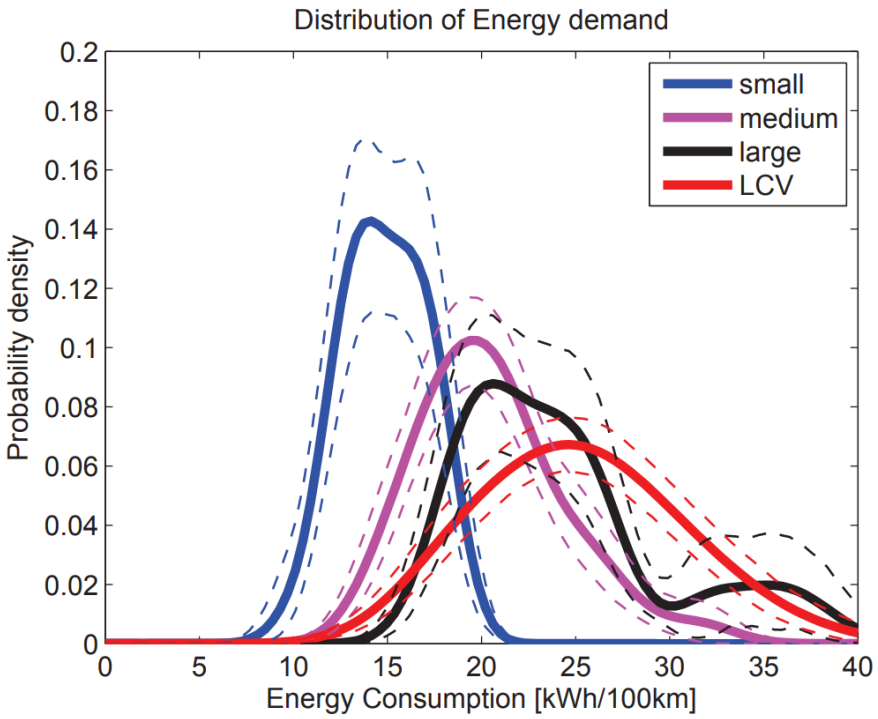

Figure 31: Energy demand distributions for different vehicle classes according to [181]. Dashed lines indicate 95% confidence intervals calculated by bootstrapping.

In all references, vehicles with greater weight show an increased energy demand compared to smaller vehicles which implies that this is mostly accountable to greater inertia. The total energy demand is the sum of several different factors, which will be described in the following section.

3.3.2 Energy Demand Modelling

To be able to assign an energy demand to mobility data that is not available in the granularity that is required to feed a holistic vehicle dynamic model, a good estimation of missing parameters for different vehicle types is required. A vehicle's energy demand E_{dem} is a function of its utilisation. E_{dem} is the product of the required power P_{req} to overcome driving resistances for time t:

$$E_{dem} = P_{req} * t \tag{17}$$

where P_{req} is composed of different driving resistances and auxiliary power demands:

$$P_{req} = \frac{P_{res}}{\eta_{res}} + \frac{P_{rec}}{\eta_{rec}} + \frac{P_{aux}}{\eta_{aux}}. \tag{18}$$

P_{res} = total driving resistance

P_{rec} = total recuperated power

P_{aux} = total power of auxiliary consumers

η_{res} = overall power train efficiency

η_{rec} = overall recuperation efficiency

η_{aux} = overall auxiliary consumer efficiency.

P_{res} is composed of the product of all driving resistances and the vehicle's velocity v:

$$P_{res} = (F_{hc} + F_{rr} + F_{ad} + F_i) * v. \tag{19}$$

F_{hc} = hill climbing force

F_{rr} = rolling resistance force

F_{ad} = aerodynamic drag

F_i = inert force.

F_{hc} is defined as:

$$F_{hc} = m * g * sin\alpha. \tag{20}$$

m = vehicle's weight

g = gravitational acceleration

$\alpha = arctan\frac{\Delta h}{\Delta x}$, with Δh as a segment's height and Δx as a segments horizontal distance.

Rolling resistance force is defined as:

$$F_{rr} = m * g * cos\alpha * f_r. \tag{21}$$

f_r = rolling resistance coefficient.

Aerodynamic drag F_{ad} is defined as:

$$F_{ad} = \frac{\rho_{air}}{2} * c_w * A * v^2. \tag{22}$$

ρ_{air} = density of the ambient air

c_w = vehicle's drag coefficient

A = vehicle's front surface.

Inert force F_i is defined as:

$$F_i = m * \lambda * a. \tag{23}$$

λ= factor for rotational and translational movement

a = vehicle's acceleration.

An EV can recover a proportion of its kinetic energy when it recuperates (see Section 2.1.2.2). While recuperating, high electric power flows can occur, which can exceed the limits of system components [182]. Hence recuperation power can vary based on the vehicle type. Also η_{rec} is usually not constant. However, due to the limited resolution of recorded data (approximately one data point per 70 m), it is feasible to assume that strong deceleration events are smoothened by the data resolution. Hence it is assumed that recuperated power is a vehicle's negative inert force F_i with a constant η_{rec}.

Auxiliary power demands are composed of:

$$P_{aux} = P_{aux_{var}} + P_{aux_{min}} \tag{24}$$

where $P_{aux_{var}}$ are variable loads, such as air conditioning or heating devices and $P_{aux_{min}}$ is the minimum power that the system requires to be operated.

The tracking devices could not be used to record the use of auxiliary consumers. Hence their power demand is modelled empirically. The ambient temperature is used to model the vehicle's interior temperature as well as the vehicle's traction

battery's temperature. The ambient temperature was obtained from a web service[11] and mapped to the vehicles' spatio-temporal data.

The thermal management of the vehicle's interior and the vehicle's battery account for the two greatest auxiliary power demands [43]. To account for their power demand, the thermal conditioning coefficient ϕ is introduced as:

$$\phi \begin{cases} 0, & \text{if } T_{amb} = T_{op} \\ 1, & \text{if } |T_{cur} - T_{op}| > |T_{amb} - T_{op}| \\ |\frac{T_{cur} - T_{op}}{T_{amb} - T_{op}}|, & \text{otherwise} \end{cases} \tag{25}$$

with

T_{cur} = Current temperature

T_{op} = Operating temperature

T_{amb} = Ambient temperature.

The coefficient accounts for the potential power demand that is created through the difference between ambient temperature and the vehicle's (targeted) interior temperature as well as the difference between ambient temperature and the batteries operating temperature. Thus

$$P_{aux_{var}} = P_{bat} * \phi_{bat} + P_{inter} * \phi_{inter} \tag{26}$$

where P_{bat} is the battery's power demand and P_{inter} is the power demand to temperate the vehicle's interior.

To account for the battery's temperature-dependent efficiency, η_{hv} is mapped to a regression function, as displayed in Figure 32.

The motor's load-dependant efficiency η_{motor} is also mapped to a regression function, as displayed in Figure 33.

[11] Dark Sky API

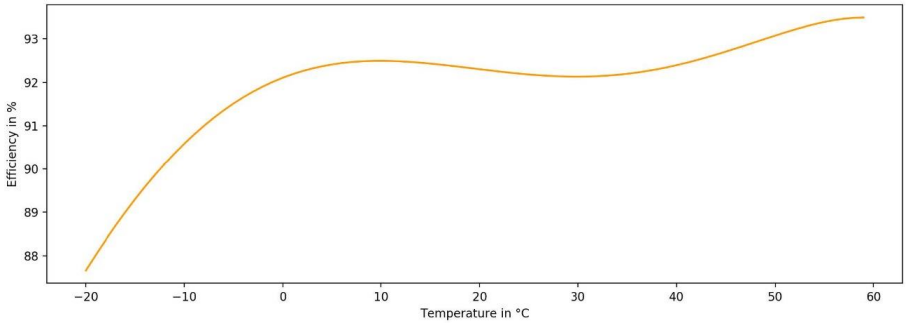

Figure 32: Battery efficiency. Values taken from [183].

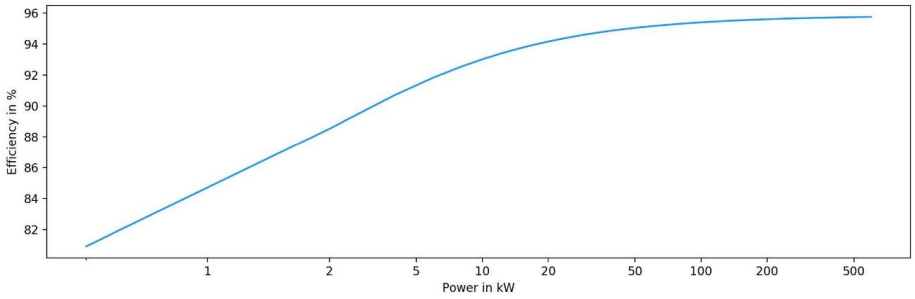

Figure 33: Motor efficiency. Values taken from [184].

3.3.3 Configuration of the EV Energy Demand Model

The previous section introduced the parameters that are used to create a simplified model for the energy demand simulation. A more detailed simulation would not be justified due to factors that cannot be simulated based on accessible data. This includes individual vehicle configurations, personal preferences, etc. Generic inputs are illustrated in Table 9. They are constant, regardless of the vehicle or trip data. The energy demand calculation is done by computing the power demand while traversing a trajectory segment. Segments are defined similarly as in Subsection 3.2.3. In the following sections, if not stated differently, the energy demand refers to the sum of energy demands of all segments of one trajectory.

Table 9: Generic model input

Description	Symbol	Value
Gravitational acceleration	g	9.81 m/s^2
Passenger mass	m_p	70.8 kg
Universal gas constant	R	8.3145 $\frac{J}{mol*K}$
Molar mass of dry air	M_d	0.029 $\frac{kg}{mol}$

Passenger mass m_p is added to a vehicle's empty weight resulting in its total weight. Vehicle specific static and conditional input parameters are listed in Table 10. The traction battery's and the motor's efficiency contribute to a significant change in power demand when they are operated outside of their optimal temperature window. Hence these parameters are modelled conditional on temperature.

Table 10: Vehicle parameters

Parameter	**Symbol**	**Type**
Empty vehicle weight	m_e	static
Rolling resistance coefficient	f_r	static
Drag coefficient	c_w	static
Front surface	A	static
Rotary translational movement factor	λ	static
Mechanical efficiency	η_{mec}	static
HV battery efficiency	η_{hv}	conditional
Motor efficiency	η_{motor}	conditional
Recuperation efficiency	η_{rec}	static
Operation temperature interior	T_{o_i}	static
Operation temperature battery	T_{o_b}	static
Idle power demand	$P_{aux_{min}}$	static

It is possible to change the input values depending on the required vehicle type simulation. For reference, two different vehicle classes are simulated for this project, as they account for a great proportion of currently used EVs. Referring to compact

vehicles, the Nissan Leaf will be simulated. Referring to a limousine style vehicle, the Tesla P100D will be simulated.

To compute segment-specific power demand for auxiliaries, the vehicle's interior and battery temperature is modelled for every segment individually. Both temperatures are used to compute the thermal conditioning coefficients ϕ_{inter} and ϕ_{bat}. P_{inter} and P_{bat} are obtained from manufacturer's data for the Tesla P100D[12] and from a large scale study for the Nissan Leaf [185] respectively. The temperature-dependent maximum and minimum power demand for auxiliary consumers is illustrated in Figure 34. The simulation chooses a random value between the curves to account for different auxiliary consumer use.

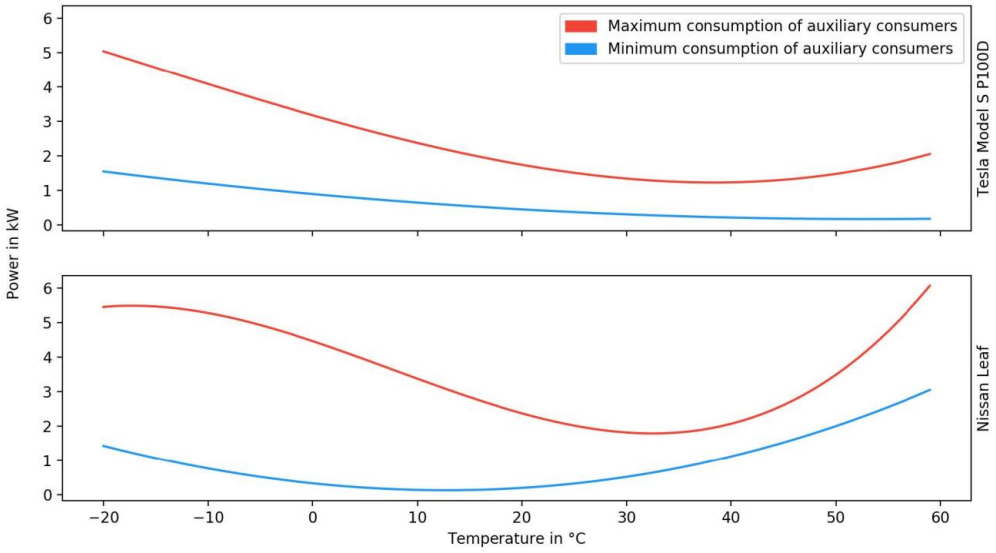

Figure 34: Power demand of auxiliary devices [172]

Thereby it is assumed that T_{o_i} is 22°C and T_{o_b} is 24°C. Both the vehicle's interior and the battery's temperature are computed for every trajectory segment. For both, active heating and active cooling different temperature gradients are estimated for driving and idling based on data of [186] [187] [188] and illustrated in Figure 35.

Static values for rolling resistance coefficient (0.01) and rotatory translational movements factor (1.1) are based on [189] and [190] respectively.

[12]https://www.tesla.com/models

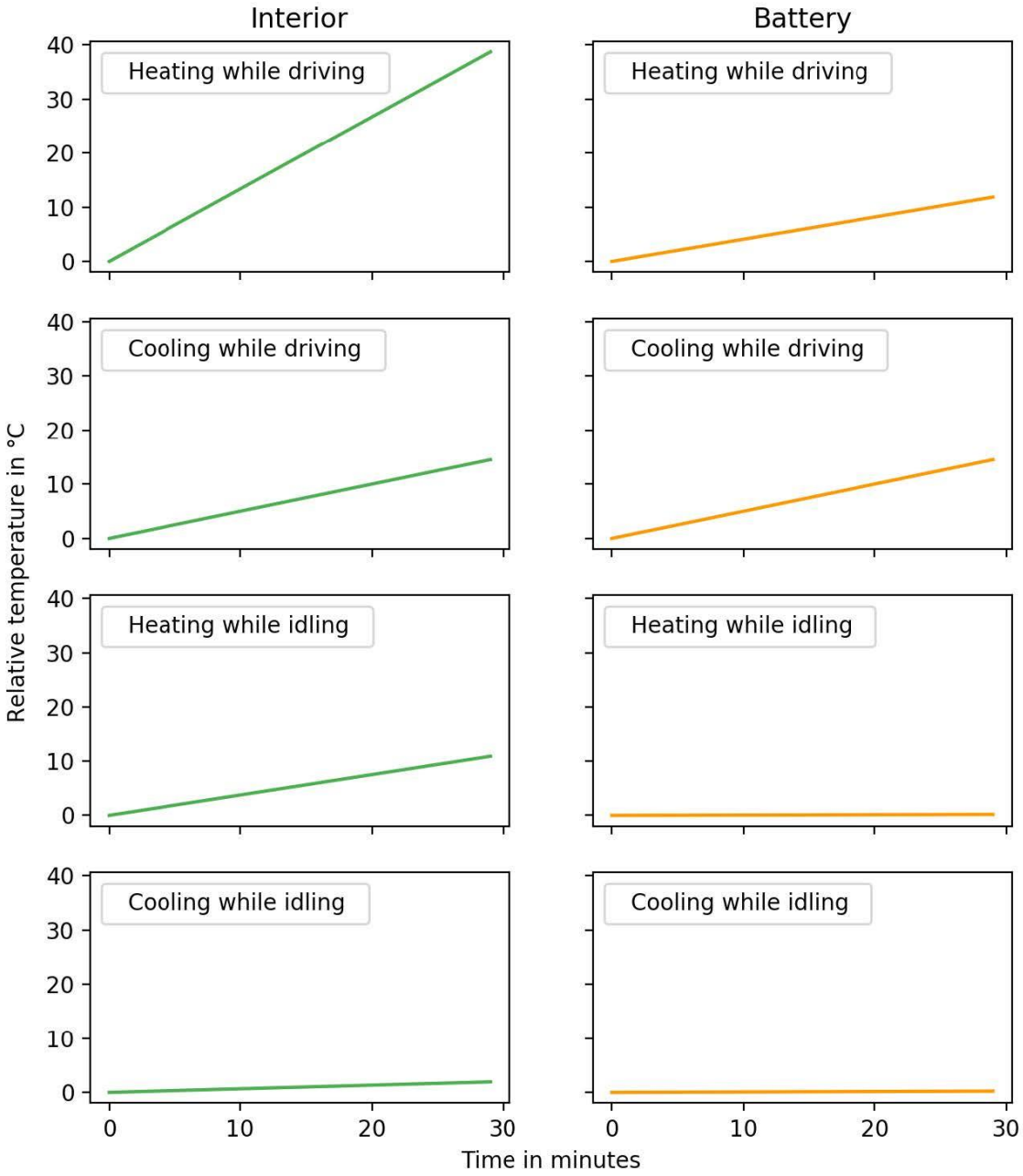

Figure 35: Interior and battery conditioning [172]. The individual graphs illustrate the change of interior and battery temperature as function of time.

3.3.4 Model Validation

The introduced model is designed to label trip data consisting of time-stamped velocity, coordinates, altitude and temperature with corresponding energy demand. The model is validated on a real-world data set, consisting of >900 km of recorded driving and corresponding energy demand data. As illustrated in Table 11, the data was collected with a "Porsche Boxster E" prototype vehicle and a Tesla P85+ and

measured via the vehicles' Controlled Area Network (CAN) bus system.

Table 11: Test vehicle data

Attributes	**Porsche Boxster E**	**Tesla P85+**
Number of trips	7	7
Total distance	213.24 km	673.19 km
Average trip length	30.46 km	96.17 km
Road type	Mostly rural	Highway
Season	Summer	Fall
Average temperature	18°C	5.6°C

The available CAN data was limited on traction components, which excludes data of auxiliaries. Hence validation of the system's output E is limited on P_{res} and P_{rec} per segment length t. Table 12 and Table 15 compare the simulated and measured energy to overcome the driving resistances for the recorded seven trips of the Porsche and Tesla. Table 13 and Table 16 correspond to the simulated and measured recuperated energy for both vehicles. Table 14 and Table 17 illustrates the simulated *combined* energy demands per trip for the Porsche and Tesla in comparison with the measured energy demand. The difference between simulation results per trip f_t with measured data y_t is given as Mean Average Percentage Error (MAPE) which is defined as:

$$MAPE = \frac{100\%}{n} \sum_{t=1}^{n} \left| \frac{y_t - f_t}{y_t} \right|. \tag{27}$$

MAPE is chosen as error measurement to account for the differences in trip lengths (Trip No. 1,...,7).

Table 12: Porsche Boxster E simulation results for traction energy (rounded values)

Trip No.	**Simulated traction E [kWh]**	**Measured traction E [kWh]**	**MAPE**
1	6.95	7.75	-10.26
2	12.21	12.00	+1.74
3	12.62	12.99	-2.84
4	5.53	6.10	-9.35
5	11.22	11.55	-2.80
6	5.48	5.48	-0.06
7	5.74	6.56	-12.54
			Average 5.83%

Table 13: Porsche Boxster E simulation results for recuperation energy (rounded values)

Trip No.	**Simulated recuperation E [kWh]**	**Measured recuperation E [kWh]**	**MAPE**
1	-0.75	-0.82	+8.83
2	-1.01	-1.01	+0.31
3	-1.05	-1.33	+20.92
4	-0.46	-0.44	-3.36
5	-0.92	-0.81	-13.99
6	-0.45	-0.30	-50.27
7	-0.54	-0.75	+27.49
			Average 17.88%

Table 14: Porsche Boxster E simulation results for total energy (rounded values)

Trip No.	**Simulated total E [kWh]**	**Measured total E [kWh]**	**MAPE**
1	6.20	6.92	-10.43
2	11.2	10.99	+ 1.93
3	11.57	11.66	-0.78
4	5.07	5.66	-10.34
5	10.30	10.74	-4.07
6	5.03	5.18	-2.84
7	5.20	5.81	-10.62
			Average 5.86%

Table 15: Tesla P85+ simulation traction energy (rounded values)

Trip No.	**Simulated traction E [kWh]**	**Measured traction E [kWh]**	**MAPE**
1	48.84	45.40	+7.59
2	45.32	50.22	-9.75
3	51.33	49.47	+3.76
4	13.29	14.00	-5.10
5	12.15	12.57	-3.34
6	8.25	8.09	+2.02
7	20.62	18.57	+11.02
			Average 6.08%

Trip No.	**Simulated recuperation E [kWh]**	**Measured recuperation E [kWh]**	**MAPE**
1	-3.72	-3.37	-10.23
2	-2.66	-2.58	-2.84
3	-3.28	-3.22	-2.00
4	-0.96	-1.35	+29.10
5	-0.81	-0.76	-5.72
6	-0.78	-1.04	+25.07
7	-1.40	-1.51	+7.20
			Average 17.88%

Table 16: Tesla P85+ simulation results for recuperation energy (rounded values)

Table 17: Tesla P85+ simulation results for total energy (rounded values)

Trip No.	**Simulated total E [kWh]**	**Measured total E [kWh]**	**MAPE**
1	45.12	42.02	+7.38
2	42.67	47.64	-10.44
3	48.05	46.26	+3.88
4	12.33	12.65	-2.54
5	11.34	11.80	-3.93
6	7.47	7.05	+6.03
7	19.22	17.06	+12.64
			Average 6.69%

It is recognised that the proposed simulation model does not capture the entire thermodynamic and dynamic structure that account for an EV's energy demand. However, the simulation results demonstrate that the model is accurate enough to

reflect increased energy demands when a vehicle is used in cold or hot environmental conditions. Apart from the power demand for propulsion, the model takes into account two relevant sources of power demand, which are the thermal conditioning of the vehicle's interior and the vehicle's battery. Considering the data resolution, the model creates small estimation errors for both reference vehicles. The MAPE for the Porsche Boxster E is 5.86% and 6.69% for the Tesla P85+. The estimation error for P_{rec} is higher than for P_{res}. Since P_{rec} accounts for a small proportion in P_{req}, the error is accepted.

3.4 Conclusion

Clustering POIs and trips allow a visual inspection of driving patterns. While this analysis, similar to other research projects, gives insights about common patterns and behaviours, this work also aims to identify individual characteristics to design and adapt a prediction and scheduling framework that takes any deviations from "regular" and well-investigated movement behaviour into account. An example for atypical travel behaviour has been illustrated with data of User 16.

The prediction of atypical travel behaviour is a more complex task than prediction of typical behaviour. A literature review shows that most researchers assume a weekly periodicity in human travel behaviour. Assuming weekly periodicity suggests to cluster days according to their day name or to separate working days from weekends. However, this assumption will falsify predictions for individuals with atypical travel behaviour (see Subsection 2.4.7).

To account for atypical travel behaviour Chapter 4 introduces a method that is based on similarity measure to provide more reliable mobility predictions and thus a better energy requirement forecast. Due to the scarcity of data that captures the real driving behaviour of EV users, the trial utilises data (DS1) that consists of travel behaviour captured with conventional vehicles. Studies indicate that individual travel choices are influenced by EV attributes such as attainable range, charging needs, etc. However, it is argued that these choices are biased through experiences with conventional vehicles and in most cases unfounded [38]. The assessment of

travel data sets introduced in Chapter 3 and the corresponding simulated energy demand indicate that the great majority of trips that are part of individual and regular travel routines, could be covered with EVs, even if they carry small capacity batteries.

Furthermore, the fact that the collected data sets are unbiased regarding EV perceptions is used to argue that individuals would not experience any disutility by using an EV instead of a conventional vehicle, given an adequate amount of charging infrastructure is available. Building upon this argument, the collected data is used to demonstrate the possibility of combining individual mobility, corresponding energy demand and smart charging.

Chapter 3 introduces and discusses a data collection trial that has been conducted specifically to set the basis for the validation of a prediction and charging scheduling framework. To enlarge the database and ensure representativeness, *DS2* is consulted. Independent from the dataset, home locations prove to be the most visited location at which individuals spend most of their time, thus being the most relevant location for potential smart charging. The working/educational location is the second most visited location and could be considered as an alternative charging location, given the EV user cannot charge an EV at home.

Based on the analysed data sets, the commute between the first and second most visited location accounts for the majority of a vehicle's energy demand. Being the most regular, thus most predictable proportion of an individual's mobility, a smart charging framework is determined to capture these mobility patterns. However, humans' tendency to randomly visit new locations must not be neglected by the framework's design, as one of the prominent reasons to possess a vehicle is being flexible in personal mobility.

To be able to use unbiased mobility behaviour on the one hand and to design a charging scheduling framework, on the other hand, a vehicle dynamic model is developed to simulate EV specific energy demands. The model uses real-world driving data and EV component-specific attributes to simulate energy demands based on the recorded vehicle dynamics and externally obtained temperature values. The

model is designed to incorporate translational and thermal attributes to account for the two greatest vehicle-related energy demands: propulsion and heating/cooling of the traction battery and the vehicle's interior. Based on findings of human mobility behaviour, specific features have been extracted, illustrated and discussed to identify characteristics that can be utilised for the design of a smart charging framework that takes individual mobility behaviour into account.

Based on the average number of trips per day and the average trip distance, the average energy demand per day can be estimated. Given the mobility behaviour that has been captured in DS1 and DS2, EVs with rather small battery capacities could cover the captured mobility demand. In only very few occasions the driven trip distance is greater than the range an EV could provide. The data also shows that the longest 10% of driven trips are not part of routines, hence being less relevant for prediction based scheduling tasks.

The most visited locations are usually visited regularly and, in most cases, show characteristic variance in dwell times. If the objective is to utilise parking times that are the byproduct of an individual's unbiased mobility behaviour for charging, these described characteristics are of specific interest as they lower an individual's mobility entropy. A low entropy indicates high predictability to the advantage of an automated scheduling scheme.

These findings provide the necessary groundwork for the subsequent investigation of adequate mobility prediction algorithms. Features that characterise DS1 and DS2 are comparable to those reported by multiple other sources. Hence it is valid to assume that they can be considered to be representative and a framework that performs well on DS1 and DS2 will also perform well on other mobility data.

Chapter 4: Mobility Prediction for Battery EV

Predicting a user's EV related mobility is an open research field with increasing relevance as markets for EVs are expected to grow significantly within the next decades. Electric mobility is linked to electric energy demand, which creates a measurable impact regarding its load on power grids. Together with investigations that addressed the risk of overstressing power grids due to simultaneously charging EVs, several types of research discovered different optimisation schemes. They aim to mitigate the impact of charging vehicles by organising grid resources and charging demand efficiently.

While optimised charging strategies for EV have also been part of recent scientific publications, the combination of individual user mobility and optimised EV grid integration was subject to comparatively few scientific investigations.

Chapter 3 discussed different aspects of mobility records, which can be used to characterise predictable travel patterns. Based on these characteristics, Chapter 4 describes how to design a mobility prediction framework to meet the requirements of an automated EV charging schedule.

The mobility behaviour analysis in Chapter 3 has highlighted the following:

- For the majority of individuals, a great proportion of their travel history originates from their commute.
- The commute is usually the trip between the first and second longest visited location.
- For individuals with typical travel behaviour, departure times for the commute can be observed in rather short periods during working days.

Based on these observations a mobility prediction framework for charging scheduling must not necessarily be capable of predicting every single trip but should be able to accurately predict dwell times on frequently visited locations, especially if they offer to charge an EV. Irregular trips are of less relevance in terms of their destination but more on their energy demand. Subsection 4.1 discusses mobility prediction in

the context of EV mobility. To realise a sensible combination of location and departure time prediction, Subsection 4.2 introduces a conceptual framework for mobility prediction, focusing on EV related issues. Section 4.3 describes the methodology that has been used to design the prediction framework. Section 4.4 addresses the problem of atypical travel behaviour in the design of a prediction mechanism. More specifically Subsection 4.5 highlights different aspects of *location prediction* to account for the relevance of frequently visited locations. To account for the temporal aspect of individual travel behaviour Subsection 4.6 introduces a method to estimate departure and corresponding arrival time. Spatio-temporal prediction accuracy is a two-dimensional unit. To account for the framework's geographic *and* temporal accuracy, Subsection 4.8 discusses possibilities to capture both aspects and how to feedback the error measures to improve the framework's performance. Parts of this section have been published in [191].

4.1 Introduction

Individual mobility prediction has been applied to address very different problems. Prediction frameworks are usually designed to solve a specific task, such as the prediction of the next location (e.g. data fetching in wireless networks) or the arrival time of transportation systems (Busses, Trains, etc.) [159]. In the context of EVs, the relevant prediction task consists of a private vehicle's future whereabouts and corresponding energy demand. Both information can be retrieved by predicting user-specific trips to locations in a period, which is a function of the driver's mobility behaviour and the capacity of the vehicle's battery. Note that this definition limits the framework's applicability to "personal mobility". This excludes, for instance, the mobility of a taxi or bus driver during work.

The necessary prediction range, which will be referred to the *prediction horizon*, is defined by the point in time in which the vehicle's battery will be depleted. The objective of the smart charging framework is to avoid situations in which an EV user is unable to reach a destination due to insufficient charge. The parking event at which the vehicle's battery will reach a state of energy (SOE) below the required

energy for the next trip defines the required prediction horizon.

For some applications, only a user's *next* location is of relevance. Data fetching applications or intelligent transportation systems, for instance, often aim to predict an individual's next location only. Based on findings in human travel behaviour (see Section 2) and due to natural constraints, the number of attainable locations in "next-step" applications is mostly limited to few locations. A human's tendency to travel between a few personal significant locations also scales down the period in which a transition can be expected, which simplifies the prediction task. Hence, transition prediction applications will be referred to as *short-term* predictions.

On the other end of the spectrum of mobility prediction there are *long-term* predictions, that reach out to months or years [192]. Long-term predictions usually do not examine location transitions as in case of short-term predictions. Also, an accurate transition time of day is usually not of specific interest. Instead, long-term predictions usually aim to gain knowledge about human migration flows and motivations to travel [193]. Sadilek et al. point out, that techniques, such as Markov models and random walk-based formalism, that work well for short term mobility prediction are of little help in the context of long term mobility [192].

In relation to the previously given examples, the prediction of EV specific use cases can be described as *medium-term* mobility prediction, which typically reaches out several days, up to a few weeks. The relevant prediction horizon can be defined as a function of the vehicle's battery capacity and a user's mobility demand. The following calculation should illustrate how the two factors influence the prediction horizon:

Let the daily driving distance be 50 km. Further, let the average energy consumption of EVs be 20 kWh per 100 km and the battery size be around 100 kWh. With a conservative safety margin of around 20% SOC, it is reasonable to assume that an EV requires to be charged around one time per week.

Relating to temporal predictions, existing frameworks often reduce their com-

plexity by binning mobility events (transitions to other places) into time slots of 15 minutes [130] , 30 minutes [117] or 60 minutes [153]. A prediction outcome may then be expressed as "Transition from A to B at time slot 16", which may be interpreted as travelling from work to home at hour 16 at that specific day. Using, for instance, 60 minutes as time slot unit reduces the number of possible prediction outcomes for the most probable transition time to 24 possible outcomes per day. Taking into account that state of the art EV can charge their batteries from 10% to 80% within 15 minutes[13], this temporal resolution for departure time prediction is rather coarse. A key disadvantage in a fixed time bin selection is that the accuracy, even in regular behaviour, is bounded to the size of the selected bin width.

Based on the previous description, a major challenge for smart charging related mobility prediction is the combination of short- and long-term prediction mechanisms. More specifically, a good departure time prediction mechanism needs to be combined with a high performing transition prediction mechanism for prediction horizons up to one week. Referencing to the temporal prediction accuracy, higher temporal accuracy than in existing works would improve the subsequent charging scheduling task.

This is realised by combining density estimation for departure time predictions and a Markov model predictor for location transitions. This concept has been published in [194] and will be explained in the following sections.

4.2 Conceptual Framework

Literature about human mobility behaviour, EVs and smart charging suggests that a smart charging framework should consist of multiple sequential steps which can be separated into three different segments (Figure 36): Data Collection (1), Prediction (2) and Scheduling (3). In this context, it is an advantage to design the framework with a generic coupling of (1), (2) and (3) to be able to implement more sophisticated models when new findings or more data are available [195].

The three segments are further separated into different sub-steps. Regarding

[13]e.g. Porsche Taycan

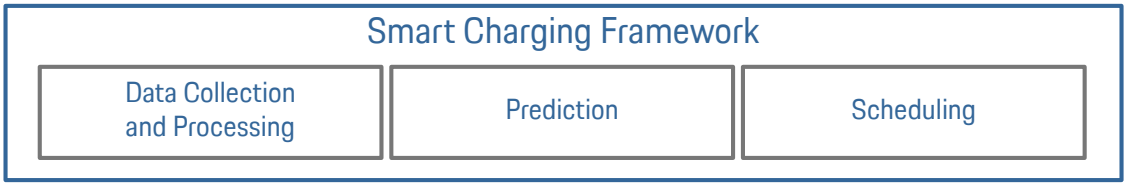

Figure 36: Illustration of three sequential tasks of data handling, prediction, and scheduling that form the conceptual smart charging framework

Data Collection and Processing (Figure 37), sub-steps consist of the collection of travel data, charging related infrastructure data and the pre-processing of corresponding data to be processable for the subsequent prediction and scheduling steps.

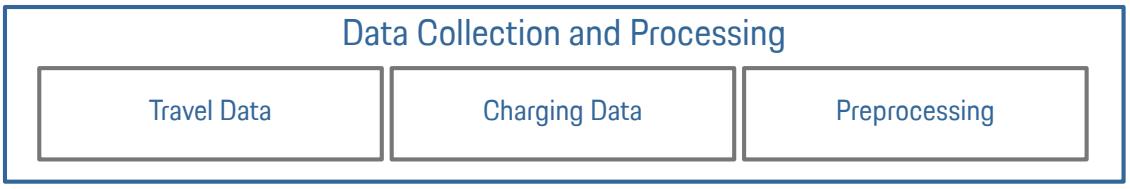

Figure 37: Three steps that form the Data Collection and Processing step. For the subsequent Prediction and Scheduling steps, the collected data must combine energy related travel data in conjunction with information about available charging infrastructure.

The prediction scheme can be further separated into three different prediction sub-steps (Figure 38), consisting of a scheme that handles atypical travel behaviour (Section 4.4), a location prediction scheme and a departure time prediction scheme.

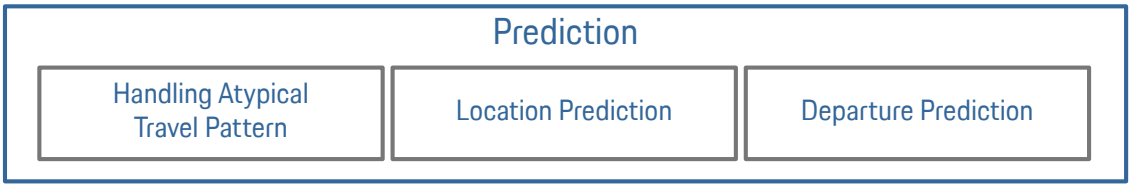

Figure 38: Prediction structure

The framework's third segment (Figure 39) consists of the scheduling segment that processes data that is relevant for smart charging and the computation of sensible charging periods and events (Section 5.2.3) based on the previously obtained mobility prediction.

Apart from the previously defined requirements, the framework must be able to

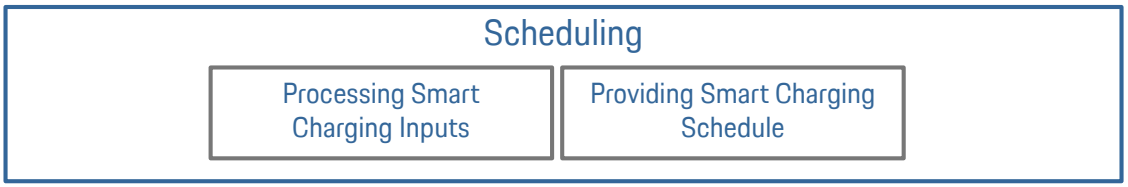

Figure 39: Scheduling structure

handle the following circumstances/conditions to provide a reliable charging schedule and to offer real-world applicability:

- Independent from the consulted prediction scheme, the situation can occur, in which the probability to visit two different locations is equal. The prediction algorithm must be able to provide a sensible prediction nonetheless to ensure that the subsequent scheduling task can be conducted.
- The prediction scheme must be able to provide a sensible trip and energy demand prediction when the vehicle visits a location for the first time.
- The system must be able to adapt to changes in a vehicle user's mobility behaviour, for example, if the location of work changes, the user moves to a new home, during holidays, etc.

4.3 Methodology

Humans tend to follow a daily (24 hours) activity rhythm [196], which is why prediction periods may be separated in multiple 24 hour periods. The prediction of mobility within 24 hours is referred to "Intra-day prediction". The framework's task is formulated to predict the mobility of 24 hour periods and to string consecutive 24 hour periods together. In "traditional" prediction approaches, day sequences are given by the natural order of weekdays. Figure 40 depicts the corresponding concept. Some researches further simplify this task by joining Monday to Friday in a "Workday" cluster and Saturday and Sunday in a "Weekend" cluster [123] [153]. In this case, the day sequence is deterministically given by five 24 hour periods followed by two weekend clusters. Recall that not all individuals follow a weekly-based periodicity, as has been illustrated on User 16 in Section 3. To be independent of a

natural order of day clusters, the order of day clusters must be determined by the framework. The task of predicting the sequence of day clusters will be referred to as "Inter-day prediction". The task of inter-day prediction consists of the identifi-

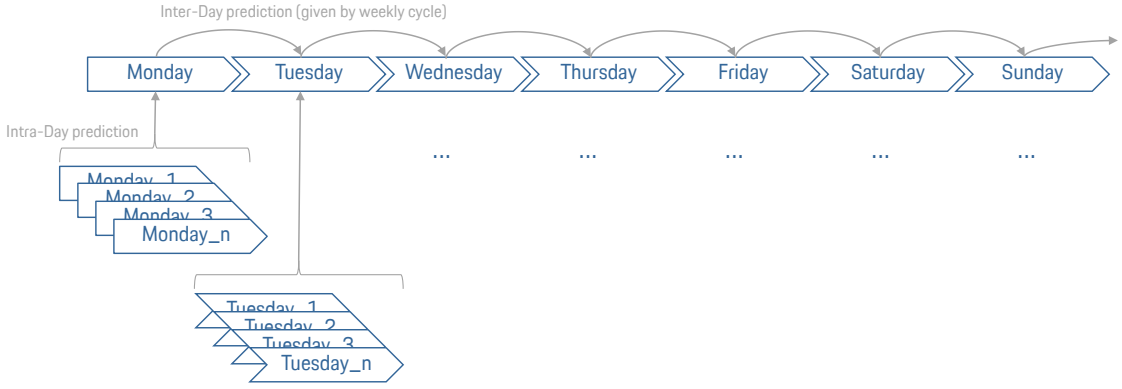

Figure 40: Traditional approach to predict day dependent mobility

cation and subsequent prediction of day (cluster) sequences, which is illustrated in Figure 41, and will be explained in more detail in Subsection 4.4. For the intended

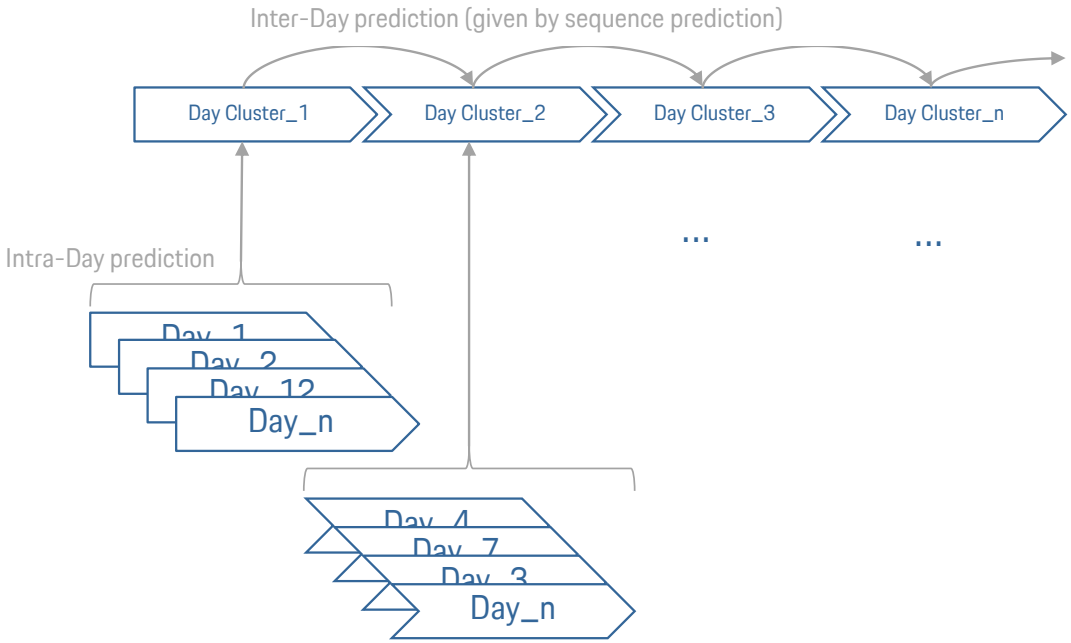

Figure 41: Artificial Neural Network based sequence prediction

framework, day clusters provide the input for day-specific location and departure time predictions. In Chapter 2 it has been discussed that Markov models of n-th order with $n < 2$ and fallback performed best under different conditions. Hence, the introduced framework is enabled to switch into a model of zeroth order, which

corresponds to a location independent (LI) state. In a location independent state, the location at which an individual was observed most often at the next time bin will be predicted as the individual's next location, *independent* from the individual's current location. The determination of the most occurring time-dependent location corresponds to the mathematical term *mode* and will be referred to in the following sections accordingly. Details about the Markov model-based location prediction scheme are given in Section 4.5.

For Markov model based location predictions of order > 0, departure time must be predicted separately. This is because a time-independent Markov models, which performed best in [130], contains no temporal information. Departure time predictions are conducted with KDE and are explained in detail in Section 4.6. Note that an LI prediction requires no separate departure time prediction. By determining the time-dependent most visited location, a departure would be assigned to the time interval at which the Mode for the location symbol changes.

Implementing two variants of an inter-day prediction and two variants of intra-day prediction results in four different combinations of prediction schemes. Depending on the actual user mobility pattern, it is expected that for some users the "traditional" approach will provide a better prediction performance than the introduced inter-day prediction. Similarly, it is expected that for some users, a location independent approach performs better than a location-dependent approach. To leverage the individually better performing approach, the implementation follows an ensemble learning approach [197]. More specifically, the system combines the individually better performing methods by executing every possible combination of aforementioned inter- and intra-day mobility prediction. The final prediction result is provided by the combination of prediction schemes that performed best for the individual user. The corresponding performance measure, which defines the best performing combination of inter- and intra-day prediction, is explained in Subsection 4.8.3. Figure 42 illustrates the overall structure of the proposed prediction framework.

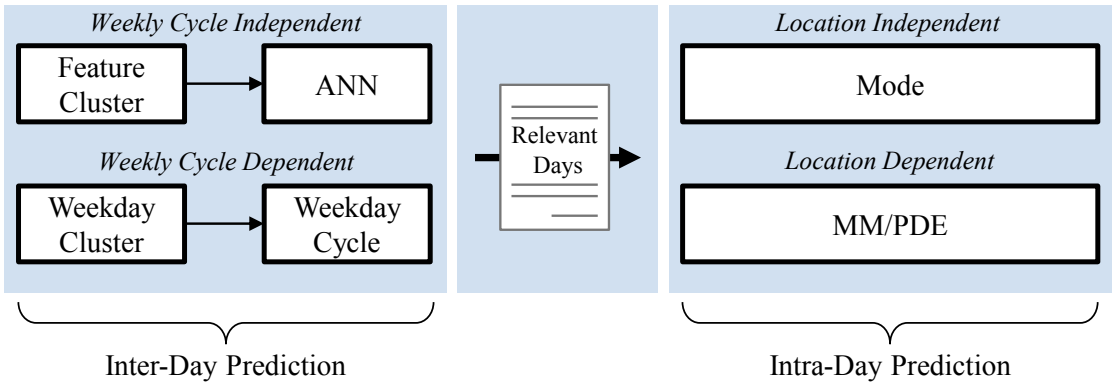

Figure 42: Two inter-day prediction methods and the subsequent two methods for the intra-day prediction.

4.4 Handling Atypical Travel Patterns

To account for travel behaviour that does not follow the periodicity of one day or week, the prediction framework is enabled to conduct an inter-day prediction, which determines the input for the subsequent intra-day prediction. This method is introduced to enable the framework to handle atypical travel behaviour, which has been explained in Section 2.4.7.

A day is a natural choice for a basic prediction interval due to the fundamental period of regularity in human activity and mobility patterns [198] [199]. Recall that the "traditional" inter-day prediction is based on the assumption that travel behaviour follows a weekly periodicity. A system that is designed on this assumption expects that observations of all Mondays provide the necessary input for the prediction of travel events on Monday. Hence all Mondays form a cluster which serves as input for the prediction of following Mondays. Furthermore, these systems assume that there is a fixed cluster sequence, given by the natural order of weekdays. To be independent of weekday names (weekday clusters) and a given sequence, the weekly cycle independent sub-method clusters 24 hour periods based on their *similarity* regarding travel behaviour.

The order of inter- and intra-day prediction remains the same for both prediction methods: The inter-day prediction forms a set of days from the recorded user profile, which is then used as input for the intra-day prediction. The "traditional" approach, in which the order of day clusters is given by the natural order of weekdays, will be

referred to as *Weekly Cycle Dependent* (WCD). The method, which is independent of the natural order of weekdays will be referred to as *Weekly Cycle Independent* (WCI). Details about the day clustering process are given in Subsection 4.4.1.

Based on the output of the inter-day prediction, the intra-day prediction forecasts the cluster-specific travel pattern. Recall that in the intra-day prediction, two approaches are possible, namely *Location Dependent* (LD) and *Location Independent*. The LD approach referrers to the Markov Model in conjunction with the kernel density estimation and the LI approach referrers to the time bin dependent *mode*.

4.4.1 Day Clustering

To detect atypical regularities in a user's travel history, days with similar movement patterns are clustered. This task is solved with a cluster analysis, which can be described in a three-step process consisting of a similarity measure, fusion algorithm and determination of an adequate number of clusters. This procedure will be referred to as *Feature Clustering* (FC).

Boriah et al. presented and evaluated several similarity measures for categorical data in [200]. The proposed method is transferred to quantify the similarity in daily movements with the *Goodall1* [200] similarity measure.

Therefore, let $T \in \mathbb{N}$ denote the last time point of a day, which must be chosen according to the desired resolution, for example, $T = 24$ for a time point each hour or $T = 1440$ for each minute. Further let $\mathcal{P}_k$ be the set of all POIs that occurred on time point k for $k = 1, \ldots, T$ for the given user profile overall days in the data. Further let $X = (X_1, \ldots, X_T)$ and $X' = (X'_1, \ldots, X'_T)$ be the mobility data of two days, where $X_k, X'_k \in \mathcal{P}_k$ describes the location at the k-th time point for $k = 1, \ldots, T$ of the first and second day respectively.

The *similarity measure* SM is then calculated with:

$$\mathrm{SM}(X, X') = \frac{1}{T} \sum_{k=1}^{T} S(X_k, X'_k), \tag{28}$$

where

$$S(X_k, Y_k) = \begin{cases} 1 - \sum\limits_{q \in Q} p_k^2(q) & \text{if } X_k = X'_k \\ 0 & \text{otherwise} \end{cases}, \tag{29}$$

with

$$Q = \{\text{POI} \in \mathcal{P}_k \mid f_k(\text{POI}) \leq f_k(X_k)\}$$

and

$$p_k^2(X_k) = \frac{f_k(X_k)(f_k(X_k) - 1)}{N(N-1)}. \tag{30}$$

$N \in \mathbb{N}$ denotes the total number of observed days of the user profile and $f_k(x)$ the total number of occurrences of POI $x \in \mathcal{P}_k$ at the k-th point of time.

This similarity measure compares whether the individual was in the same location for each point in time within two days. Rarely visited locations are weighted higher to lessen the effect that an individual mostly stayed in one POI, e.g. at home.

Since this is a similarity measure for categorical data, the hierarchical clustering algorithm is utilised. Furthermore, a *silhouette-coefficient* is used to evaluate the cluster quality and to determine a reasonable number of clusters [201]. It compares the mean intra-cluster distance and the mean inter-cluster distance of each object (day). To identify a reasonable number of clusters, the amount of clusters to be formed is incremented in multiple cycles and the average silhouette coefficient is calculated. The number of clusters is determined by the highest average silhouette coefficient.

4.4.2 Day Sequence Prediction with ANN

The previous subsection described how clusters are formed. For a user record of n days, this results in a sequence of n cluster symbols, as illustrated in Figure 43. Since the order of this sequence is not bound to the periodicity of weekdays, this approach makes it necessary to learn and predict the cluster sequence separately. To account for this, it is assumed that successive clusters provide information about

subsequent clusters.

Hence the ratio of a variable number of known clusters to a subsequent unknown cluster is to be formed and learned by the framework. The framework is designed to consider different inputs for the sequence prediction. The information on known holidays and the current weekday will be considered in particular. The principle for two exemplary input clusters for a searched output cluster is illustrated in Figure 44. The cluster assigned to the respective day is indicated by each number and colour.

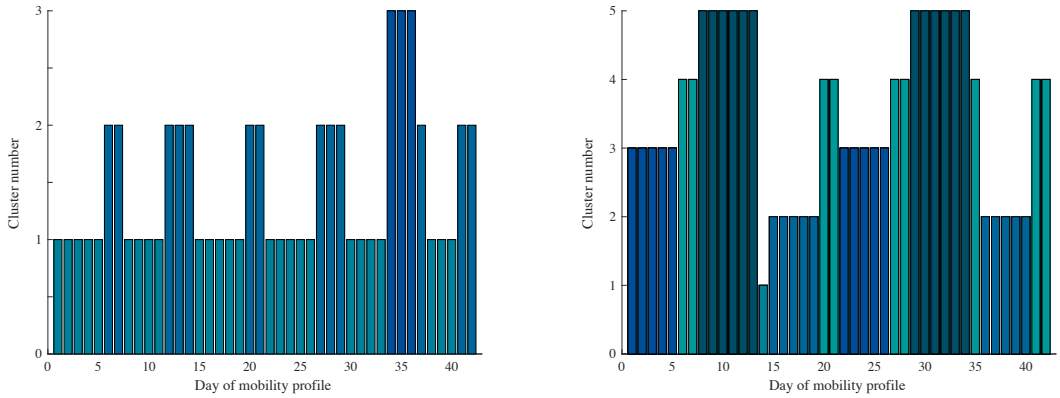

(a) (b)

Figure 43: (a) represents a cluster sequence of an individual. The sequence follows a fairly one week periodicity. (b) represents the cluster sequence of another individual with a periodicity of three weeks. In both cases, a period of six weeks is displayed. Each cluster is highlighted with an individual colour.

	Mo	Tu	We	Th	WD_t	Sa	Su
CW 1	1	1	2	1	1	3	3
CW 2	4	1	1	1	1	3	2
CW 3	4	1	1	1	1	3	3
CW 4	2	1	Cl_{t-2}	Cl_{t-1}	Cl_t		

Figure 44: Illustration of cluster sequence prediction. The number and colour represent the determined cluster for the respective day. The example illustrates two input days for the Input layer ($Cl_{t-2} = 1$, $Cl_{t-1} = 1$) with the predicted day being a Friday ($WD_t = Fr$). In this case the ANN would predict $Cl_t = 1$ as an output.

The combination of different information types results in a complex non-linear

relationship between input and output [191]. Therefore, an ANN is explored to find existing patterns in the cluster sequence by combining additional information. The ANN's structure allows to integrate additional (categorical) information into the forecast of the next cluster (public holidays, etc.). The NN's number of layers is calibrated to be equal to half the number of input neurons.

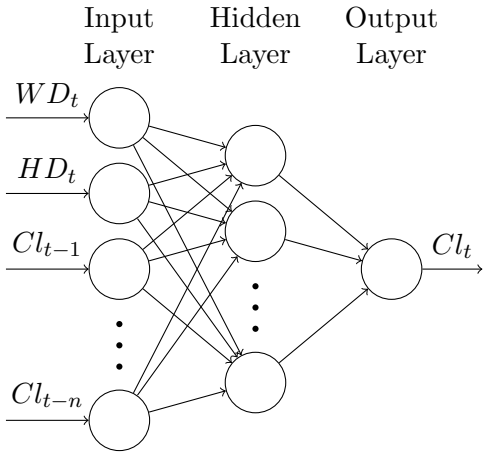

Figure 45: Feedforward ANN for next cluster prediction. The input layer can include the corresponding weekday (WD_t), the information of a public holiday (HD_t) and a number of previous cluster numbers ($Cl_{-1}, ..., Cl_{-n}$).

All described input factors of the ANN are categorical variables. In order to be able to process them, they must be *one-hot encoded* [202]. The output of the ANN shows which cluster most likely occurs for the next day. Therefore it must also be one-hot encoded. In addition, the *Softmax-Function* [155] is applied to the output (see Paragraph 2.4.5.2). Thus the values of the individual outputs range between zero and one with output neurons summing up to 1. The normalised output can be interpreted as probabilities for each cluster of the following day.

The coded data is used to train the ANN in order to find a functional relationship between the input and output clusters. The ANN's structure is shown in Figure 45. To recognise the patterns in the respective profile, several ANNs with a different number of input clusters Cl_{t-n} are trained for each profile ($n = 2, ..., 7$). The one with the highest cluster prediction performance (in sample test) is selected. The trained ANN is then used to obtain a forecast of the next cluster for the upcoming day. All days in the recorded user profile assigned to this predicted cluster will now provide the input for the subsequent intra-day prediction (see Figure 42).

The described scheme for atypical travel pattern prediction can be considered as an addition to existing MM based prediction methods. It is designed to provide an alternative approach to the "traditional" process of clustering days. With the parallel implementation of the different prediction methods, it is ensured that the individually better performing approach provides the final mobility prediction.

4.5 Location Prediction

In Chapter 3 specific characteristics of human mobility have been identified and discussed. Based on findings illustrated in Chapter 3, a human's mobility can be described as a network of visited locations, as illustrated in Figure 46. In this network, for instance, a location's relevance grows proportionally with its number of visitations and/or the time spent at the location. The following section reviews existing methods to determine a location's relevance in an individual's network of visited locations and methods to determine departure times. Based on this review, Sections 4.7 introduces the concept of a new prediction method.

4.5.1 Review of Existing Methods

Along with different prediction methods, discussed in Chapter 2, (MM) based prediction methods anticipate that trends in an underlying state sequence provide important information about the probabilities of the next occurring state [155]. As has been illustrated in a number of different research projects, it is valid to describe human mobility as a Markovian process [113] [140]. Humans tend to follow repetitive patterns in their mobility which is one explanation for the good performance of Markov models in mobility prediction [130].

Based on findings illustrated in [119] and [122], location-dependent prediction methods generally perform better than location independent prediction methods. Furthermore, different combinations of spatial and temporal features were combined in [130] to investigate their performance in a MM based prediction approach. To this end, Baumann combined a user's current location (l_1), a user's current and previous location ($l_1 l_2$), time of day, day of the week and weekday/weekends to 18 different

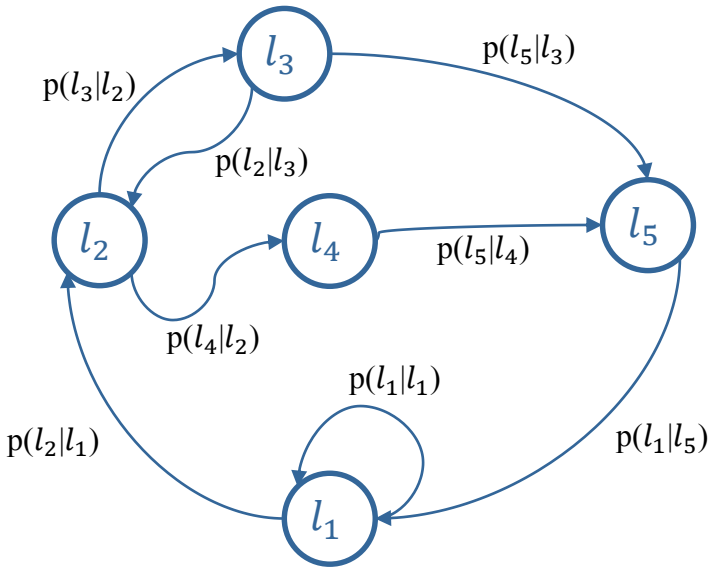

Figure 46: Example for an EV user's location network. Circles $(l_1, l_2, ...)$ mark an individual's relevant locations. A Mobility Markov Model creates edges between visited locations (states). The edge's weight is defined by the transition probability (p) between corresponding states.

Markov predictors and measured their ability to predict a user's next place 1-time step ahead. Time steps were defined as 15-minute time slots. The experiment was conducted on a recorded mobility data set of 37 users (MDC-Dataset[14]).

Baumann was able to confirm findings of Song et al. and demonstrate that a first order Markov model, in which solely a user's current location is used to predict the next destination, is performing best in terms of prediction accuracy. Baumann defined the predictor's accuracy as the ratio of correct predictions to all prediction attempts.

Another example of the utilisation of a Markov model derived location prediction scheme is [153]. In her dissertation, Burbey used a Markov model to predict future locations and departure times. Pointing out a similar separation of spatial and temporal features as in [130], Burbey proposes to predict future locations based on a sequence prediction (Markov model) and assigns a Market Basket Analysis for temporal predictions. Further variances of Markov model applications for mobility prediction have been presented in [123], [203] and [204].

The principle of a location-dependent transition prediction is illustrated in Fig-

[14] www.idiap.ch/dataset/mdc

ure 47. Example probabilities to transition from l_0 to l_4, l_6 and l_{12} are marked in red.

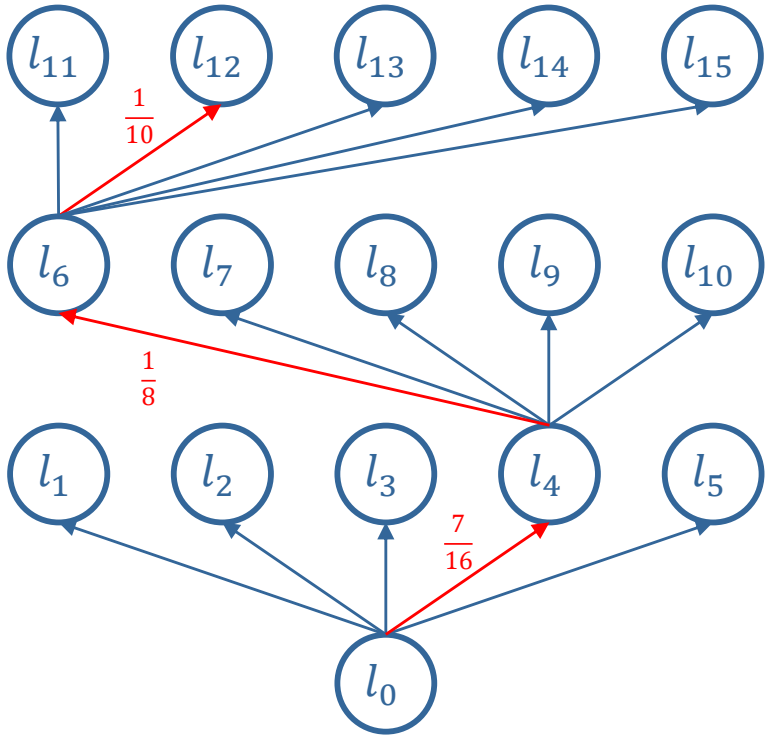

Figure 47: Illustration for location prediction steps. Every destination is associated to a location specific transition probability.

4.5.2 Markov Process

Based on [155] and the definition given in Paragraph 2.4.5.1 Markov processes can be described with the "Probability Theory". Let X be a set of POIs that represent *Origins* and Y be a set of POIs that represent *Destinations*. X can take any value of x_i where i=1,..., M, and Y can take any value of y_j where j=1,...,L, forming a L×M matrix. Let N be an individual's POI sequence where the last item is the individual's current location $x = x_{cl}$. If the number of visits in which $X = x_i$ is denoted c_i and similarly the number in which $Y = y_j$ is denoted as r_j, the probability p for the event $(X = x_i, Y = y_j)$ is called *joint* probability and calculated with

$$p(X = x_i, Y = y_j) = \frac{n_{ij}}{N} \tag{31}$$

where n_{ij} is the cell i, j as fraction of all cells of the matrix L×M. The probability for instances of $Y = y_j$ given $X = x_i$ is called the *conditional* probability and is written as $p(Y = y_j|X = x_i)$.

The location prediction task can be described as finding the probabilities for transitioning to a specific node in a network of destinations, given that a POI sequence is used to count the number of transitions between X and Y. Since the Origin (cl) is known ($x = x_{cl}$), the conditional probability for known destinations can be calculated with

$$p(Y = y_j|X = x_{cl}) = \frac{n_{cl,j}}{N_Y} \tag{32}$$

where $n_{cl,j}$ is the number of transitions from cl to y_j and $N_Y(cl) = \sum_{j=1}^{L} n_{cl,j}$.

With Equation (32) it is possible to determine the probabilities of travelling to all known locations, which must by definition add up to 1. Based on the MM, the *Destination* with the highest probability would be considered to be the next destination. Note that this calculation does not include any temporal information yet and can be described as a simple stochastic process. This, however, is a drawback for the application of MM for mobility prediction. More specifically, if data has been collected for a long period, high counts for known locations will outweigh new locations simply due to their long existence in the network, but not necessarily due to higher relevance [140]. Naturally, the longer the data is being collected, the longer it takes the system to adapt to changes in behaviour. While this feature avoids that irregular transitions faze the prediction of routines it becomes challenging for the system to distinguish between new/relevant and outdated data.

4.5.3 Baseline Scenarios

A system that is based on a Markov process will fail to provide a transition probability if an individual visits locations in a sequence that has not been presented to the model before (in higher-order models) or when a location is visited for the first time.

Failing to provide a transition prediction is a significant disadvantage for medium-term prediction horizons. Whenever the system fails to provide a prob-

ability p for the *next* transition, the prediction for the entire transition chain fails. To avoid that the system is not able to predict a location for the next transition there are different options available, also referred to as "fallback" or "escape" solutions [113]:

- When the model's order $n > 1$, the order can be decreased until $p > 0$.
- When a vehicle is used to visit a location for the first time, $n = 1$ does not resolve the issue. This is because the MM approach is location dependent. In this case, the system "escapes" into a location independent state (zeroth order, see Subsection 4.5.5).

Also, in situations where the probabilities for the next locations are equal, for instance, 50% for POI1 and 50% for POI2, the system is calibrated to select the location that has been visited more recently, under the assumption that more recent data contains more information.

4.5.4 Location Dependent Prediction

The location-dependent prediction in the proposed framework is based on a Markov model of first order. Recall that in a MM system of first order only the current state, an individual's current location, is used to calculate the transition probability to the next state S_{t+1}. A user's recorded POI sequence N is used to create a transition matrix T with POIs (see Subsection 3.2.4), as illustrated in the following example:

N=1, 2, 3, 1, 3, 1, 3, 2, 4, 5, 6, 2, 3, 1, 3, 1,...,cl where cl is a user's current location. The corresponding transition matrix is depict in Figure 48.

Origin
x_i

Destination y_j	1	2	3	4	5	6
1	0	0	4	0	0	0
2	1	0	1	0	0	1
3	3	2	0	0	0	0
4	0	1	0	0	0	0
5	0	0	0	1	0	0
6	0	0	0	0	1	0

Figure 48: Transition matrix example

Naturally, a user's actual *current location* is only known for the first prediction step. Since the framework requires a prediction for up to several days (prediction horizon), the system assumes a user's transition to the most probable destination and repeats the prediction task until the "transition chain" is long enough to cover the required prediction horizon. The transition to the most probable destination is checked for plausibility in conjunction with the expected departure time. The process of checking the plausibility for transition and departure time prediction is explained in detail in Subsection 4.6.

4.5.5 Location Independent Prediction

A MM of zeroth order corresponds to a location independent prediction [153]. This prediction variant is implemented as alternative method to let the framework switch into a different prediction mechanism in situations in which a MM of first order is not able to provide a transition probability, for instance, if an EV user parked at a location that has not been visited yet (see Subsection 4.5.3).

To implement the model, a day is divided into 1440 bins (one bin per weekday minute). If a user is at the location with the POI symbol '1' from midnight until 6:00 am, time bin No. 1 to No. 360 are assigned to the corresponding symbol. The method uses no context (previous locations) and will, independent from the user's

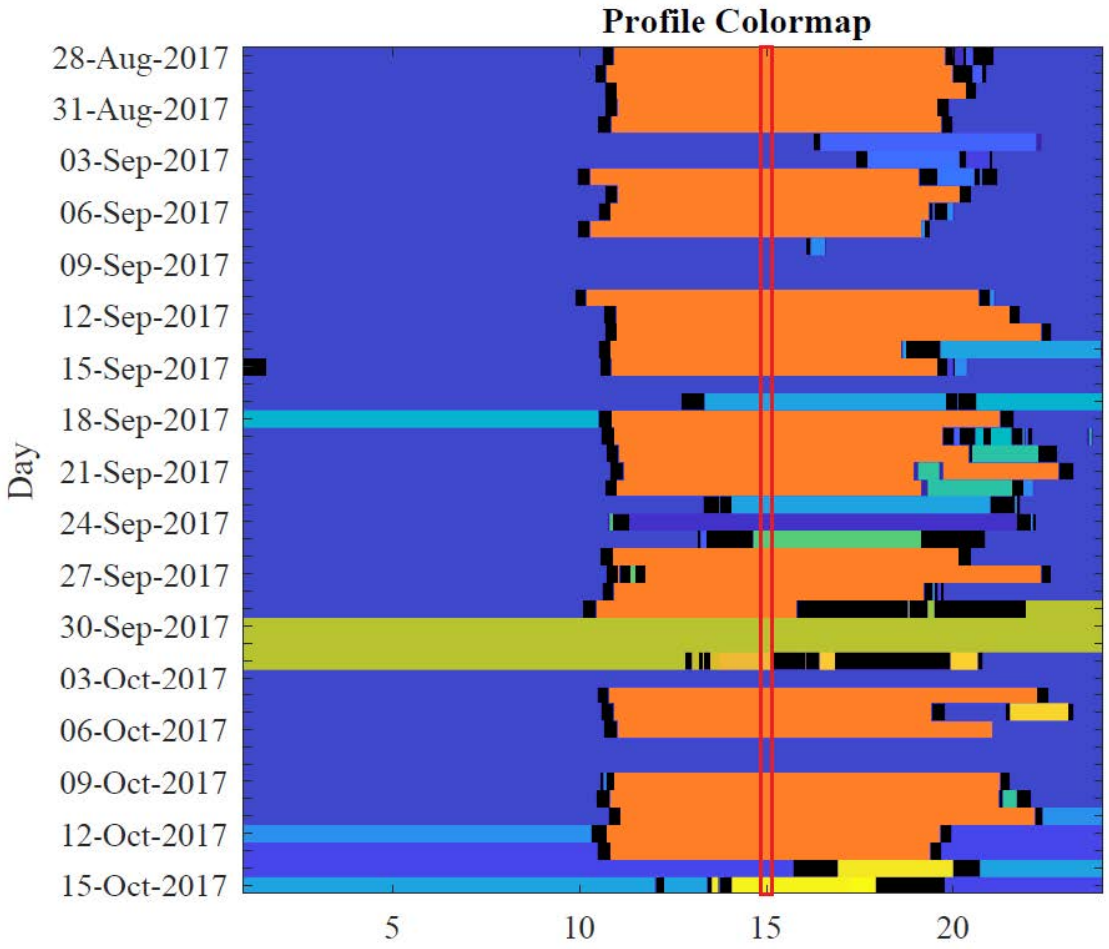

Figure 49: Example Colourmap of a six-week mobility record. Trips are indicated in black. The area framed in red illustrates the input for hour 15 for which the mode predicts the most probable location. To predict a day specific most probable location for hour 15, for instance on a Monday, only Mondays serve as input.

current location, predict an individual's next location to be the one that has been the most visited location at the day-specific time bin in the past. This method is location independent, which especially for long prediction periods should be more robust against error propagation. If A describes a matrix where the columns are minute of days (1440) and the lines are days of records, starting from the current minute t_i, t_{i+1} is calculated with

$$mode\{ar_x m_{i+1}, ..., ar_n m_{i+1}\} \tag{33}$$

where x is the first relevant day and n is the last relevant day.

As this method picks the most occurring POI identifier per time bin, it can be referred to the mathematical operation *mode* [151]. Note that it is not ensured that

this method predicts a trip duration correctly or a trip between location transitions at all. To this end, a subsequent step must be added to this method, which ensures that between every predicted location transition a trip symbol is existing. In the tested implementation a trip's duration is the median trip duration of the predicted trip ID. The predicted trip ID is the ID that occurred most often between the departure location and the predicted destination. Figure 50 gives an example for

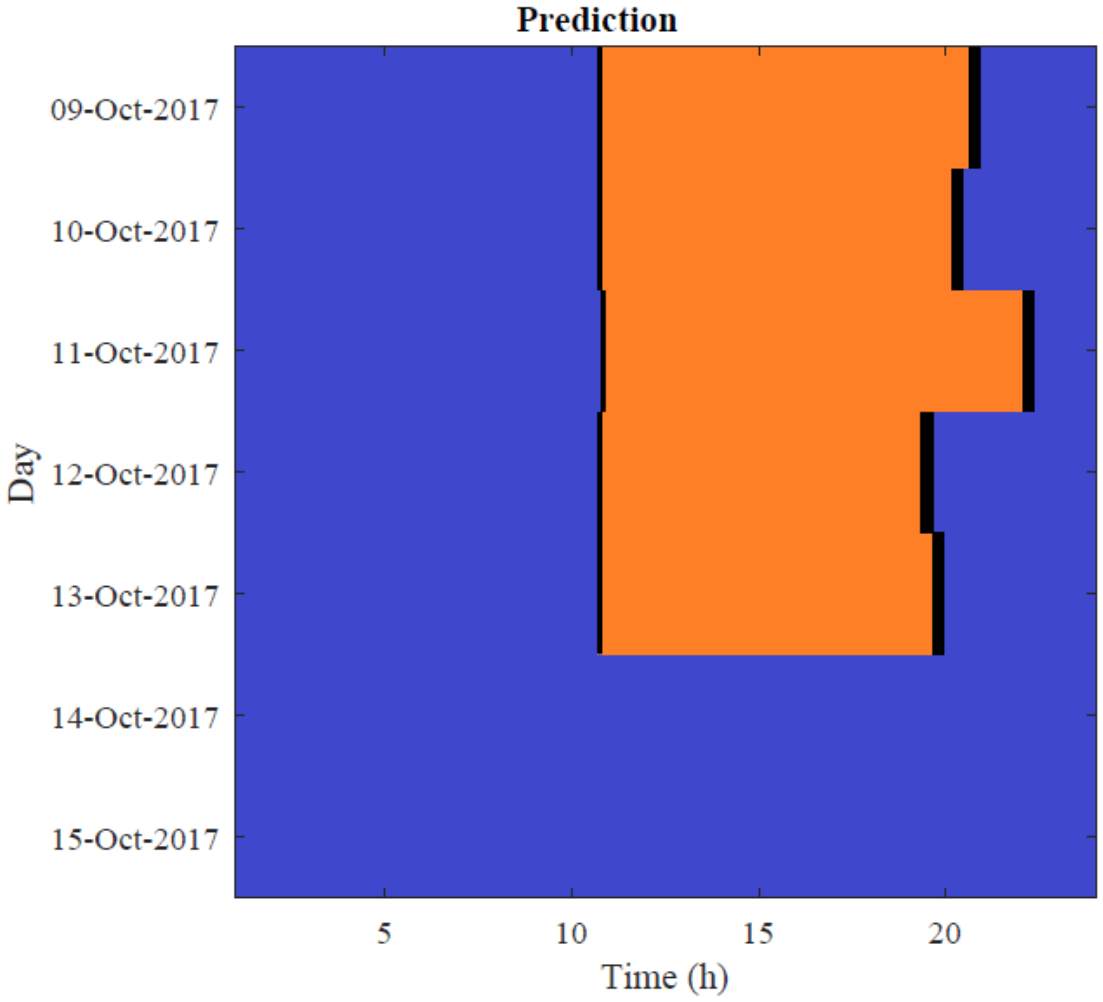

Figure 50: Example of predicted colourmap.

the prediction result, using six weeks of sample data of the example user, displayed in Figure 49.

4.6 Departure Time Prediction

This section introduces a non-parametric departure time prediction method that is based on kernel density estimation (KDE). A separated departure time prediction

is required since the previously described Markov model's transition prediction is decoupled from the departure time prediction.

4.6.1 Review of Existing Methods

Temporal behaviour is generally more difficult to predict than spatial behaviour [122] [205]. The temporal aspect of mobility prediction can be investigated from two different angles. One approach is to identify characteristic periods (time of day), in which an individual is usually on the move. By investigating different mobility profiles, the beginning of these periods can be observed in the morning hours, when people usually commute to work. A higher probability to be at *different* places results in a higher mobility entropy. The hourly mobility entropy of different users is illustrated in Figure 51. The illustration is the result of an analysis in [123] to illustrate periods in which humans are more mobile, hence less predictable.

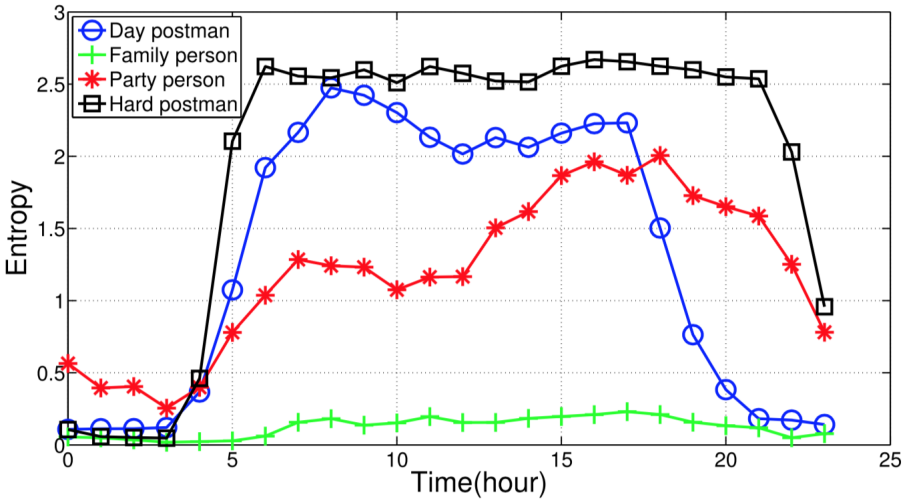

Figure 51: Entropy of different User Clusters [123]

Another approach is to focus on the prediction of stay time at a distinct location, as demonstrated in [205] and [122]. Based on the MDC data set, Baumann demonstrated that stay times show lower entropy than arrival times. A lower entropy indicates higher predictability (see Section 2.4.8). Baumann showcases relevant findings for EV specific predictions. Recall that a smart charging framework aims to schedule charging events based on the location and expected dwell time. An overestimation of dwell time for a location at which a charging event is scheduled

could lead to an insufficient battery charge when the objective is to reach the level of charge before the user departs.

By comparing eight different dwell time prediction methods, a location independent Markov model of first order produced the smallest number of overestimated dwell time predictions [205]. Similar findings regarding the dwell time prediction accuracy are illustrated in [113]. Baumann argues that the presence of temporal data forces the predictor to be "riskier" in predicting place transitions, which leads to a smaller dwell time estimation.

In its simplest form, dwell time prediction is only useful for *one* next-step predictions in which the end of a stay could mark the probable departure time [113]. Recall that a smart charging framework is required to provide *medium-term* predictions. Hence a dwell time based "next-step" prediction is not considered to be sufficient for the necessary prediction horizon for EV specific predictions.

Although the aforementioned references state higher entropy for departure time predictions, a location-specific departure time prediction appears to be the more appropriate prediction scheme for a smart charging framework. This is because by predicting departure times independent from arrival time, the medium-term prediction is less prone to error propagation. By predicting arrival and departure periods independent from each other, errors for the arrival time do not necessarily have an impact on the prediction accuracy of departure periods. Figure 52 illustrates the correlation of dwell time prediction and its variance and arrival-departure time prediction.

Different departure time prediction schemes have been presented in recent literature. A common approach is to create time bins and count transition events within these time bins. The discretisation of time intervals is an established method to simplify temporal prediction tasks. To incorporate time bins into Markov models, in [205], [206] and [164] time bins were randomly defined as 15 minute intervals. The downside of this approach is that the temporal prediction accuracy is limited to the discrete time bin scale. For instance, two departure events, separated by only one minute (on different days) could be assigned to two different 15-minute intervals,

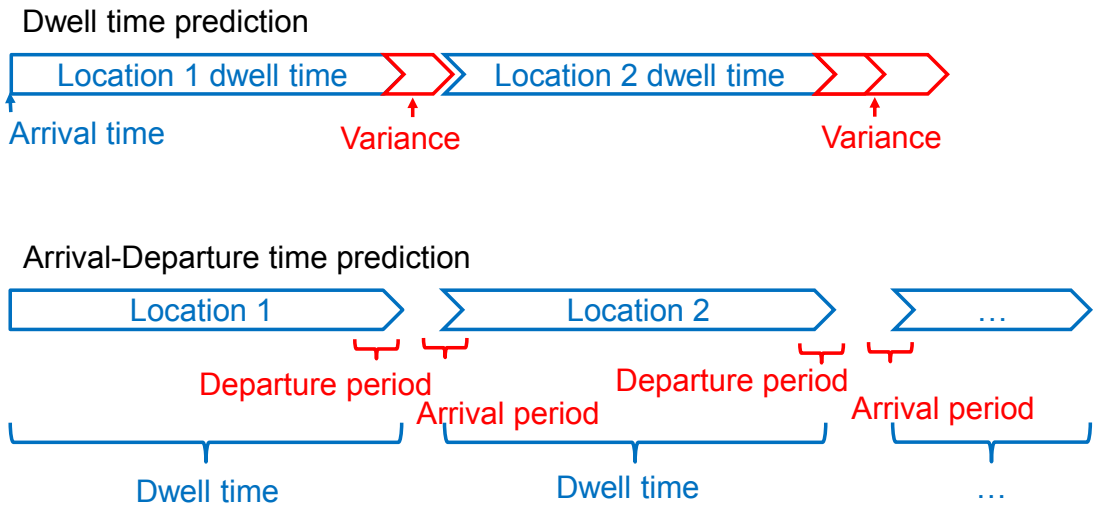

Figure 52: Dwell time prediction vs. departure and arrival time prediction.

creating a potential departure interval of 30 minutes. In an EV context, 30 minutes of charging time could account for a significant change in the attainable range. Hence, a non-parametric approach, such as a kernel density estimator, promises a more accurate estimation method for the intended use case.

The previously discussed aspect creates special requirements regarding the temporal prediction task for a smart charging framework. Based on a study[15] conducted in 2018, 86% of EV charging takes place at the EV owner's home. Hence an accurate prediction of arrival and departure times, especially at home, is a priority for the smart charging framework. According to [205] the predictability of residence time for the most visited location, which is usually an individual's home, is lower than for the second and third most visited location, the following section will introduce a non-parametric method to predict departure time for scheduled charging.

4.6.2 Kernel Density Estimation

This section discusses how departure and arrival events will be predicted. In the previous section, it has been discussed why departure and arrival times play an essential role in the task of scheduling charging events. Both events define periods

[15] http://www.electricnation.org.uk/wp-content/uploads/2018/10/Electric-Nation-What-weve-learnt-so-far-Oct18.pdf

in which the vehicle can be charged for its future trips. Charging schedules and their optimisation benefit from high accuracy for the prediction of departure and arrival events.

The corresponding problem statement can be formulated as follows: What time of day features the highest probability to leave a location to a known destination? More specifically, the problem can be formulated to find the probability X that a location-dependent departure event falls into the period (a,b). Given that the corresponding probability density function (PDF), also referred to as kernel density estimation, f is known, X can be quantified with

$$P(a < X < b) = \int_a^b f(d)dx \tag{34}$$

where $a < b$ [207]. Based on observations illustrated in Chapter 3, human's tendency to move following distinctive travel patterns suggests that departure events follow a distinctive probability distribution which, however, is unknown. Considering a scenario in which an individual is observed for a limited period, the observation data provides samples for the underlying probability function $f(x)$. As the true probability density function is unknown, it must be estimated. The required kernel density estimator for a nonparametric approach is defined as

$$\hat{f}(x) = \frac{1}{nh} \sum_{i=1}^{n} k\left(\frac{x - X_i}{h}\right) \tag{35}$$

where $i = 1, 2, ..., n$ are samples of relevant departure times, k defines the kernel density function and $h > 0$ is the bandwidth [207]. Apart from the actual samples, the shape of the corresponding density estimation is influenced by the selection of the kernel k and the bandwidth h.

The kernel function k defines the shape of weight function that usually satisfies $\int_{-\infty}^{\infty} k(x)dx = 1$ and is symmetric over 0 [207] [208]. In relation to the kernel's shape, the choice of the density estimator's bandwidth has a greater impact on the shape of the density estimation, as it defines the width of the kernel (see in Subsection 4.6.3 for a detailed discussion).

The set of samples, that is used to create a density estimation, consists of data that is classed as relevant for the estimation. More specifically, departure times provide data points that are classed as relevant when the origin and destination of the corresponding trip correlate with the transition prediction (see 3.2.4). Figure 53 visualises a histogram of relevant departure events in the morning (Home-Work) from User 6 and the corresponding density estimation.

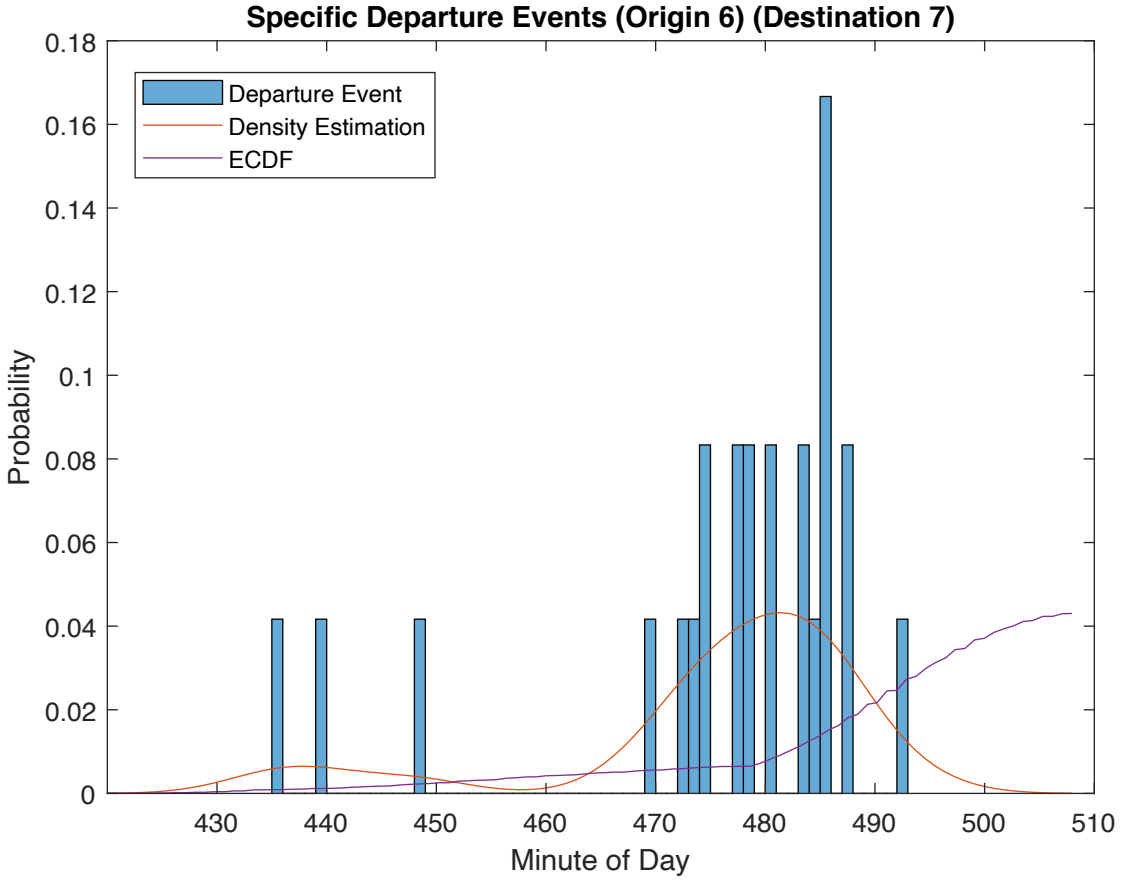

Figure 53: KDE Example. Departure events are illustrated as histogram with a bin width of one minute. The red function displays the kernel density estimation. The purple function illustrates the empirical cumulative distribution function (ECDF) which can indicate a departure's "certainty" for EV charging purposes.

4.6.3 Bandwidth Selection

A density estimation's bandwidth, also referred to as *hyper-parameter*, defines the smoothness of an estimated function [149]. Recall that the bandwidth defines the width of the kernel function. Hence a larger bandwidth creates a smoother density curve. Selecting an adequate bandwidth is a non-trivial task. It is challenging in

particular if the underlying density has long tails.

If a small bandwidth is chosen, samples at the tails of a distribution create noise. If the bandwidth is too large, the information in the main part of the distribution is lost (over-smoothing) [208]. The "optimal" bandwidth can be inferred with different methods. For instance, the goodness-of-fit of the density estimate can be quantified with an error criterion. A sensible choice of bandwidth h minimises this error [209]. Note that, since *f(x)* is unknown, the error can only be approximated asymptotically. A measure to quantify the estimated error is to compute the Mean Integrated Squared Error (MISE) [210] with

$$\mathrm{MISE}(h) = \mathrm{E}\left[\int (\hat{f}_h(x) - f(x))^2 \, dx\right]. \tag{36}$$

If the kernel k is assumed to be Gaussian

$$k(x) = \frac{1}{\sqrt{2\pi}} \exp\left(-\frac{1}{2}x^2\right) \tag{37}$$

then

$$h = \left(\frac{4\hat{\sigma}^5}{3n}\right)^{\frac{1}{5}} \approx 1.06\hat{\sigma}n^{-1/5}, \tag{38}$$

where $\hat{\sigma}$ is the sample set's standard deviation, minimises the MISE [207]. Equation (38) is referred to as Silverman's rule of thumb. Note that there are different methods to obtain h [208]. For departure time prediction, the peak's location is more relevant than the estimation of the probability function. For simplicity, the built-in MATLAB function *ksdensity* is employed to minimise MISE(h), which determines h according to the Scott's estimate (see Figure 54).

Transferred into a scenario of departure time observation, a long-tailed distribution would be created when an individual departures to a specific destination most of the time within a short period but sometimes at very different day times. Statistically the appearance of departures at "unusual" times might be negligible, however, the total number of these unusual departures could sum up to a significant proportion of the overall number of relevant departure events.

Using a bandwidth that is dependent on the sample size n instead of being static

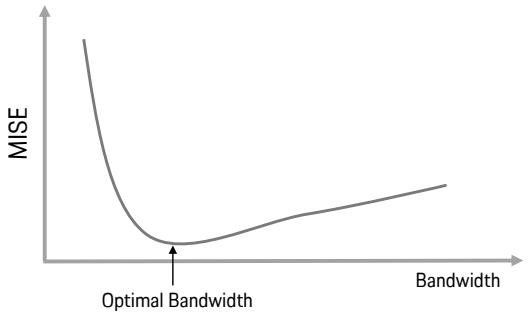

Figure 54: Optimal bandwidth based on MISE.

is useful as it adapts to the underlying data distribution. Given a system that observes a user's movement, the sample set should evolve from sparse to dense. This means that the density estimation could be improved with every additional sample by choosing a variable bandwidth. This promotes the utilisation of KDE for departure time prediction as locations of specific interest, such as an individual's home, are visited most frequently and will proportionally provide the most sample points for the density estimation. Based on departure time observations in Chapter 3, it is valid to assume that eventually, location-specific departure times will form a near Gaussian distribution around a typical departure time. To this end, the KDE's bandwidth is computed based on Equation (38). Concluding the concept of departure time estimation, departure time is predicted at the time of the day at which $\hat{f}(x)$ reaches its maximum.

4.7 Multi-step Prediction

The separation of location prediction (via MM) and departure time prediction (via KDE) requires to design the prediction as a sequential process. The most reliable predictor for a destination is an individual's current location [130]. Hence, the process starts with the MM based prediction of the next destination. Once the destination with the highest probability is being determined, the process proceeds with the probability estimation of the corresponding departure time. The predicted location is used as input for the determination of relevant departure events, that are all departure times of trips that originated from the current location and ended at the predicted destination.

In this process, predicted departure times overrule transition probabilities. If, for instance, the most probable departure period to the most probable destination elapsed, the system falls back to the location-dependent second most probable destination. If the same applies to the departure time to the second most probable destination, the process is repeated for the (current) third most probable destination. Algorithm 1 illustrates the conceptual process.

Algorithm 1 Markov Model with density estimation

1: N = POI sequence
2: *CDT* = Current Daytime
3: *Current Location (CL)* = Last element of N
4: Create transition matrix T:{1,...,m}×{1,...,n}
5: *First Most Probable Destination (FMPD)* = max{T[cl,n]}
6: Execute probability density estimation for day specific departure times from *CL* to *FMPD*
7: Highest Peak of density estimation = Day specific *Most Probable Departure Time (MPDT)*
8: **if** *MPDT* > *CDT* **then return** *Destination* = *FMPD*, *Departure Time* = *MPDT*
9: **else** *Second Most Probable Destination (SMPD)* = max{T[cl,n]\{*FMPD*}}
10: Execute probability density estimation for day specific departure times from *CL* to *SMPD*
11: Highest Peak of density estimation = *MPDT*
12: **if** *MPDT* > *CDT* **then return** *Destination* = *SMPD*, *Departure Time* = *MPDT*
13: **else** *Third Most Probable Destination (TMPD)* = max{T[cl,n]\{*FMPD, SMPD*}}
14: Execute probability density estimation for day specific departure times from *CL* to *TMPD*
15: Highest Peak of density estimation = *MPDT*
16: **if** *MPDT* > *CDT* **then return** *Destination* = *TMPD*, *Departure Time* = *MPDT*, *CDT* = *Arrival Time at predicted location*
17: **else** assume no more trips at that specific day, *CDT* = 0:00 (+1 day)
18: **end if**
19: **end if**
20: **end if**

This iterative process ensures that the predicted departure time is "valid". The system would be forced to predict transitions if the process would not be stopped after the consideration of the location dependant three most probable destinations. The three most probable destinations are considered as they account for almost 90% of all visits for most users (see Section 3). Note that the *location dependent* most probable destinations are considered and not the *global* most relevant destinations.

The first, second and third most probable destination as well as the most probable departure time are *maximum* values that can be determined with a "*sort*" function. The operation must be executed once per prediction step. For destination probabilities, the results with indices (0), (1) and (2) are the corresponding first, second and third most probable destination. Given the applied code uses the *Quicksort* method, as for instance in MATLAB, the algorithm has a complexity of $\mathcal{O}(n \cdot \log(n))$ if n is the number of possible destinations [211].

At this stage, the system determined the most probable (next) destination and the most probable departure time. The first prediction step is concluded by the estimation of arrival time at the predicted destination under consideration of the expected trip duration. The trip duration is determined by the median trip duration

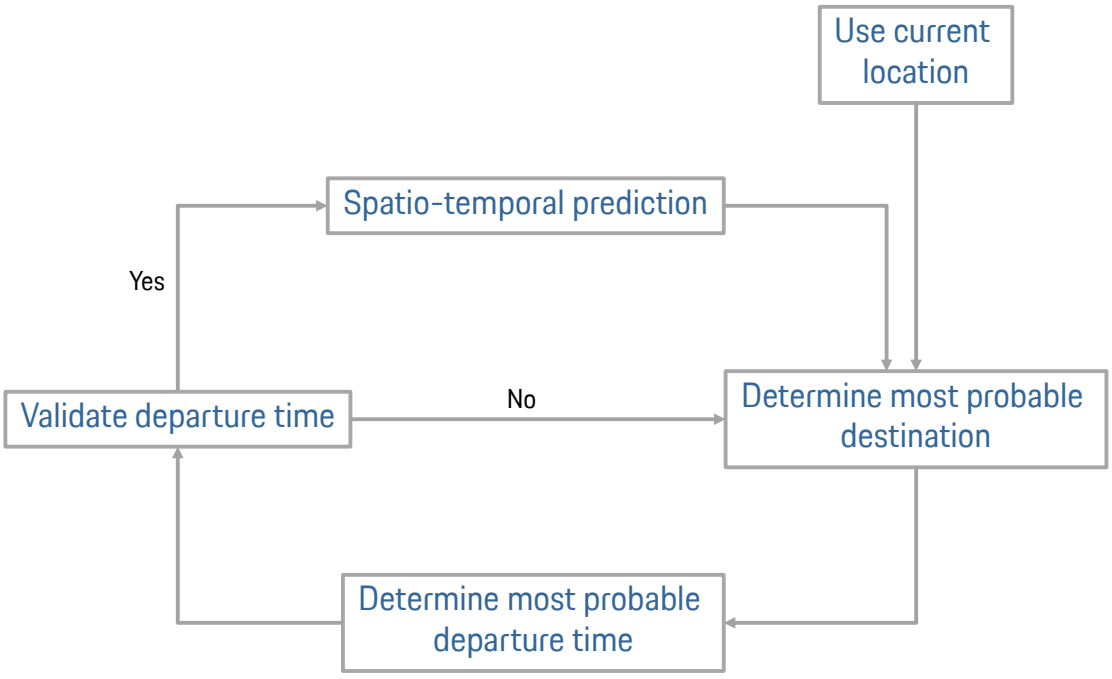

Figure 55: Sequential steps of location based transition prediction and subsequent departure time prediction. A departure time is valid if it is yet to come for the predicted day (*most probable departure time* > *current day time* (see Algorithm 1)).

of all trips that lead from the origin to the destination. A schematic view of the prediction process is illustrated in Figure 55.

4.8 Validation and Experiment

This chapter introduces the conceptual framework for a novel spatio-temporal mobility prediction method. This subsection depicts results that were obtained with an implementation of the introduced methods in MATLAB on DS1 and DS2. To illustrate the results that were obtained with the method that has been introduced in Subsection 4.4, results of the MM/PDE and *mode* approach are illustrated. More specifically, Subsection 4.8.2 discusses the framework's transition prediction accuracy as well as its spatial (Subsection 4.8.3) and temporal accuracy (Subsection 4.8.4). A definition of the different measures is given in the following sections.

4.8.1 Error Matrices

To schedule charging based on spatio-temporal predictions, both spatial *and* temporal accuracy is of high relevance. Wrong location predictions can lead to wrong assumptions about the mobility-related energy demand and false expectations concerning the charging infrastructure availability. Inaccuracies for arrival and departure times could result in insufficient vehicle charging, for instance, due to shorter dwell times.

The performance of prediction algorithms is typically measured with a set of different metrics. Well known performance indicators for prediction algorithms are *accuracy*, *precision*, *recall* and *F1-score* [110] [212]. Accuracy, precision and recall are computed based on classifications given by a confusion matrix. The matrix contains four different classes: true positive (TP), true negative (TN), false positive (FP) and false negative (FN). The corresponding definitions are:

$$\text{Accuracy} = \frac{TP+TN}{TP+TN+FP+FN}$$
$$\text{Precision} = \frac{TP}{TP+FP}$$
$$\text{Recall} = \frac{TP}{TP+FN}.$$

A fourth metric is given as F1-score, which is defined as the harmonic average of precision and recall:

$$\text{F1-Score} = \frac{2*Precision*Recall}{Precision+Recall}.$$

The F1-score indicates how well a prediction algorithm can balance precision and recall [130]. A high F1-score indicates a good prediction performance. Based on this definition, three different metrics are of specific relevance to the framework's prediction task:

- Transition prediction performance: The algorithm's transition prediction performance is measured with three different scores: *precision*, *recall* and *F1-score*. The predicted transition precision is defined as the ratio of correctly predicted transitions and the total number of predicted transitions, which, in this context corresponds to the definition of accuracy. The score is computed with a ratio of six weeks of training data and one week of predicted data (out of sample test). The second score is the transition recall which is defined as the ratio of correctly predicted transitions and the total number of actually occurred transitions. The definitions of transition precision and recall are resumed from [205]. The transition is considered as being correct if the predicted origin-destination couple is equal to the observation, regardless of the predicted transition time.

- Spatial accuracy: The spatial prediction accuracy refers to the framework's ability to correctly predict an individual's (vehicle's) presence at a specific location. Every prediction consists of seven days with one predicted location symbol per minute (7 days $\times$1440 minutes = 10080 location predictions). The spatial accuracy in percent corresponds to the fraction of correctly predicted location symbols.

- Temporal accuracy: The departure time prediction accuracy is measured for correctly predicted transitions. The error is indicated as difference in minutes from the predicted departure event time to the observed departure time.

Referring to the aforementioned performance measures, an adequate comparison of different prediction models is difficult for multiple reasons: One reason is that most investigations use different data sets which often show different characteristics that influence predictability. Another is that there are divers measurements that

indicate the accuracy of a prediction method.

Focusing on medium-term mobility predictions, three different accuracy metrics are introduced to indicate the model's prediction performance. For the measurement and to ensure similar conditions for all user profiles, the available profiles are cut in periods of seven consecutive weeks. The last week (7th) from each mobility profile is separated from the data. This single week is not presented to the prediction models and serves for testing the prediction accuracy for each individual (out-of-sample test). This results in a training data set of six weeks and a validation data set of one week per profile.

4.8.2 Transition Accuracy

Both prediction schemes underestimate the number of trips in a week. The average ratio of the number of predicted and observed trips is 0.87 in DS1 and 0.52 in DS2 for MM/KDE. The Mode based prediction achieved a ratio of 0.73 for DS1 and 0.83 for DS2.

An underestimation of transition predictions was expected for both prediction methods and can be attributed to the framework's limitation to predict regular trips. The observations indicate that in addition to regular mobility behaviour, there is a proportion of random mobility, which does not follow a logic that is captured by the framework. Part of this random behaviour is captured by the number of trips that headed to destinations that have not been visited in the six weeks of sample data.

In average, 15.6% of trips in DS1 and 16.3% in DS2 headed to a destination that has not been visited in the six weeks of training data. The probability of heading to an unknown destination can be computed for every profile individually and, in addition to a profile's entropy, indicates the uncertainty that is associated with the transition prediction.

Besides the fact that in DS1 15.6% and 16.3% in DS2 of transitions could not be predicted due to the framework's logic, both prediction schemes performed better on DS1 than on DS2. A tendency for better predictability of vehicle data was expected as the data indicated a higher degree of regularity, as has been discussed in Section

3 and will be further analysed in Section 4.8.3.

The transition prediction accuracy (fraction of correct predictions over the total number of predictions) for both methods is slightly lower than stated in other publications, for instance in [149]. However, note that the results are obtained from predictions for an entire week, thus up to seven days into the future. Results illustrated in [149] for transition accuracy refer to intervals of one to three hours. Taking error propagation into account, both introduced models performed satisfactorily on DS1 and DS2.

Details of both scheme's transition prediction precision, recall and F1-Score distribution are depicted in the Appendix.

4.8.3 Spatial Accuracy

The spatial accuracy is defined as the proportion of predicted time instances in which the individual/vehicle was present at the location that has been predicted and the total number of predicted time instances. For an individual with typical travel behaviour, a separated test week would be a good representation of the remaining six weeks. However, this does not apply to individuals that show atypical travel behaviour. A source of error for the performance measure is that there is a risk of separating a week that has no similarities to the remaining six weeks. For instance due to holidays, the end of a semester, etc. In the best-case scenario, the test week shares 100% similarity with the previous weeks. However, any deviation from regular behaviour in the test week would lead to a decrease in accuracy, even if an algorithm learned the past behaviour correctly. To provide a general indication of the predictions scheme's performance and to ensure comparability to other prediction schemes, three different methods for the comparison of the prediction outcome to the input data are introduced:

- **One Day comparison (1Day):** In this metric, the first day of prediction is compared to the first day of the test week regarding the location accuracy. This measure indicated the framework's ability to provide short term predictions. However, the measure is prone to errors as the selected day could be a poor

representation of the user's mobility.

- **One Week comparison(1Week):** For this metric, an entire predicted week is compared to the test week regarding its location accuracy. This measure indicates the framework's ability to provide medium-term predictions, however, similar as in *1Day*, there is a risk of selecting a poor representation of the user's mobility, for instance, a week of holiday etc.

- **Seven Weeks (7Weeks):** In this metric, the predicted week is compared to the *average* of the seven recorded profile weeks. More specifically, the normalised fraction of correct overlap accounts for the achieved accuracy. This corresponds to an in-sample test.

By using three different, instead of just one comparison method, the impact of inconsistency in the test data can be lowered. For instance, if an atypical test week would have been selected for the "One week comparison" the prediction performances would be significantly lower than in the "Seven weeks comparison". This would falsify any assumption about the prediction method's performance. Similarly, the outcome of the "One day comparison" should be better than for the two other methods due to error propagation in the medium-term prediction. If the "One day" performance were significantly lower, this would be an indication for an atypical test day.

For a direct comparison, Table 18 shows the achieved accuracy results for the proposed models for DS1, while Table 19 shows the achieved accuracy results for the proposed models for DS2.

In general, the mode method achieves higher accuracy in all three accuracy metrics for both DS1 and DS2. The Mode in conjunction with WCD achieves a slightly higher accuracy for 1Week and 7Weeks than the Mode based on WCI. This can be attributed to the fact that most profiles show a weekly cycle based rhythm. Only for the one-day comparison, the Mode with WCI in DS1 achieves a comparably high accuracy as the Mode with WCD.

Based on the exhaustive search approach, the framework calculates each intra-day prediction for both inter-day predictions. The better performing inter-day pre-

Table 18: Achieved prediction accuracy on DS1.

Approach		**1 Day**	**1 Week**	**7 Weeks**
WCD + MM/KDE	Mean	52%	36%	34%
	Median	53%	34%	34%
WCI + MM/KDE	Mean	53%	41%	38%
	Median	56%	37%	35%
Auto-Select + MM/KDE	Mean	60%	44%	41%
	Median	66%	41%	38%
WCD + Mode	Mean	76%	68%	71%
	Median	81%	72%	72%
WCI + Mode	Mean	77%	66%	66%
	Median	86%	70%	68%
Auto-Select + Mode	Mean	83%	70%	69%
	Median	86%	75%	70%

Table 19: Achieved prediction accuracy on DS2.

Approach		**1 Day**	**1 Week**	**7 Weeks**
WCD + MM/KDE	Mean	46%	32%	28%
	Median	45%	31%	30%
WCI + MM/KDE	Mean	46%	38%	34%
	Median	47%	35%	32%
Auto-Select + MM/KDE	Mean	53%	40%	35%
	Median	56%	36%	33%
WCD + Mode	Mean	53%	55%	57%
	Median	57%	56%	57%
WCI + Mode	Mean	49%	49%	49%
	Median	52%	49%	48%
Auto-Select + Mode	Mean	58%	56%	55%
	Median	61%	58%	57%

diction is chosen (Auto-Select) based on the average prediction accuracy (of 1Day, 1Week, 7Weeks). The selection is executed individually for each user profile.

The results show that location-dependent prediction is more prone to errors caused by atypical travel behaviour. In 60% of the data profiles (DS1 and DS2), the ANN improved the prediction accuracy by 13.9% on average. Location-independent prediction is less prone to atypical movement, as the accuracy for 22% of data profiles was improved by 5.8% on average through the ANN approach.

Figure 56 shows a detailed distribution of the achieved accuracy per user profile over the profile's respective entropy. The plots marked with (a) in Figure 56, 57 and 58 correspond to the data in row "Auto-Select + MM/KDE" of Table 18 and

19, while the plots marked with (b) in Figure 56, 57 and 58 correspond to the data from row "Auto-Select + Mode" of Table 18 and 19. The coloured marking of the data is used to distinguish between DS1 and DS2.

To illustrate the differences in performance, Figure 56, 57 and 58 illustrate the location accuracy over the corresponding profile entropy with the previously defined measurement methods.

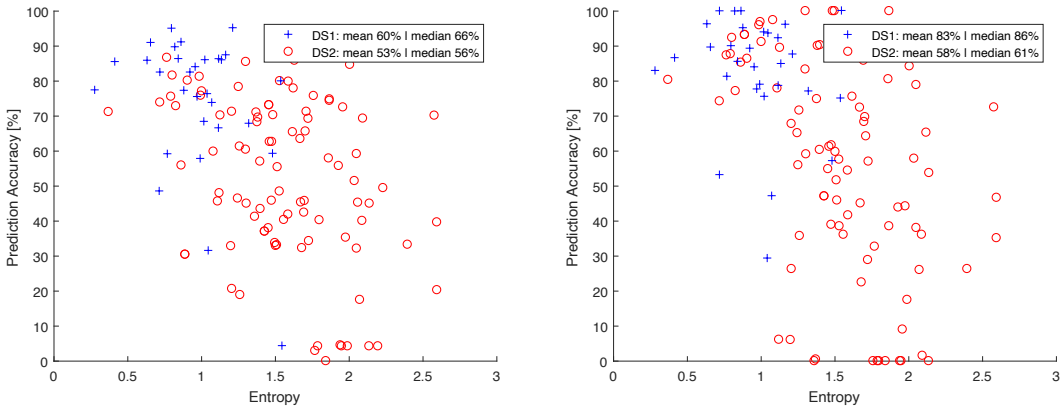

(a) (b)

Figure 56: Accuracy over entropy: a) 1Day MM/KDE, b) 1Day Mode.

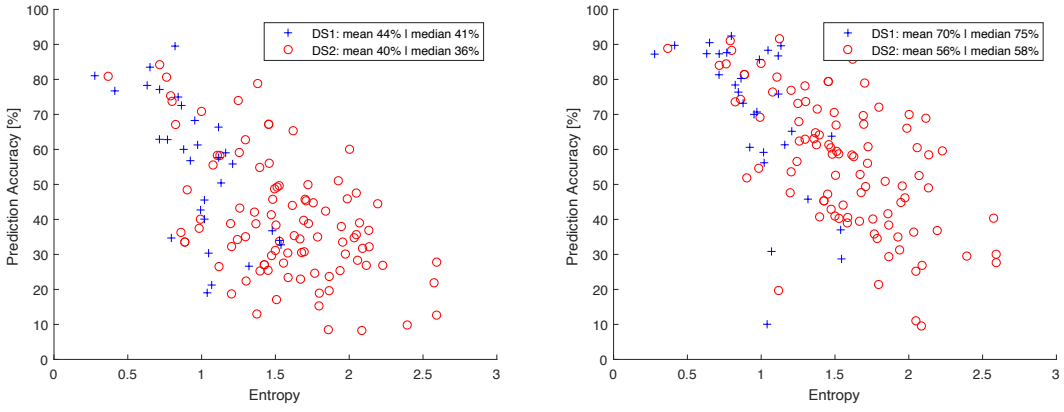

(a) (b)

Figure 57: Accuracy over entropy: a) 1Week MM/KDE, b) 1Week Mode.

Figure 56 illustrates the correlation between prediction accuracy and entropy for the introduced accuracy metrics. Vehicle data (blue cross) shows a systematically lower entropy and hence a better prediction accuracy compared to smartphone data (red circle). Better predictability for vehicle data can be concluded as vehicles are "less mobile" compared to human beings in terms of freedom of movement.

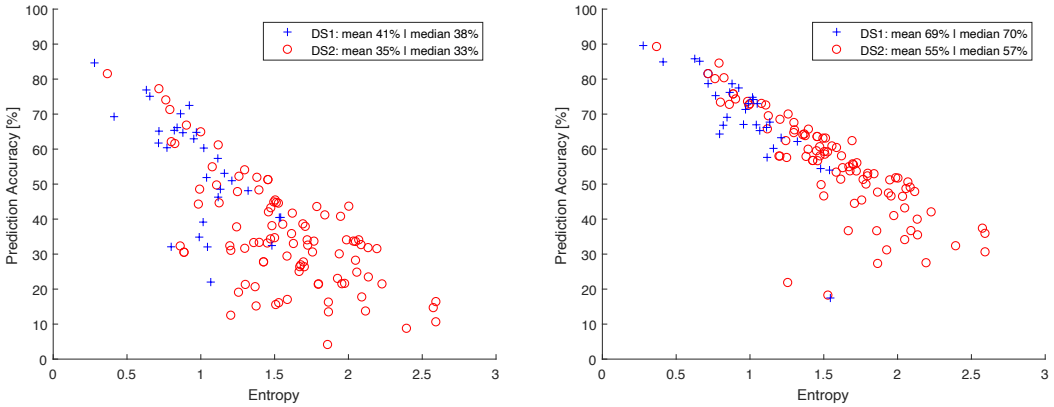

(a) (b)

Figure 58: Accuracy over entropy: a) 7Weeks MM/KDE, b) 7Weeks Mode.

Furthermore, fewer detection errors can be assumed for DS1 as it, other than DS2, requires no assumption about the transportation mode and hence should provide a better base for prediction.

The three different performance measures visualise the challenge of choosing an adequate performance indicator for location prediction data. While a day by day comparison of observation and prediction data is prone to outliers (Figure 56 (a) and (b)) for both MM/KDE and Mode, a comparison with the movement of an entire week shows a stronger correlation between entropy and prediction accuracy. The "limits of predictability" become most obvious in Figure 58 (a) and (b), where one week of prediction data is compared to seven weeks of observation data. A decrease in prediction accuracy has to be expected for longer predictions due to error propagation.

4.8.4 Temporal Accuracy

The analysis of departure time accuracy reveals that the introduced KDE-based departure time prediction performs better than a location independent departure time prediction (mode-based). The results underline that the separation of the transition prediction task and the departure time prediction task increases the temporal prediction performance significantly. Figure 59 depicts the KDE-based departure time prediction error in minutes for both DS1 and DS2. The error is calculated as the difference of observed and predicted departure time of correctly predicted

transitions. A negative error is the result of a too early predicted departure time. Table 20 shows key statistics for the tested prediction schemes.

Table 20: Mean and standard deviation for departure time prediction

	KDE	**Mode**
Mean DS1	- 17.7 minutes	24.7 minutes
Standard deviation DS1	188.9 minutes	382.3 minutes
Mean DS2	- 66.0 minutes	20.4 minutes
Standard deviation DS2	249.2 minutes	385.5 minutes

The departure time prediction for DS1 has fewer and smaller errors than for DS2 with the KDE-based method. Recall that DS1 has higher predictability than DS2, as illustrated in Section 4.8.3. The histogram in Figure 59 and Figure 60 illustrate 5-minute bins. The results are obtained from an out of sample test in which six weeks of individual user data is used to train the model. The prediction is tested on a separated seventh week.

The KDE-based prediction method underestimates departure time by 17.7 minutes for DS1 and 66.0 minutes for DS2 on average. This means that the prediction scheme expects departures on average earlier than observed in the test data. An underestimation is considered as less critical as an overestimation since a charging event that is finished earlier than necessary is less disruptive than an unfinished charging event.

Note that values illustrated in Table 20 are obtained from spatio-temporal predictions of seven consecutive days, hence already including propagation errors.

The standard deviation for mode-based departure time prediction is higher for both DS1 and DS2 in comparison to the KDE-based prediction. Figure 60 illustrates that the error values are more distributed than in Figure 59. Based on the almost random distribution of mode-based departure time prediction error, this method fails to provide a sufficient departure time prediction for charging purposes.

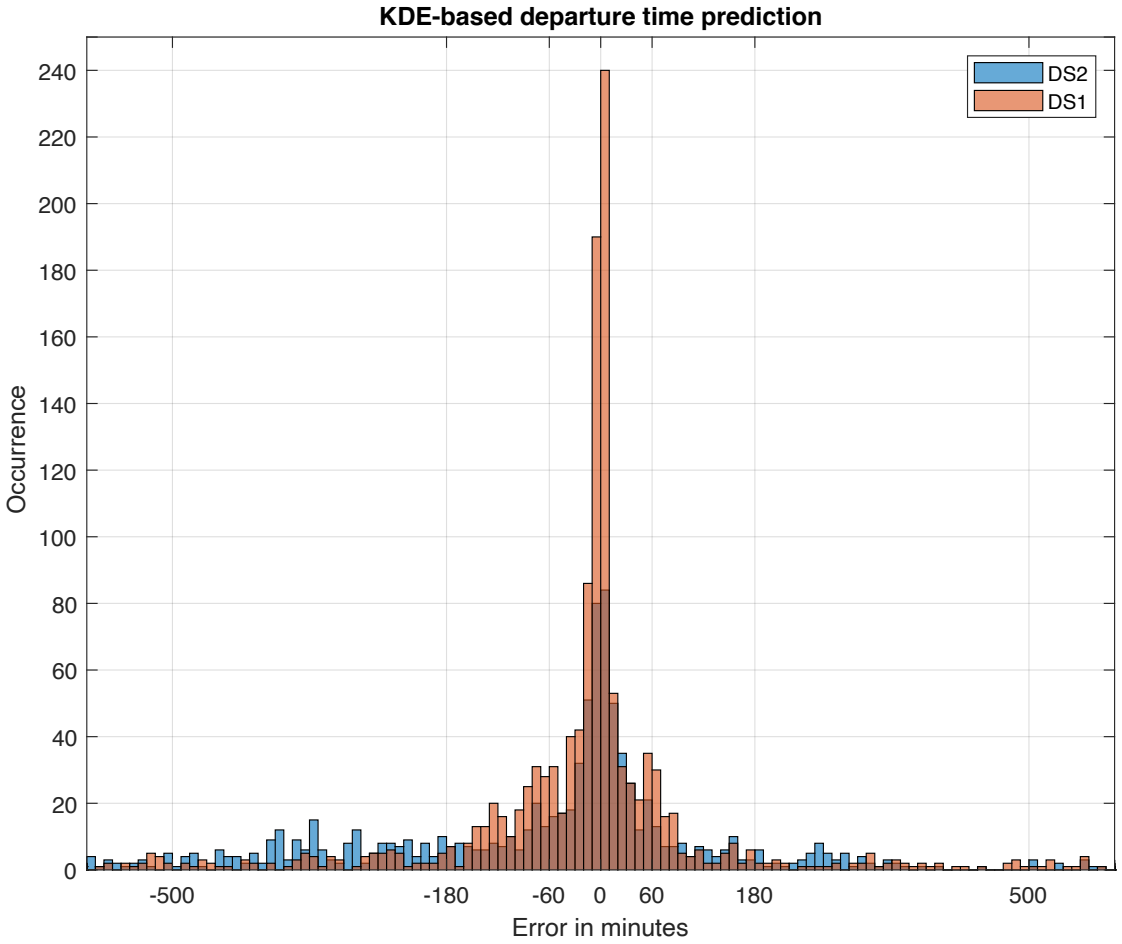

Figure 59: Temporal accuracy for KDE-based departure time prediction. Departure time deviations from 2192 samples.

4.9 Discussion and Conclusion

This chapter introduces a mobility prediction scheme that combines a location dependent and a location independent transition prediction method. Furthermore, the introduced scheme combines both transition prediction methods with a WCD or a WCI inter-day prediction. The framework is configured to select the individual better performing combination automatically and to adjust the corresponding framework output leading to better real-world applicability.

With the help of real-world data sets, it has been demonstrated that not in all cases a weekday-specific prediction, which is used by several state-of-the-art prediction methods, leads to the best user-specific mobility prediction. Instead, for individuals that follow atypical travel patterns, a feature-related clustering method outperforms the weekday-specific prediction method. For 22% of individuals in the

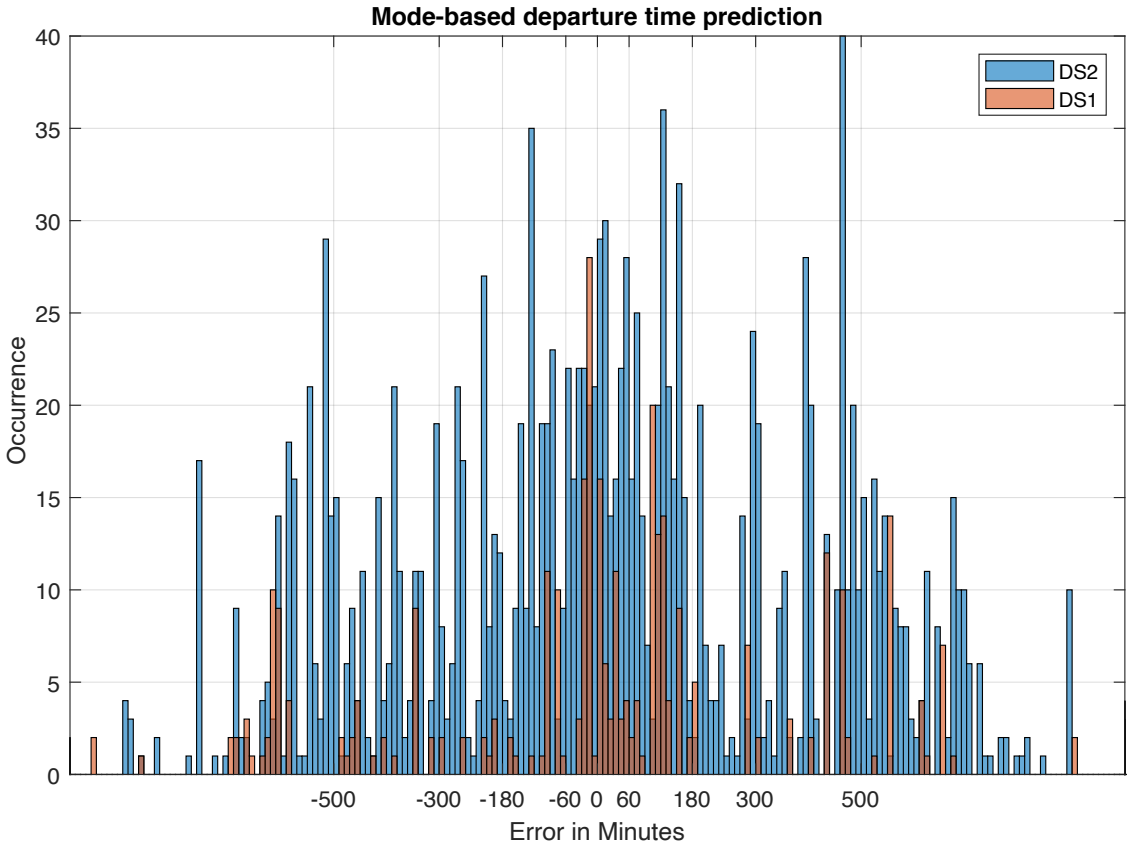

Figure 60: Temporal accuracy for mode-based departure time prediction. Departure deviations from 1914 samples.

available data sets, the framework improves the prediction accuracy by choosing the weekday independent prediction method.

Overall, the framework achieves a median location prediction accuracy of 75% for vehicle-based mobility profiles and 58% for smartphone-based mobility profiles for a one-week mobility forecast and demonstrates that the prediction outcome corresponds to the individual's profile entropy. The location prediction accuracy is an important indicator for a smart charging framework. It contains information about the framework's ability to correctly predict a vehicle's destination but also the corresponding departure times. Incorrect departure time prediction will lower the location prediction accuracy. A high location prediction accuracy also indicates a good estimation regarding the required energy for transitioning between the predicted locations.

On average, for 75% of time in a seven-day period, vehicles are parked at the location that the framework expected. A high location prediction accuracy improves the chance to schedule a charging event at a location and in a period in which the

location is in fact visited.

The introduced KDE-based departure time prediction demonstrates good performance. In relation to other publications, which predict departure events for short periods, the introduced prediction method creates small errors for departure time prediction of an entire week. On vehicle data, the mean error is -17.7 minutes on a seven-day mobility prediction. On less predictable smartphone data, the average error is -66.0 minutes. Both the mean prediction accuracy and the standard deviation could be used for the subsequent scheduling task. For individuals with small departure time deviations, the scheduling scheme can schedule charging events close to the corresponding predicted departure time. For individuals with high standard deviations in the historic departure time prediction, the charging schedule can be created more conservatively.

Independent from the prediction method, the subsequent scheduling task requires a predicted schedule for the vehicle parking and driving times. The predicted schedule must include charging parameters, such as trip associated energy requirements, the available charging power at charging location, etc.

Chapter 5: Prediction Based Charging Schedules

This chapter introduces the third part of the conceptual smart charging framework, which schedules charging events based on the preceding mobility prediction, as presented in Chapter 4. The scheduling scheme's concept is deduced from findings in the field of human travel behaviour and requirements that are derived from existing smart charging implementations. To this end, EV charging related scheduling schemes are introduced and reviewed in Section 5.1. Aspects that can be transferred to a smart charging framework will be highlighted specifically.

The applied methodology of this chapter is explained in Subsection 5.2. Building upon findings in human travel behaviour, power grid requirements, current charging infrastructure and EV communication protocols, the introduced scheduling scheme follows a generic design. The generic design enables to adapt the scheduling scheme to different inputs, which allows a continuous adaption to changes in both vehicle and infrastructure development. The introduced framework is also able to process user preferences, given they are provided manually by the EV user. The proposed concept is tested and validated in a simulation experiment in Section 5.3.

The scheduling schemes performance is illustrated and discussed in Section 5.4. Section 5.5 concludes this chapter.

5.1 Introduction

Scheduling charging events based on predicted travel behaviour should be treated as unidirectional process. This means that a charging schedule must not cause any changes in an EV user's predicted mobility. In this context, the quality of a predicted charging schedule is dependent on the travel prediction accuracy. Wrong predictions about destinations will result in inaccurate assumptions about the vehicle's energy demand, the expected dwell times, potential charging times as well as the available charging infrastructure. Furthermore, inaccuracies about the departure and arrival time can lead to insufficient charging due to too short dwell times. However, the process is explicitly treated as unidirectional, since a bidirectional treatment would

potentially compromise an individual's mobility. Recall that some individuals' mobility behaviour is challenging to predict and prediction outcomes can be vague. Therefore the concept of the scheduling scheme is supposed to embrace uncertainties of the preceding prediction and adapt the charging schedule accordingly.

The scheduling concept in Chapter 5 is designed to account for the specific requirements that are derived from human travel patterns and EV specific charging demands. Different scheduling schemes for EV charging (and discharging) were part of different proposals in the context of smart charging. Based on corresponding publications, existing scheduling schemes can be separated into different classes, according to their original motivation. One class of scheduling scheme in the context of EV charging is designed to reduce waiting time on charging stations [213]. These systems must not be confused with the original concept of smart charging as they limit their focus on the optimisation of one parameter. Aspects such as the grid load and/or charging prices are neglected in these schemes.

Another class of scheduling frameworks focuses on the utilisation of EV batteries to mitigate grid constraints and congestion [214]. Motivated by the impact assessment of charging EVs on the power grid, these scheduling schemes rely on potential monetary benefits that could be created by grid friendly charging behaviour (see Section 2.3). These systems require an infrastructure that can forward price information towards the user and rely on a user's price sensitivity. Besides all associated user interaction requirements, the incentive must be great enough to compensate the effort to provide smart charging relevant data (required energy, desired departure time, etc.) and potentially losings in terms of range.

The review of existing scheduling schemes in Chapter 2 reveals a bias towards infrastructure-centric approaches. Independent from the original purpose of existing charging scheduling schemes, the proposed systems rely on a few basic inputs, which are explained and discussed in the upcoming sections. The assessment of existing and transferable scheduling schemes reveals two major deficits, which restrains their suitability for the intended automated smart charging framework. One deficit is characterised by the strong entanglement of smart charging and monetary benefits

(see Subsection 5.1.1), the second is the dependency on manual user input (see Subsection 5.1.3). Both aspects are described and discussed in detail in the following subsections.

5.1.1 Background

Charging an EV is a means to an end and thus is originally engineered to be as simple as possible. Functions such as "Plug and Charge" (PnC) are developed to simplify a user's authentication process at charging infrastructure to save time and make charging more comfortable. Automated wireless charging (AWC) systems are developed to eliminate the necessity of plugging in a vehicle, to relieve a user and to streamline the charging task.

Existing smart charging concepts oppose the tendency to streamline EV charging processes by creating an additional task, independent from the actual smart charging realisation. This task consists at least of the provision of charging requirements and/or preferences. Hence, a user must be encouraged to participate in smart charging. The majority of scientific investigations focus on charging costs, which can be minimised by shifting charging sessions into periods of cheap power availability. Relying on the availability of flexible price information limits the applicability of smart charging to locations which offer an interface for price information. The dissemination of price incentives in private infrastructure requires additional smart metering equipment and energy management systems (EMS) that can coordinate power consumers or can relay price information to an EV in conjunction with flexible tariffs. In Germany, for instance, the roll-out of required smart metering hardware will not be finished until 2032 (see Chapter 2).

Differences in national regulations and power prices make it challenging to provide a general assumption about the response to price incentives and customer-willingness to install the aforementioned systems. Moreover, as users are used to virtually omnipresent and instant mobility from their ICEV, it must be questioned that compromised mobility by EVs due to smart charging solutions would be widely accepted. Smart charging solutions that rely on flexible tariffs lack a motivation

to be used when no flexible tariffs are available. Hence, it is argued that the attractiveness of smart charging could be improved by the decoupling of charging and monetary incentives. Instead, monetary incentives should be considered as an additional benefit, that could be enabled if flexible tariffs in conjunction with the required infrastructure are available.

5.1.2 Motivation

The realisation of an automated smart charging scheduling scheme is motivated by the original purpose of smart charging and drawbacks of existing smart charging solutions. This includes environmental as well as monetary and technical aspects. An additional aspect, which refers to the drawbacks of existing methods, addresses the user experience that is associated with smart charging. Seamless integration of smart charging technology is considered to contribute to a widespread adaption, similar to other technology that is developed to facilitates EV charging and prevalent adaption to environmentally-friendly electric mobility.

5.1.3 Review of Existing Methods

Existing scheduling schemes require detailed information about the location, the time, the level of power and the amount of energy that is related to a charging event. The provision of these information creates user engagement for every single charging event [215]. For this reason, other works elaborated user interfaces which intend to make charging calibrations "intuitive and easy" to handle [38]. Figure 61 provides an example for a simplified interface for smart charging calibration.

Even tough the choice of charging settings, as illustrated in Figure 61, can be provided in a reasonable simple interface, the selection of corresponding charging choices creates a charging related task for a user. This task must be assessed critically. Under the consideration of the aforementioned influencing factors, it should be assumed that charging choices are not always made rationally. EV-related range anxiety has been identified as one reason for opportunistic charging behaviour which could lead to charging decisions which do not reflect an "optimal" charging choice [38].

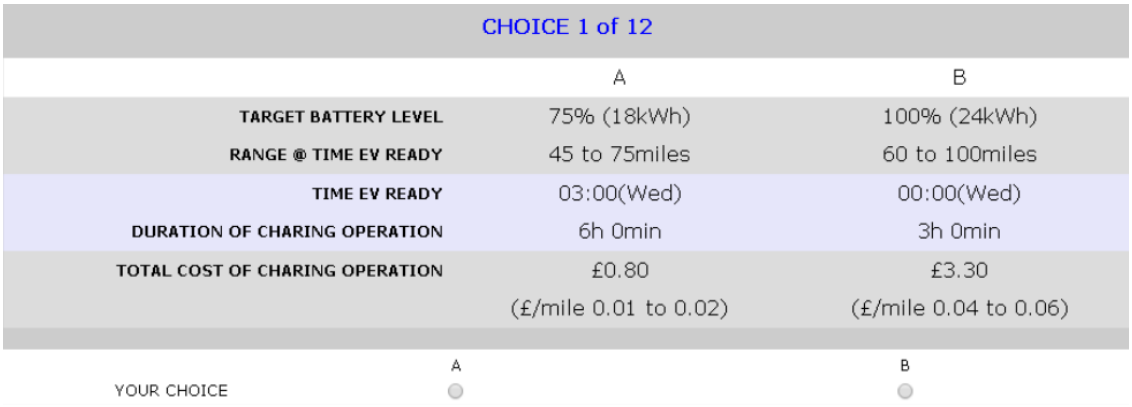

CHOICE 1 of 12		
	A	B
TARGET BATTERY LEVEL	75% (18kWh)	100% (24kWh)
RANGE @ TIME EV READY	45 to 75miles	60 to 100miles
TIME EV READY	03:00(Wed)	00:00(Wed)
DURATION OF CHARING OPERATION	6h 0min	3h 0min
TOTAL COST OF CHARING OPERATION	£0.80 (£/mile 0.01 to 0.02)	£3.30 (£/mile 0.04 to 0.06)
	A	B
YOUR CHOICE	○	○

Figure 61: Example for charging choices. Example taken from [38].

Charging choices as proposed in [38] do not consider a user's individual travel patterns. Thus, there is always a risk of not offering a charging choice that satisfies a user's mobility demand. Forcing an EV user to choose from a set of charging choices that mismatches an individual's mobility behaviour is comparable to situations presented in [216] in which EV user's were reported to be forced to extend working hours to be able to charge their vehicle sufficiently.

Ideally, a smart charging framework is able to schedule charging without the necessity of user interactions while also being able to respect a user's mobility wishes in case they are communicated. More specifically, a smart charging framework should anticipate a user's charging preferences and provide the deduced information to the infrastructure if the information is not provided by a user.

5.1.4 Preliminary Conditions and Requirements

An EV charging process involves at least two parties which are the vehicle and infrastructure. Smart charging requires communication between these parties to organise the exchange of electrical energy. With the upcoming relevance of intelligent vehicle to grid integration, there are several efforts to standardise the communication between the involved instances [217].

In the context of a vehicle to grid integration, the following communication interfaces are of specific relevance:

- IEC 62196 - which defines the types of plugs, socket outlets, vehicle connectors and vehicle inlets for conductive charging,

- IEC 61851 - which standardises EV conductive charging systems based on either AC or DC and defines general EV and EV Supply Equipment (EVSE) requirements and different modes for charging,
- ISO/IEC 15118 - which defines a complementary Vehicle-to-Grid Communication Interface to IEC 16851-1 for bi-directional digital communication based on Internet Protocols.

Features of charging infrastructure, that comply with the standardisation protocols, can be used to evaluate a charging infrastructure's compatibility for a specific EV. For instance, according to the plug definition in IEC 62196, a system can verify if charging infrastructure is, in general, usable for a specific vehicle. Likewise, an infrastructure that complies with ISO 15118 will be able to provide bi-directional communication, which is required to make use of flexible tariffs. The following subsections will give an overview of protocol features which are of specific interest for the intended smart charging framework. As these features are part of defined standards, they can be used to compare charging infrastructures with each other. Being able to compare infrastructure and corresponding charging events will be an essential part of the introduced scheduling scheme. The scheme follows the concept of scoring infrastructure according to its features. An infrastructure that offers suitable user/vehicle-specific features will receive a higher score than an infrastructure that offers less valuable features. After the introduction of existing charging related standards and an assessment of their features, the aforementioned scoring scheme is deduced and explained in detail in Section 5.2.2.

5.1.4.1 IEC 62196

The IEC 62196 standard specification defines a series of plug types and charging modes, specifically for EVs. Regarding charging modes, IEC 62196 describes four different variants. **Mode 1** - single-phase charging. **Mode 2** - allows charging with up to three phases and currents up to 32 Ampere or up to 70 Ampere on a single phase. **Mode 3** - charging on three phases with up to 250 Ampere and **Mode 4** - DC charging with up to 400 Ampere.

The assignment of a charging location to one of the IEC charging modes can be used to make assumptions about the **available charging power**. Furthermore, the mode allows excluding specific charging locations for vehicles which do not support the corresponding **plug type**.

5.1.4.2 ISO 15118

The main purpose of ISO 15118 is to establish a more advanced and autonomously working charge control mechanism between EVs and charging infrastructures [217]. Summary of charging parameters included in ISO 15118 are:

- Charging station service: **AC, DC, wireless power transfer, automatic connection device**.
- Charge Parameter Discovery: max/min/target Energy, max/min Current and max Voltage. These values are used to determine the **maximum charging power** and can be used to communicate the requested **energy transfer**.
- Plug and Charge (PnC): as function to ensure a secured communication between infrastructure and vehicle for billing purposes via digital certificates and public-key infrastructures. This function enables to exchange all necessary credentials to **start a charging event automatically**.
- Load management (smart charging) for all charging modes (as described in IEC 62196), which includes the provision of **dynamic price information**.
- Renegotiation of charging schedules while charging to react upon unforeseen changes in the grid.

For more details regarding the content of the communication interfaces, the reader is advised to [217].

5.2 Methodology

The scheduling scheme's task is to identify periods in which a vehicle should be charged and to what level it should be charged while respecting different factors.

Some of these factors are mandatory, such as a vehicle compatible charging infrastructure. Other factors are optional, such as a low energy price. Hence, it is required to differentiate between factors that enable charging in the first place and factors which improve a charging schedule in terms of, for instance, efficiency or comfort. The following sections introduce relevant factors and how they are processed in the scheduling scheme.

5.2.1 Charging Time Identification

Assuming a user's mobility and corresponding energy demand does not exceed a vehicle's energy-storing capabilities, charging periods can be described as a subset of parking periods (dwell periods at known locations). Note that this assumption describes a scenario in which no stops need to be made purposely for charging. The subset is created under consideration of various variables.

For instance, the subset excludes parking periods at locations where no or no suitable charging infrastructure is available. Information about the presence of corresponding charging infrastructure can be obtained from different sources: The vehicle's individual parking/charging history records or any kind of information platform e.g. navigation system, online platform, etc. The quality of information could be enriched with real-time information, such as the charging station's occupation status.

In its simplest iteration, the identification of charging periods is defined by predicted parking periods at locations, at which the vehicle has been charged in the past. Figure 62 gives a simplified overview of the proposed charging periods identification scheme.

5.2.2 Scheduling Concepts

As mentioned earlier, mobility data serves as input for an EV's charging schedule. Recall that mobility can be expressed with dwell times at personal POIs and transitions between these POIs, which more specifically can be organised as a set of trips (see Section 3.2.3). To this end, the definition of mobility features, as introduced in Chapter 3 and 4 are resumed and extended. As illustrated in Figure 37, the Data

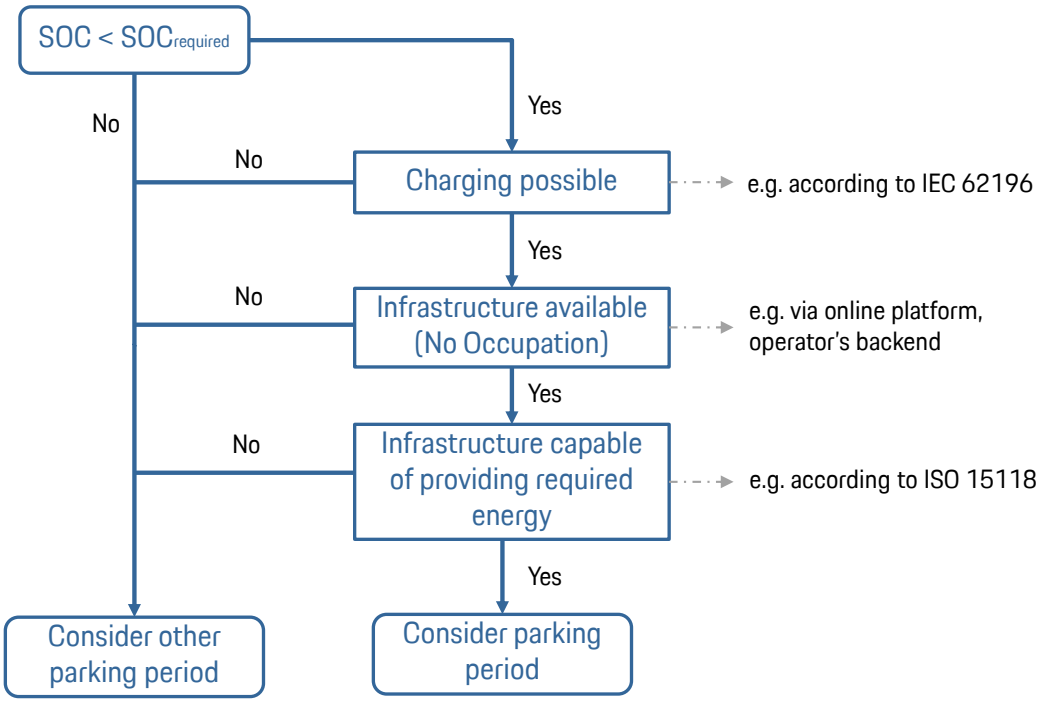

Figure 62: Charging period identification.

Collection and Processing phase is used to aggregate charging related data. These features include but are not limited to:

1. Vehicle compatible charging infrastructure
2. Available charging power
3. Infrastructure's ability to conduct smart charging (Infrastructure requirements are discussed in Subsection 5.1.4.2)

The third point is mainly concerned with soft- and hardware requirements which enable communication between infrastructure and vehicle (see Subsection 5.1.4). Charging infrastructure is characterised by different factors, for instance the "available charging power" or "occupation status". Some infrastructures, for example in the private environment, will usually offer less power than a public charging infrastructure. Also, the occupation status of a private infrastructure that is installed exclusively for one vehicle will be more reliable than the occupation's status of public charging infrastructure. Both factors should have an impact on the scheduling process of a charging event.

The assessment of variables that influence the appropriateness of charging periods suggests, that some factors should be treated as "static", e.g. the presence of charging infrastructure at known locations and some as "dynamic", e.g. the infrastructure's occupation status or the price for charging. Furthermore, the variables can be separated into two classes. One class should be considered as a binary variable, which either allows charging in the first place (see Figure 62) and variables that decrease the "attractiveness" of a charging session.

More specifically, a charging location may allow charging a vehicle based on the infrastructure, however, the predicted parking time may be too short to ensure the required energy transfer under the consideration of the available charging power. A charging event at such location would be less attractive as it would require additional charging within the prediction horizon to satisfy the mobility demand or cause user disutility [38]. The latter is a factor that is influenced by the predicted mobility behaviour rather than the charging location.

Considering the two involved parties of a smart charging event (see. Section 5.1.4), the scheduling task could be described as a process that finds the best trade-off between the interests of both parties. In this process, two variables should be considered as given: the user's mobility demand (in the form of the predicted demand) and the available charging infrastructure. The user's mobility should be considered as given as it ensures a user-centric smart charging solution.

Based on findings regarding human mobility behaviour that were presented in Chapter 3, EV dwell times would allow several *different* charging schedules. Based on this assumption, some schedules may combine the interests of involved parties better than others. To select the most appropriate charging schedule, two conditions must be satisfied:

1. All possible charging schedules must be known to the system.

2. Charging schedules must be comparable to each other.

A charging schedule can consist of multiple charging events. Hence the sum of the ratings of single charging events provides the score for an entire charging schedule.

The introduced method to identify charging periods in Section 5.2.1 can be considered as a preceding step which ensures that the predicted mobility demand can be fulfilled. After successful identification and rating of potential charging periods, the charging event can be scheduled according to "traditional" optimisation schemes (cost optimisation, peak shaving, etc.), that are described as smart charging solutions.

5.2.3 Automated Scheduling of Charging

This section describes variables that need to be considered to rate charging periods in the predicted mobility behaviour of an individual. Note that this differentiates the proposed scheduling scheme from other smart charging scheduling systems, that were presented in other research work (see Section 2.3.1).

In general, periods in which a vehicle is predicted to be parked can be considered for scheduled charging events. Given that information about the existing charging infrastructure is available, features of the installed charging infrastructure can be consulted to rate a charging event at the corresponding location. The features include but are not limited to:

- Availability of Automated wireless charging (AWC)
- The available charging power
- Availability of renewable energy
- Dynamic price information
- Preferred parking location (e.g. Home)[16]

To account for these charging parameters, the proposed scheduling scheme *rates* potential charging locations and the predicted dwell time according to location-specific charging features. Note that the rating scheme is designed generically and the listed features, such as AWC, are examples. Features that may be discovered by other research work can arbitrarily be included and assigned to a rating accordingly.

[16] A user might prefer to charge at home (the most visited location) to make use of infrastructure that has been installed specifically for the EV.

The rating of different charging infrastructure features influences the charging schedule. In the process, the scheduling task needs to respect multiple objectives. Referring to the aforementioned aspects, the scheduling task can pursue a strategy that minimises the cost of charging. Similarly, the strategy to form a charging schedule could aim to schedule charging events in a manner that maximises the comfort of an EV user. This could be achieved by planning to charge preferably at locations which offer AWC, thus making it unnecessary to plug-in the vehicle. Referring to [38], the scheduling task could also pursue the minimisation of range anxiety and create a schedule that maximises the vehicle range at any time. Different optimisation goals, however, can lead to conflicting goals. For instance, cost-optimal charging may require shorter, thus more charging events, which reduces comfort. Similarly, a cost-optimal charging schedule could require to use more of the vehicle's range, which may result in range anxiety.

5.2.4 Model Description

An "expert system" is developed that scores every predicted POI based on a defined rating system naming it POI Rating Algorithm (PRA). Exemplary ratings for predicted parking periods are illustrated in Figure 63. The concept of PRA is to schedule a charging event in periods in which the vehicle will be present at the highest rated POI. In Figure 63, for instance, the POI with a rating score of 3.9 would have been selected and the charging event would have been scheduled in the night between Monday and Tuesday. Note that for simplicity the vehicle's simulated battery capacity is 100 kWh in the following examples. A SOC of 10% corresponds to a SOE of 10 kWh.

The predicted dwell time and available charging power is used to calculate the chargeable energy and the achievable SOC at every POI. Therefore the arrival SOE at the POI is determined by the predicted schedule and the chargeable energy ($E_{chargable}$)is defined by the following equation:

$$E_{chargable} = min((dwellTime \times availablePower), \\ E_{Bat} - SOE_{arrival}). \tag{39}$$

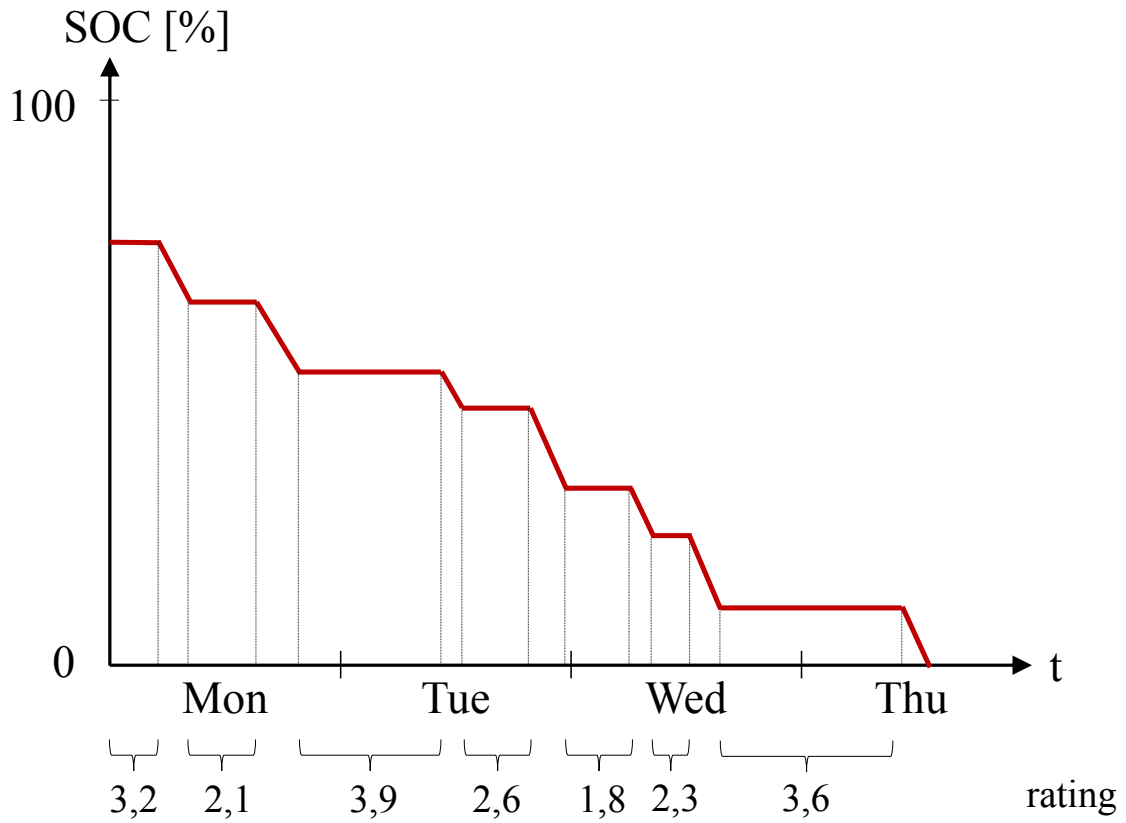

Figure 63: The course of a vehicle's predicted state of charge (SOC). The SOC stagnates when the vehicle is parked and decreases when it is on a trip. Numbers show exemplary ratings for POIs that are eligible for charging.

The scheduling scheme in this section is designed to respect a user's individual preferences. To respect a user's preferences, it is possible to convey an initial calibration for the framework. In contrast to most existing methods, this calibration is only necessary once; however, a user would be free to change it at any time. For convenience, a user could also provide a minimum SOC (minSOC), that is not undercut in the scheduling process. If no minSOC is provided, a lower threshold > 0 is applicable to ensure that the system does not allow the battery to be completely emptied. For consistency, the minSOC, by definition in percent, is replaces with minSOE in kWh.

Users may have different preferences regarding comfort and flexibility. Studies also observed a change in EV user behaviour and range awareness the more experience they gained with EVs [218] [219]. Hence, their preferences regarding charging priorities may also change over time. The system is designed to account for these differences by prioritising comfort *or* flexibility. While a charging schedule with comfort as priority aims for a minimum number of charging events, a charging

schedule with maximum flexibility aims for high SOC at any time, providing maximum range at any time. Based on this definition, comfort and flexibility oppose each other. Therefore their calibration is realised with a slider, as illustrated in Figure 64. For the scheduling task, the slider generates linear values between 1 (maximum comfort) and 0 (maximum flexibility). The slider value S_v is used to generate a flexibility SOC ($Flex_{SOC}$) with:

$$Flex_{SOC} = \frac{(E_{Bat} - minSOE) \times (1 - S_v) + minSOE}{E_{Bat}} \tag{40}$$

where E_{Bat} is the battery's capacity in kWh and $minSOE$ is the minimum required energy in kWh. To respect a user's flexibility preference, the vehicle's scheduled SOC should not fall below the flexSOC. Therefore, POIs with charging possibility are scored higher when they can be reached with a predicted SOC above the flexSOC. Note that, other than for the minSOC, the predicted SOC curve is allowed to fall below the flexSOC. However, Figure 64 illustrates higher ratings for POIs that are reached with a SOC higher than the flexSOC.

The proposed POI's rating score consists of a static and a dynamic part.

$$Rating_{POI} = Rating_{static} + Rating_{dynamic}. \tag{41}$$

A POI's static rating remains identical for as long as the charging infrastructure is not changed, for instance through a subsequent installation of an AWC system. The dynamic rating is a function of the predicted dwell time and the vehicle's SOC at arrival. However, both the static and dynamic rating outcome depends on a user's preset preferences. The static value can be understood as a representation of the POI's charging feature's *quality*. Therefore every POI is checked for the availability of AWC and PnC. Furthermore, the assignment of a POI to the most visited location is checked and rated. Charging the vehicle wirelessly can provide flexibility without compromising comfort, hence POIs with AWC infrastructure receive the highest static rating, followed by the most visited POI (MVP), given the user prefers to charge at this location, for instance at home. Both conditions are rated binary.

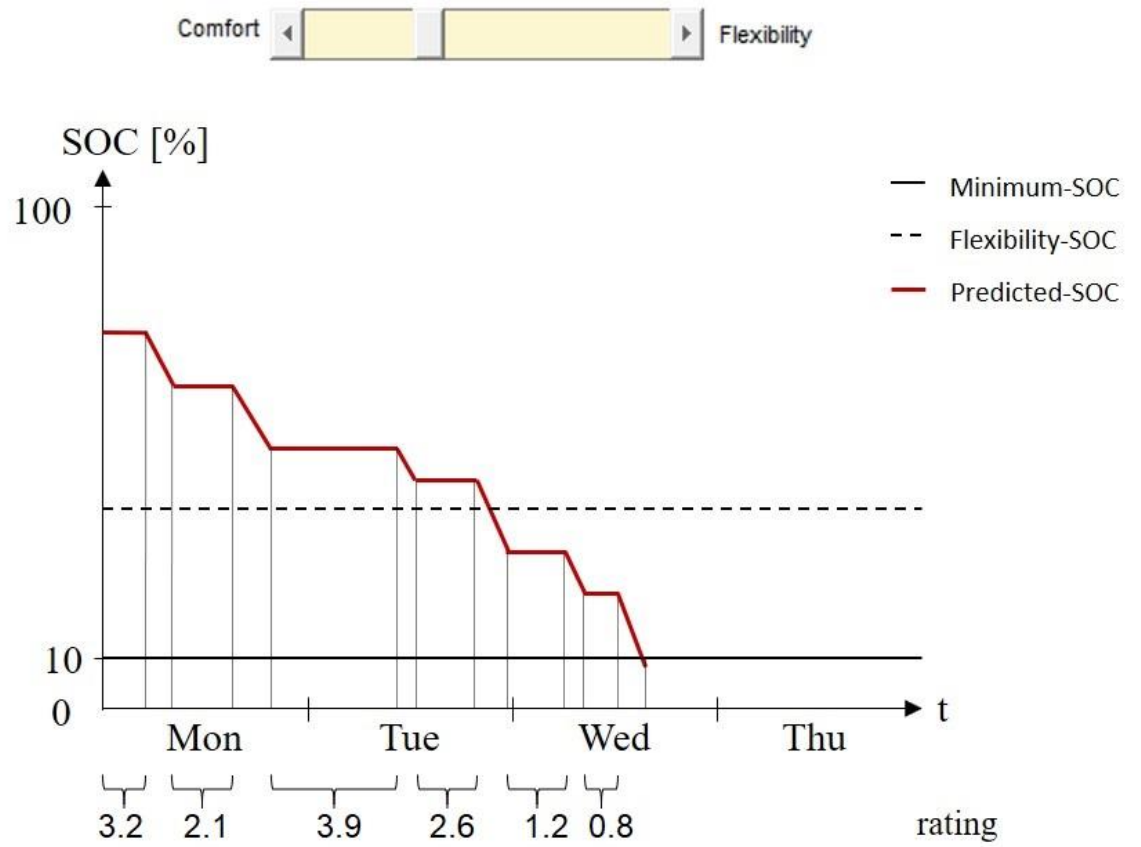

Figure 64: POI rating illustration

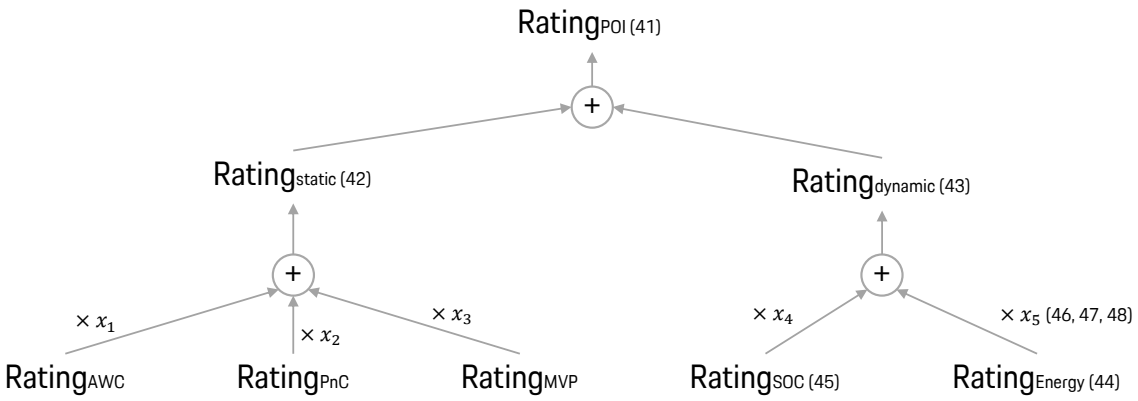

Figure 65: POI rating scheme overview. The illustrated numbers (41-48) next to the Ratings refer to the equation numbers.

$$Rating_{static} = Rating_{AWC} + Rating_{PnC} + Rating_{MVP}. \tag{42}$$

The dynamic rating evaluates a potential charging session. Hence, the vehicle's expected SOC at arrival and the available energy at the corresponding POI influence

the score.

$$Rating_{dynamic} = Rating_{SOC} + Rating_{Energy}. \tag{43}$$

The available energy ($E_{available}$) is a function of the available power and the predicted dwell time at a POI. Dwell time defines the time between predicted arrival and departure time at the reviewed POI. To rate the available energy ($Rating_{Energy}$) a linear equation (44) is chosen.

$$Rating_{energy} = \frac{E_{available}}{E_{Bat} \times (1 - \frac{minSOE}{100})}. \tag{44}$$

Note that $Rating_{Energy}$ becomes greater with the available energy. Hence, a predicted stop at a location at which more energy is available than necessary will be preferred over a location which may offer just enough energy. This is done to address uncertainties in $E_{available}$ for instance due to fluctuations in the power production. The rating of the SOC at the arrival is divided into three different sections, as displayed in Figure 66. For a SOC higher than the flexSOC a linear rating is used. By charging the EV at the flexSOC two objectives can be reached: the user's desired flexibility and a great SOC-swing. A great SOC-swing is wanted as it reduces the necessary number of charging events. Thus, an arrival SOC that equals the flexSOC achieves the highest rating. A similar effect is wanted for SOCs between the minSOC and the flexSOC. As a SOC in this area falls below a user's desired flexibility it must be rated with a significantly lower value.

The dotted interpolation line in Figure 66 is supposed to rate this area with an empirically determined rating of 0.7 at the flexSOC and a rating of 0 at 0% SOC. A drop below the flexSOC was implemented to rate SOCs below the flexSOC significantly lower then SOCs above the flexSOC. To achieve a continuous rating the following equation is chosen to rate the values between the minSOC and the flexSOC (in this illustration between 20% and 38%).

$$\begin{aligned} Rating_{SOC} = 1.31 * 10^{-7} * x^5 - 9.12 * 10^{-6} * x^4 + \\ 1.75 * 10^{-4} * x^3 + 2.25 * 10^{-5} * x^2. \end{aligned} \tag{45}$$

The equation was created by interpolating a function with six equally distributed values between the flexSOC and the minSOC. Note that this equation was chosen to get a function that is close to the interpolation line while fulfilling the requirement of being significantly below the rating factor of the flexSOC. However, any other function can be chosen that creates a similar rating for a SOC between min and flexSOC. The value 0.7 at the flexSOC is substituted by the highest possible rating. This is because it is wanted that charging events are scheduled when the battery's SOC is equal to the flexSOC. Recall that the flexSOC represents the user's charging preferences. As SOCs below the minSOC must not occur they are rated with 0. Figure 66 displays the rating for the entire SOC range [0-100]. To respect the

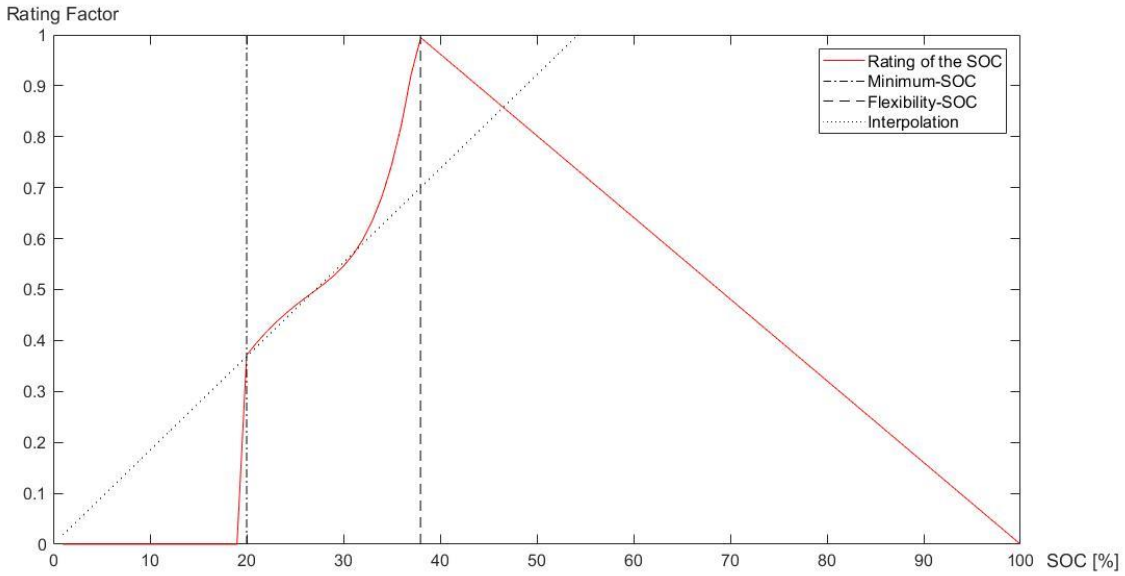

Figure 66: Key features of the arrival SOC rating at a POI: SOC smaller than the minSOC are rated with 0. SOC between the minSOC and the flexSOC is rated according to Equation (45). The highest rating factor is achieved at the flexSOC.

user's preferences, the rating of different factors have to be weighted. In Figure 65 these factors are named with x_n. Therefore the slider position shifts the maximum value that can be scored by the different factors, with respect to their weight. As AWC combines both comfort and flexibility it receives the highest score. If AWC is available at one POI in the predicted schedule, the corresponding POI receives the doubled maximum value of all dynamic factors combined to ensure that it outweighs all other factors. Furthermore, if charging at the most frequently visited POI has been prioritised, the theoretic maximum dynamic rating will be added to the most

visited POI's rating.

All influencing factors are ranked in a hierarchy that represents their weight to the scheduling part. Thereby AWC is rated twice as high as all other dynamic factors plus the availability of PnC.

$$Rating = AWC \gg MVP > (Rating_{dynamic} + PnC). \tag{46}$$

$$Rating_{SOC} = Rating_{SOC} \times (slidervalue \times 3 + 1). \tag{47}$$

$$Rating_{Energy} = Rating_{Energy} \times (slidervalue \times 2 + 1). \tag{48}$$

5.3 Simulation Experiments

To demonstrate the framework's functionality and to evaluate its performance, the scheduling scheme is tested with predicted mobility data. Real driving data, which has been introduced in Chapter 3, was used to create "predicted driving schedules". These predicted schedules consist of a user-specific sequence of predicted departure times, predicted energy demand (per trip) and predicted destinations. The corresponding charging schedules are created under the assumption of different flexible prices and with different priorities. Details about the simulation set up are given in the subsequent sections.

5.3.1 Scenarios and Experiment Conditions

The scheduling framework is tested with three different priorities on 12 different predicted mobility data profiles. As previously described, the available mobility data does not contain any information about the availability of charging infrastructure. Hence the availability of charging infrastructure at the visited locations needs to be estimated. The probabilities to find charging infrastructure at visited locations are insinuated (denoted as POI) displayed in Table 21. Note that the probability of finding a charging infrastructure in the individual's network of POIs can be considered as generic input. Values in Table 21 are estimated based on the current development and roll-out of charging infrastructure. Also, note that true charging

power availability is subject to several dynamic factors. Other power consumers can lower the charging power output in private infrastructures. Hence, the probability to have access to little charging power (3.6 kW) is assumed to be greater than high charging power (7.2 kW - 22 kW). However, the geographic area in which the corresponding user lives and travels influences power availability. To this end, Table 21 should be understood as an example only.

Note that the probability distribution in Table 21 is assigned to every individual mobility network, created by the Markov model. Charging infrastructure is only simulated *at* POIs and not "en-route" to investigate if predicted parking periods are sufficient to cover the predicted charging demand.

Table 21: Probabilities for different charging infrastructure

Probabilities	**Charging Infrastructure**
(Semi-)Public Charging POI	
50%	no charging possibility
12.5%	3.6 kW
12.5%	7.2 kW
12.5%	11 kW
12.5%	22 kW
Most frequently visited POI (25% wireless)	
62.5%	3.6 kW
12.5%	7.2 kW
12.5%	11 kW
12.5%	22 kW

To implement the possibility to schedule charging events based on minimal (average) costs, different dynamic energy prices are provided to the framework. Note that dynamic prices are used as input parameter as they are often referred to as greatest motivation to participate in smart charging. For simplification, other factors such as charging service fees are excluded from this consideration but could be

added in a real world application.

To demonstrate the impact of energy prices on the framework's scheduling results, three different price curves are implemented. Tariff 1 is based on average unit prices from 2017 on the German spot market[17]. Prices per kWh are displayed as a function of time in Figure 67.

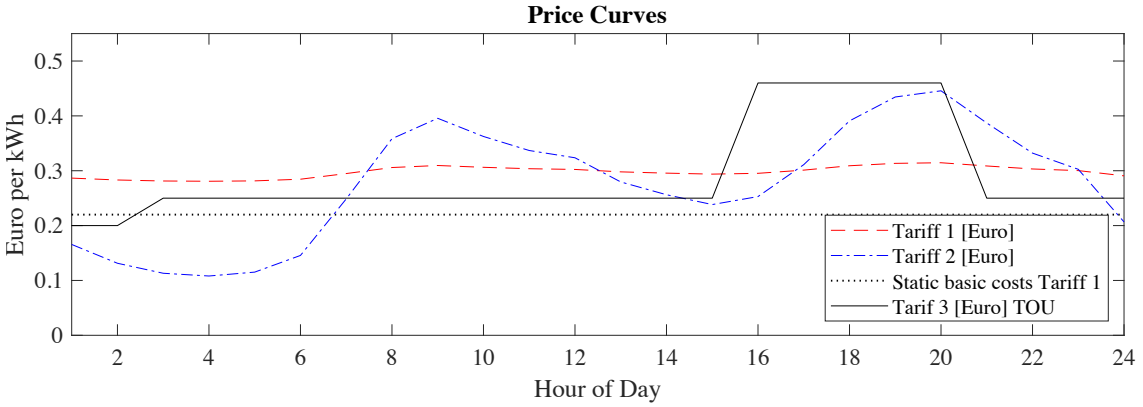

Figure 67: Tariff 1, 2 and 3 over the course of 24 hours. The single dotted line marks the fixed part of Tariff 1 (Tariff 3 has been converted from Dollar to Euro with a conversion rate of 0.86).

Note that, due to the price structure in Germany, only 20% of Tariff 1 is considered as dynamic. The average price per kWh for Tariff 1 is 0.29 Euros at the time of writing. As the German price structure is an example for little spreads in power prices, the framework is also tested with a more volatile price curve, represented as Tariff 2. The gradient of Tariff 2 is based on Tariff 1, however, the fixed basic costs are removed and the whole price per unit is considered as dynamic. Thereby the price minimum is lowered from 0.28 to 0.10 Euros, the price maximum is raised from 0.31 to 0.47 Euros, the average remains 0.29 Euros.

At last a third price curve is generated, based on a Time of Use (TOU) tariff that is currently, at the time of writing, available in California[18] specifically for EV-owners. The average price per kWh is 0.33 Dollar. The displayed curve shows the price converted to Euros per kWh on working days during summertime (June 1 - October 31). Starting with a SOC of 50%, charging is scheduled based on the

[17]https://transparency.entsoe.eu/

[18]https://www.sdge.com/residential/pricing-plans/about-our-pricing-plans/electric-vehicle-plans

corresponding predicted schedule for one week with priority on *Comfort* (Comf.), *Flexibility* (Flex.) and *Costs* (Cost).

- *Scenario 1:* Since it is considered to be most comfortable when a user must not charge more often than necessary to fulfil its mobility wishes, it is aimed to minimise the number of charging events disregarding the costs for the charging event in this scenario. Inherently, scheduling with this priority requires fewer but longer charging events. Therefore long parking duration or shorter parking duration with high charging power receive high ratings.

- *Scenario 2:* A user's flexibility is prioritised by providing the maximum range in every situation possible. The framework schedules a charging event at every location that offers the possibility of charging, disregarding the charging costs and number of plug-in events. This scenario is comparable to a situation in which a user charges every time he can due to range-anxiety.

- *Scenario 3:* Charging events are scheduled with respect of available price information, aiming for minimum average costs per kWh for the entire predicted schedule, disregarding the number of necessary charging events or location. Note that in this scenario the tariff function could be replaced by other factors, such as renewable energy availability.

5.3.2 Simulation Results

Figure 68 shows the predicted and scheduled SOC for User 3 for all of the three different optimisation goals (Scenario 1-3.) with Tariff 1. This user is chosen since all optimisation goals led to different charging schedules. The red graph shows the predicted and scheduled SOC with the framework's priority set on comfort (Scenario 1). According to the system's response, the vehicle is only scheduled to be charged once from around 25% SOC up to around 70% within the predicted time. Note that in this scenario, the flexSOC is ignored and only the adjusted minSOC (dotted line) is of relevance.

The green graph shows the SOC that is based on the same predicted schedule of User 3, however, the framework's priority was set to schedule charging events for

maximum flexibility. Therefore a charging event is scheduled for every parking event in a location that offers charging possibilities, resulting in eight charging events and a high SOC at any time. In this scenario the flexSOC is set to 100% SOC, the minSOC remains at 20% (20 kWh SOE).

The blue graph accordingly displays the predicted energy demands of User 3 but with priority set on minimal costs. It can be seen that other than in Scenario 1 and 2, charging events are scheduled into time slots in which charging is relatively cheap. In this scenario, a minimum average price per kWh is prioritised, disregarding the number of charging events but with respect of the adjusted minSOC.

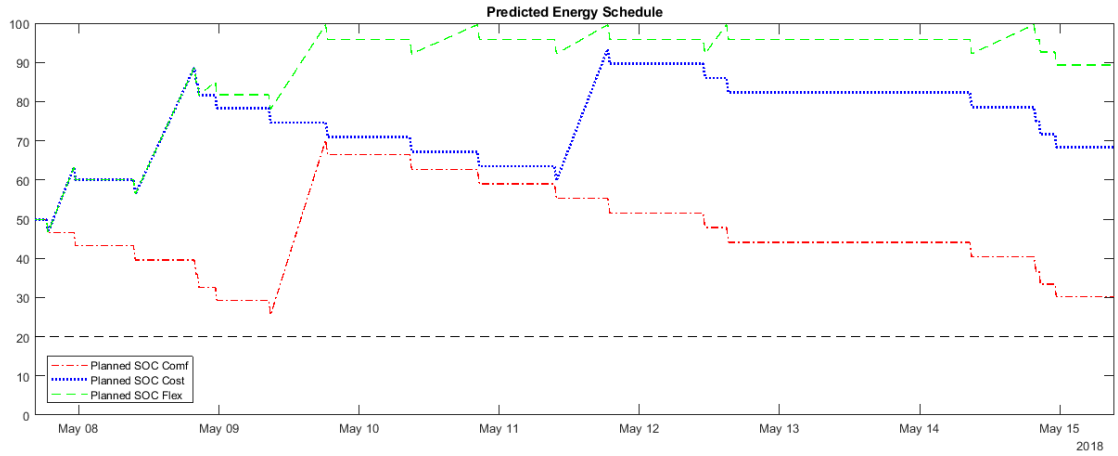

Figure 68: Comparison of scheduled SOC curves for the three scenarios.

The different curves per scenario illustrate that different optimisation goals lead to different charging schedules and may have an effect on the system's recommendations to the user. It also demonstrates that the framework can prevent, in any scenario, that the vehicle undercuts the calibrated minSOC. For simplification, the SOC curve for charging events in Figure 68 is illustrated as a linear function between the beginning and end of the parking event.

5.3.3 Performance Analysis

Different charging strategies on similar predicted travel behaviour are expected to translate to different charging schedules. Thus, a cost-related charging strategy's effectiveness should be evaluated according to the average price per unit energy that it achieved. Likewise, the effectiveness of a comfort-related charging strategy is

reflected by a minimum number of scheduled charging events. Hence, the associated number of charging events per charging strategy is also compared and evaluated.

5.3.3.1 Average Price

By comparing the total costs it must be taken into account, that the amount of charged energy differs per scenario and the price per kWh is dynamic. For a representative comparison, the *average* price per kWh per scenario is displayed to evaluate the benefit that can be created by the framework's scheduling strategy. Note that the displayed average price per kWh takes into account a system efficiency of 85% and therefore represents the price a user would have to pay for the actual stored kWh energy in the battery including losses[19]. The expected results for the order of charging strategies regarding the average price per kWh is Cost $<$ Flex. $\leqslant$ Comf.

- Tariff 1: The results show that, given the German price structure with little price dynamics, the achievable benefit per kWh is marginal. Only two out of 12 users achieve a positive price difference for the average kWh of 0.01 Euros compared to both other scheduling strategies. For six users, there is a price benefit compared to one other scheduling strategy, however, the average price difference is 0.01 Euro only. With an average energy demand of 0.22 Wh/km and a yearly driven distance of 15,000 km, this would result in a difference of 33 Euros per year (0.22 Wh/km * 15000 km * 0.01 Euro/Wh).

- Tariff 2: Compared with Tariff 1, Tariff 2 offers a higher price spread between energy price maximum and minimum. As a result, the framework can create a relevant price benefit for five out of 12 users. Note that for four further users the framework achieves a price advantage compared to one other scheduling strategy.

- Tariff 3: Apart from offering a greater price spread than Tariff 1, Tariff 3 creates a price benefit for two out of twelve users as well. Similarly for six out of the remaining ten, the framework achieves a price benefit compared to one other scheduling strategy. However, the price difference between the cheapest

[19] Typical value for EV charging systems including battery efficiency.

and the most expensive scheduling strategy per user is 0.02 Euro per kWh on average.

5.3.3.2 Number of charging events

The expected result for the number of charging events is Comf. $\leqslant$ Cost $<$ Flex.

- Tariff 1: The results show that the target of reducing the number of charging events for the first scenario can always be achieved. For seven users the framework was able to create a charging schedule that required fewer charging events than the other charging strategies would have required. For four users the most comfortable charging strategy resulted in an equal number of charging events as the most cost-efficient strategy. User 5 is an exception as the predicted SOC would not have dropped below the minSOC within the predicted time, which is why the framework did not schedule a charging event for the entire week.

- Tariff 2: For the number of required charging events the framework achieved similar results for Tariff 2 and Tariff 1 as the gradient of Tariff 1 and 2 is identical.

- Tariff 3: With the less dynamic Tariff 3 the framework was able to create a benefit for even more users than with Tariff 1. Eight users would have benefited from a comfort-oriented charging strategy, for three users the number of scheduled charging events with priority on comfort would be equal as for a priority set on costs.

5.4 Discussion

In contrast to most existing work, the scheduling scheme was tested with real driving data, which allows gaining practical results. By using travel behaviour that has been captured with ICEV it has been demonstrated that all users would not have been compromised by an EV, given that there is a charging possibility in at least one location that is frequently visited by the user. Relating to the probability

distribution of charging infrastructure in Table 21, the predicted parking periods would have been sufficient to cover the charging demand, even if it is assumed that 50% of (predicted) POIs would not offer any charging possibility and 62.5% of the individual MVP offers 3.6 kW charging power only.

The different results for Tariff 1, 2 and 3 emphasise that the user-benefit of smart charging solutions is directly connected to the available price structure. The results show that the automated smart charging framework can schedule charging events for all users, in all scenarios and with all tariffs. With Tariff 1, the maximum difference in average price per kWh between different optimisation strategies is 0.01 Euros. This is a relevant finding as it emphasises that, assuming a required infrastructure is in place, smart charging offers very little monetary benefit for an EV-user when the tariff's price spread is small and hence should not be considered as the only reasonable motivation to participate in smart charging. In reverse, a greater price spread can create relevant benefits. The higher price spread for Tariff 2 led to differences of up to 0.13 Euros per kWh between different charging scenarios.

Tariff 3 is the only tariff in this simulation that is available for EV-users. However, the difference between an "expensive" and a "cheap" charging schedule with Tariff 3 is only marginal. Only two users benefited from a charging schedule that prioritises low average costs per kWh. With this specific TOU tariff, the energy supplier may create a motivation to influence a user towards a grid friendly load generation. Users, however, would only benefit marginally from the offered tariff, given the recorded travel behaviour.

The little monetary advantage that can be created confirms the initial statement that the existing price structures are not adequate to justify a user's effort to participate in smart charging, even with an automated framework. Given a user has to analyse power price forecasts and provide all necessary smart charging information manually, the benefit may become even smaller.

Based on real-world mobility data (see Section 3) it is known that vehicles are only used for a small fraction of time per day. The remaining time during the day can be used to shift charging of EVs according to different charging strategies, given

a suitable charging infrastructure is available.

Mobility can be broken down into a binary variable that indicates predicted periods in which a vehicle can be charged or not. Furthermore, predicted mobility creates a time-dependant energy demand which serves as input for a charging schedule. A charging schedule can be created with respect to different charging strategies, which may pursue various goals, such as low charging costs, little grid impact, high renewable energy proportion, etc.

The provision of individual charging schedules contributes to an advanced smart charging concept. Based on the expected energy demand and time of load, the grid operator and utilities can prepare the grid for the corresponding charging event. Although the load of a single charging EV creates a rather insignificant impact on a grid, the aggregation of multiple charging schedules could be used as an efficient tool for the mitigation of congestion and utilisation of renewable energy.

5.5 Conclusion

Based on the identified input parameters, this chapter introduced an expert system, which is designed to create charging schedules based on *rated* potential charging periods. The chapter has discussed and identified different generic inputs that can be consulted to schedule charging with respect to an individual's mobility and existing charging infrastructure. A charging schedule is created by scheduling charging events which achieved the highest ratings. The rating mechanism is designed to be biased towards a user's preferences. If a user prefers to charge with minimal costs, the system will rate charging periods with low costs higher than others.

Besides the framework's functionality to prioritise a user's mobility demand, it is designed to combine different interests. A grid operator can forward his interests in the form of a price signal via flexible tariffs. A user's predicted mobility serves as a basis for the scheduling task and ensures that the user's interests are taken into account.

The framework's functionality is demonstrated with a combination of real-world data and generic variables. Generic inputs, such as the probability distribution

of charging infrastructure in an individual's network of POI's allows the network to be applicable in different geographic regions, which may offer different coverage regarding the charging infrastructure.

The PRA is designed to process generic mobility data to ensure that it could be used in conjunction with other prediction methods. Predicted charging schedules can be utilised for different purposes, such as providing charging guidance or recommendations to the EV user. Another benefit is created when a charging schedule is communicated to the charging infrastructure that is capable of smart charging. Finally, the individually predicted charging and energy demand could also serve utilities to organise their resources efficiently and early in advance.

Chapter 6: Conclusions and Future Work

EVs have the potential to play an essential role in the decarbonisation of the transportation sector. The technology that is used for EV charging is a key element that influences their impact on the environment for multiple reasons. Electric mobility is only sustainable if renewable energy is used for charging EVs. A second aspect is the potentially harmful impact that charging vehicles can create on the existing electric power grids.

Both aspects are being addressed with the concept of smart charging. Smart charging concepts apply different strategies to mitigate stress on power grids and aim to shift charging events into periods of cheap and/or excessive renewable power production. A shortcoming of existing smart charging solutions is their dependency on user involvement. Regardless of the smart charging strategy on hand, basic information about the required energy and the time at which the EV will be driven are mandatory to ensure that the vehicle can fulfil its original purpose: providing mobility to its user.

The effectiveness of smart charging solutions can be facilitated by designing them seamless and attractive to use. A high priority must be set on the indemnification of a user's mobility, since the creation of smart charging related disutility contradicts the purpose of an EV.

6.1 Summary and Conclusions

This thesis explores the possibilities to advance existing smart charging schemes. The focus is set on a solution that combines the interests of all parties that are involved in a smart charging process.

An EV's charging demand is a function of the EV user's mobility demand. To this end, real-world mobility data is collected, reviewed and analysed. The representativeness of the collected data is ensured by a comparison of key indicators with other mobility data sets. The collected mobility data is used to investigate typical and atypical travel patterns and sets the groundwork for the subsequent design of

an enhanced mobility prediction mechanism. Furthermore, the collected mobility data set is used to simulated EV energy demand with the help of a vehicle dynamic model.

The analysis of mobility data is also used to answer the research question: What characterises human travel behaviour and are these characteristics eligible to make useful assumptions about smart charging parameters? The characterisation of human mobility shows that the majority of human travel behaviour, more specifically repetitive and long dwell times at relevant locations, create sufficient flexibility regarding potential charging times. Smart charging can be shifted towards a more user-centric approach by utilising this flexibility. However, this can be accomplished without a user's involvement. With an advanced smart charging framework an EV user is not required to hand over charging parameters such as departure times or required energy. This task can be eliminated when a smart charging framework has access to an EV- and user-specific travel history to anticipate future mobility and corresponding energy demand.

Human mobility is characterised by transitions between regular visited locations and location characteristic dwell time. The second part of the framework picks up identified travel characteristics and introduces a combination of location-dependent and location-independent mobility prediction methods. A combination of LD and LI prediction methods is implemented to benefit from the individually better performing scheme on the characteristics of individual travel patterns. Further, the introduced prediction scheme is designed to be independent of weekly periodicity in travel behaviour and to provide a holistic spatio-temporal mobility prediction, consisting of departure time, route information and arrival time. To be independent from weekly periodicity, an ANN is explored to predict the sequence of characteristic travel patterns. The framework's independence from week cycles improved the prediction accuracy for 60% of the investigated data profiles by 13.9% on average. The prediction scheme provides a detailed "predicted mobility schedule", which allows deducing a location and time-dependant EV energy demand.

A predicted driving schedule provides the basis for the third part of the intro-

duced smart charging framework. Predicted parking time and parking locations in conjunction with a time-dependant energy demand are used to identify sensible charging periods. The introduced scheduling scheme rates potential parking periods and follows a generic design, adaptable to personal preferences or new scientific findings and methods. The analysis of the rating scheme in conjunction with the mobility prediction data is used to illustrate relevant findings. First, vehicle-related travel behaviour is eligible for smart charging and, as demonstrated with the available data set, offers sufficient flexibility for shifting charging into different periods of the day. With its features, the scheduling scheme takes into account the uncertainty that is associated with human mobility prediction. In rare occasions, in which individuals deviate from regular hence predictable mobility behaviour, the scheduling scheme adapts quickly by recalculating the charging schedule every time the vehicle stops at a location.

Another finding is that available tariffs, even if they forward the stock market prices for electric energy to the end-user, do barely justify the application of smart charging strategies. This finding implies necessary changes to energy tariff structures to create a convincing smart charging benefit.

The scheduling scheme successfully scheduled charging events in periods of cheap power production while respecting a user's predicted mobility demand. The introduced smart charging scheme can also pursue a strategy that minimises the number of necessary charging events. For all tested mobility profiles, the framework reduces the number of scheduled charging events compared with an opportunistic charging plan. In average, the number of charging events was reduced by 67%.

The introduction of the scheduling scheme answers the fourth research question: What characterises a scheduling scheme that combines individual predicted mobility, predicted energy demand, and charging infrastructure features to a smart "charging schedule"? It eliminates the necessity of handing over charging preferences manually, which is necessary for existing smart charging schemes to apply smart charging strategies.

A strength of the introduced framework is its compatibility with existing smart

charging proposals. Other works, which introduced different methods for shifting EV charging concerning dynamic prices or renewable energy generation, will apply to the introduced framework. However, both a user as well as grid operators would benefit from an automatic provision of charging requirements. This is because individual EV charging requirements could not only be provided for every single parking event but also early in advance, as a predicted schedule contains energy-related information for several days in advance. While EV-users are liberated from manual charging calibration, utilities could aggregate power demands from a fleet of EVs to organise their resources efficiently or create dynamic power prices, based on the expected grid load.

6.2 Limitations

The framework's effectiveness is limited by several factors. The impact of a single charging EV is usually too small to create threat to a power grid, nor will smart charging of a single vehicle make a significant impact to the utilisation of renewable energy. To this end, a sufficient number of predicted schedules and detailed forecasts about power availability for a specific region are required to create measurable positive impacts.

Furthermore, the introduced smart charging scheme is designed to be robust against a great variation in travel patterns, which includes typical and atypical travel behaviours. However, as demonstrated in several research projects [151] [165], mathematical limits regarding the predictability of human travel behaviour exist. These limits as well as unpredictable mobility behaviour may affect the generation of a sensible charging schedule, which may limit the framework's applicability to predictable user groups.

The simulation results regarding the achievable monetary benefits imply necessary changes in power price policies. A greater variance in dynamic power prices increases the effectiveness of smart charging solution and the implementation of a smart charging framework. At the time of writing, barely any available flexible tariff provided a sufficient motivation to participate in smart charging. This is even more

relevant when the costs for the required communication and smart charging infrastructure are considered. Without sufficient monetary incentives, the motivation to use a smart charging framework is limited to environmental awareness and potential comfort gains.

6.3 Future Work

During the writing of this thesis, the EV market has experienced significant growth. With more EVs on the market, new insights and findings regarding technology and user experience were made available.

In the course of this research, the influence of charging behaviour and battery wear became significantly more relevant. Studies regarding charging behaviour implied that the opportunistic charging behaviour of many EV users leads to greater battery wear than originally expected [220]. Using the introduced smart charging framework as a basis, this effect could be part of future investigations.

Furthermore, this thesis was intentionally set to prioritise a user's mobility in the design of the charging scheduling mechanism. EVs, however, could also be utilised as energy storage, which could feed back to power grids in times of low energy generation. This process is referred to as bi-directional charging. Bi-directional charging requires specific infrastructure and is regulated by national laws but could be investigated as part of future iterations of this smart charging framework.

EV charging offers further potential for improvement. With "smart charging hardware", the introduced smart charging framework could help to establish a physical connection between vehicle and infrastructure. Automated hardware in conjunction with individually scheduled charging events would make any user involvement redundant for charging events.

Further potential for EV sharing concepts is given by the possibility to connect individuals who share similar mobility demand. A centralised system that combines individual travel patterns, humans with complementing mobility demands could be motivated to share EV and charging infrastructure. The promotion of ride-sharing concepts could contribute to a reduction in the number of required vehicles.

A subject for further research is the secure operation of a smart charging framework. As has been discussed and demonstrated, EV user mobility prediction requires sensitive user data. A system that reveals or predicts a home owner's absence, for instance, must be operated securely.

References

[1] Y. Zhou, M. Wang, H. Hao, L. Johnson, and H. Wang, "Plug-in electric vehicle market penetration and incentives: a global review," *Mitigation and Adaptation Strategies for Global Change*, vol. 20, no. 5, pp. 777–795, 2015.

[2] "Global emissions," Jan 2018. [Online]. Available: https://www.c2es.org/content/international-emissions/

[3] R. Graham *et al.*, "Comparing the benefits and impacts of hybrid electric vehicle options," *Electric Power Research Institute (EPRI), Palo Alto, CA, Report*, vol. 1000349, 2001.

[4] J. McLaren, J. Miller, E. O'Shaughnessy, E. Wood, and E. Shapiro, "Emissions associated with electric vehicle charging: Impact of electricity generation mix, charging infrastructure availability, and vehicle type," National Renewable Energy Lab.(NREL), Golden, CO (United States), Tech. Rep., 2016.

[5] P. Wellbrock, M. Fette, J. Gabriel, and K. Janßen, "Bewertung der co2-emissionen von elektrofahrzeugen–stand der wissenschaftlichen debatte," *Techn. Ber., Bremer Energie Institut*, 2011.

[6] C. Thiel, J. Schmidt, A. Van Zyl, and E. Schmid, "Cost and well-to-wheel implications of the vehicle fleet co2 emission regulation in the european union," *Transportation Research Part A: policy and practice*, vol. 63, pp. 25–42, 2014.

[7] O. Van Vliet, A. S. Brouwer, T. Kuramochi, M. van Den Broek, and A. Faaij, "Energy use, cost and co2 emissions of electric cars," *Journal of power sources*, vol. 196, no. 4, pp. 2298–2310, 2011.

[8] L. C. Casals, E. Martinez-Laserna, B. A. García, and N. Nieto, "Sustainability analysis of the electric vehicle use in europe for co2 emissions reduction," *Journal of Cleaner Production*, vol. 127, pp. 425–437, 2016.

[9] W. J. Smith, "Can ev (electric vehicles) address ireland's co2 emissions from transport?" *Energy*, vol. 35, no. 12, pp. 4514–4521, 2010.

[10] E. Hahne, *Technische Thermodynamik: Einführung und Anwendung.* Oldenbourg Verlag, 2011.

[11] J. Dickert and P. Schegner, "Residential load models for network planning purposes," in *2010 Modern Electric Power Systems.* IEEE, 2010, pp. 1–6.

[12] S. W. Edison and G. L. Geissler, "Measuring attitudes towards general technology: Antecedents, hypotheses and scale development," *Journal of targeting, Measurement and Analysis for Marketing*, vol. 12, no. 2, pp. 137–156, 2003.

[13] M. Modahl, *Now or never: How companies must change today to win the battle for internet consumers.* HarperCollins Publishers, 1999.

[14] O. Egbue and S. Long, "Barriers to widespread adoption of electric vehicles: An analysis of consumer attitudes and perceptions," *Energy policy*, vol. 48, pp. 717–729, 2012.

[15] B. K. Sovacool and R. F. Hirsh, "Beyond batteries: An examination of the benefits and barriers to plug-in hybrid electric vehicles (phevs) and a vehicle-to-grid (v2g) transition," *Energy Policy*, vol. 37, no. 3, pp. 1095–1103, 2009.

[16] D. Dallinger, *Plug-in electric vehicles integrating fluctuating renewable electricity.* kassel university press GmbH, 2013, vol. 20.

[17] M. Duvall *et al.*, "Comparing the benefits and impacts of hybrid electric vehicle options for compact sedan and sport utility vehicles," *Final Report*, vol. 1006892, 2002.

[18] G. Nischler, C. Gutschi, M. Beermann, and H. Stigler, "Auswirkungen von elektromobilität auf das energiesystem," *e & i Elektrotechnik und Informationstechnik*, vol. 128, no. 1-2, pp. 53–57, 2011.

[19] R. Kasper and M. Schünemann, "Elektrische fahrantriebe topologien und wirkungsgrad," *MTZ-Motortechnische Zeitschrift*, vol. 73, no. 10, pp. 802–807, 2012.

[20] "Worldwide number of electric cars 2018." [Online]. Available: https://www.statista.com/statistics/270603/worldwide-number-of-hybrid-and-electric-vehicles-since-2009/

[21] M. Lackner, F. Winter, and B. Geringer, "Chemie im motor: Verbrennungsmotoren versus brennstoffzelle und elektromotor," *Chemie in unserer Zeit*, vol. 39, no. 4, pp. 246–254, 2005.

[22] A. Pina, P. Baptista, C. Silva, and P. Ferrão, "Energy reduction potential from the shift to electric vehicles: The flores island case study," *Energy Policy*, vol. 67, pp. 37–47, 2014.

[23] C. Holman, R. Harrison, and X. Querol, "Review of the efficacy of low emission zones to improve urban air quality in european cities," *Atmospheric Environment*, vol. 111, pp. 161–169, 2015.

[24] A. D'Avignon, F. A. Carloni, E. L. La Rovere, and C. B. S. Dubeux, "Emission inventory: An urban public policy instrument and benchmark," *Energy Policy*, vol. 38, no. 9, pp. 4838–4847, 2010.

[25] W. Sierzchula, S. Bakker, K. Maat, and B. Van Wee, "The influence of financial incentives and other socio-economic factors on electric vehicle adoption," *Energy Policy*, vol. 68, pp. 183–194, 2014.

[26] M. A. Tamor, P. E. Moraal, B. Reprogle, and M. Milačić, "Rapid estimation of electric vehicle acceptance using a general description of driving patterns," *Transportation Research Part C: Emerging Technologies*, vol. 51, pp. 136–148, 2015.

[27] P. Hertzke, N. Müller, and S. Schenk, "The global electric-vehicle market is amped up and on the rise," *McKinsey, May*, 2018.

[28] U. Köhler, "Aufbau von lithium-ionen-batteriesystemen," in *Handbuch Lithium-Ionen-Batterien*. Springer, 2013, pp. 95–106.

[29] M. Yilmaz and P. T. Krein, "Review of battery charger topologies, charging power levels, and infrastructure for plug-in electric and hybrid vehicles," *IEEE transactions on Power Electronics*, vol. 28, no. 5, pp. 2151–2169, 2013.

[30] S. Sen, L. Zhang, T. Chen, J. Zhang, and A. Q. Huang, "Three-phase medium voltage dc fast charger based on single-stage soft-switching topology," in *2018 IEEE Transportation Electrification Conference and Expo (ITEC)*. IEEE, 2018, pp. 1123–1128.

[31] D. Dujic, "Electric vehicles charging-an ultrafast overview," in *KEYNOTE at PCIM Asia 2019; International Exhibition and Conference for Power Electronics, Intelligent Motion, Renewable Energy and Energy Management*, no. POST_TALK, 2019.

[32] M. Murnane and A. Ghazel, "A closer look at state of charge (soc) and state of health (soh) estimation techniques for batteries," *Internet: http://www. analog. co m/media/en/technical-documentation/technical-articles/A-Closer-Look-at-State-Of-Charge-and-State-Health-Estimation-Techniques-.... pdf*, 2017.

[33] S. Pang, J. Farrell, J. Du, and M. Barth, "Battery state-of-charge estimation," in *Proceedings of the 2001 American control conference.(Cat. No. 01CH37148)*, vol. 2. IEEE, 2001, pp. 1644–1649.

[34] E. Karden, S. Ploumen, B. Fricke, T. Miller, and K. Snyder, "Energy storage devices for future hybrid electric vehicles," *Journal of Power Sources*, vol. 168, no. 1, pp. 2–11, 2007.

[35] A. Khaligh and Z. Li, "Battery, ultracapacitor, fuel cell, and hybrid energy storage systems for electric, hybrid electric, fuel cell, and plug-in hybrid electric vehicles: State of the art," *IEEE transactions on Vehicular Technology*, vol. 59, no. 6, pp. 2806–2814, 2010.

[36] O. Sundström and C. Binding, "Optimization methods to plan the charging of electric vehicle fleets," in *Proceedings of the international conference on control, communication and power engineering*. Citeseer, 2010, pp. 28–29.

[37] H. He, Y. Zhang, R. Xiong, and C. Wang, "A novel gaussian model based battery state estimation approach: State-of-energy," *Applied energy*, vol. 151, pp. 41–48, 2015.

[38] N. Daina, A. Sivakumar, and J. W. Polak, "Electric vehicle charging choices: Modelling and implications for smart charging services," *Transportation Research Part C: Emerging Technologies*, vol. 81, pp. 36–56, 2017.

[39] F. L. Mapelli, D. Tarsitano, and M. Mauri, "Plug-in hybrid electric vehicle: Modeling, prototype realization, and inverter losses reduction analysis," *IEEE Transactions on Industrial electronics*, vol. 57, no. 2, pp. 598–607, 2009.

[40] C. Botsford and A. Szczepanek, "Fast charging vs. slow charging: Pros and cons for the new age of electric vehicles," in *International Battery Hybrid Fuel Cell Electric Vehicle Symposium*, 2009.

[41] S. Haghbin, K. Khan, S. Lundmark, M. Alaküla, O. Carlson, M. Leksell, and O. Wallmark, "Integrated chargers for ev's and phev's: examples and new solutions," in *The XIX International Conference on Electrical Machines-ICEM 2010*. IEEE, 2010, pp. 1–6.

[42] N. Sakr, D. Sadarnac, and A. Gascher, "A review of on-board integrated chargers for electric vehicles," in *2014 16th European Conference on Power Electronics and Applications*. IEEE, 2014, pp. 1–10.

[43] W. Tober and H. Lenz, *Praxisbericht Elektromobilität und Verbrennungsmotor*. Springer, 2016.

[44] G. A. Pagani and M. Aiello, "The power grid as a complex network: a survey," *Physica A: Statistical Mechanics and its Applications*, vol. 392, no. 11, pp. 2688–2700, 2013.

[45] O. Veneri, L. Ferraro, C. Capasso, and D. Iannuzzi, "Charging infrastructures for ev: Overview of technologies and issues," in *2012 Electrical Systems for Aircraft, Railway and Ship Propulsion*. IEEE, 2012, pp. 1–6.

[46] T. Franke and J. F. Krems, "Understanding charging behaviour of electric vehicle users," *Transportation Research Part F: Traffic Psychology and Behaviour*, vol. 21, pp. 75–89, 2013.

[47] J. Bailey and J. Axsen, "Anticipating pev buyers' acceptance of utility controlled charging," *Transportation Research Part A: Policy and Practice*, vol. 82, pp. 29–46, 2015.

[48] M. Neaimeh, G. Hill, P. Blythe, R. Wardle, J. Yi, and P. Taylor, "Integrating smart meter and electric vehicle charging data to predict distribution network impacts," in *IEEE PES ISGT Europe 2013*. IEEE, 2013, pp. 1–5.

[49] G. Pasaoglu, D. Fiorello, A. Martino, G. Scarcella, A. Alemanno, A. Zubaryeva, and C. Thiel, "Driving and parking patterns of european car drivers-a mobility survey," *Luxembourg: European Commission Joint Research Centre*, 2012.

[50] N. Daina, "Modelling electric vehicle use and charging behaviour," Ph.D. dissertation, Imperial College London, 2014.

[51] S. Á. Funke, T. Gnann, and P. Plötz, "Addressing the different needs for charging infrastructure: An analysis of some criteria for charging infrastructure set-up," in *E-Mobility in Europe*. Springer, 2015, pp. 73–90.

[52] B. Kang and G. Ceder, "Battery materials for ultrafast charging and discharging," *Nature*, vol. 458, no. 7235, p. 190, 2009.

[53] E. Herder and P. Siehndel, "Daily and weekly patterns in human mobility." in *UMAP Workshops*. Citeseer, 2012.

[54] A. Di Giorgio and F. Liberati, "A model predictive control-based approach for plug-in electric vehicles charging: Power tracking, renewable energy sources

integration and driver preferences satisfaction," in *Plug In Electric Vehicles in Smart Grids*. Springer, 2015, pp. 203–240.

[55] H. Han, H. Xu, Z. Yuan, and Y. Zhao, "Interactive charging strategy of electric vehicles connected in smart grids," in *Proceedings of The 7th International Power Electronics and Motion Control Conference*, vol. 3. IEEE, 2012, pp. 2099–2103.

[56] M. Agsten, "Einfluss gesteuerten ladens von elektrofahrzeugen auf die netzbetriebsführung bei volatiler windeinspeisung," *Dissertation*, 2011.

[57] M. F. Shaaban, M. Ismail, E. F. El-Saadany, and W. Zhuang, "Real-time pev charging/discharging coordination in smart distribution systems," *IEEE Transactions on Smart Grid*, vol. 5, no. 4, pp. 1797–1807, 2014.

[58] Z. Xu, Z. Hu, Y. Song, Z. Luo, K. Zhan, and J. Wu, "Coordinated charging strategy for pevs charging stations," in *2012 IEEE Power and Energy Society General Meeting*. IEEE, 2012, pp. 1–8.

[59] D. Steen, O. Carlson, L. Bertling *et al.*, "Assessment of electric vehicle charging scenarios based on demographical data," *IEEE Transactions on Smart Grid*, vol. 3, no. 3, pp. 1457–1468, 2012.

[60] N. Zimmerman and R. Bass, "Impacts of electric vehicle charging on electric power distribution systems," Ph.D. dissertation, Portland State University, Portland, 09.2013.

[61] K. Clement-Nyns, E. Haesen, and J. Driesen, "The impact of charging plug-in hybrid electric vehicles on a residential distribution grid," *IEEE Transactions on power systems*, vol. 25, no. 1, pp. 371–380, 2009.

[62] C. Ma, J. Rautiainen, D. Dahlhaus, A. Lakshman, J.-C. Toebermann, and M. Braun, "Online optimal charging strategy for electric vehicles," *Energy Procedia*, vol. 73, pp. 173–181, 2015.

[63] Z. Jiang, H. Tian, M. J. Beshir, S. Vohra, and A. Mazloomzadeh, "Analysis of electric vehicle charging impact on the electric power grid," City of Los Angeles Department, Tech. Rep., 2016.

[64] L. Zhou, F. Li, C. Gu, Z. Hu, and S. Le Blond, "Cost/benefit assessment of a smart distribution system with intelligent electric vehicle charging," *IEEE Transactions on Smart Grid*, vol. 5, no. 2, pp. 839–847, 2013.

[65] C. Leitinger and M. Litzlbauer, "Grid integration and charging strategies for e-mobility," *Elektrotechnik & Informationstechnik*, 2011.

[66] DoE, US, "Evaluating electric vehicle charging impacts and customer charging behaviors-experience from six smart grid investment grant projects, office of electricity delivery and energy reliability, us department of energy," 2014.

[67] L. Pinter and C. Farkas, "Impacts of electric vehicle chargers on the power grid," in *2015 5th International Youth Conference on Energy (IYCE)*. IEEE, 2015, pp. 1–6.

[68] R. V. Solé, M. Rosas-Casals, B. Corominas-Murtra, and S. Valverde, "Robustness of the european power grids under intentional attack," *Physical Review E*, vol. 77, no. 2, p. 026102, 2008.

[69] S. Meier, S. Norrga, and H.-P. Nee, "New voltage source converter topology for hvdc grid connection of offshore wind farms," *Citeseer*, 2004.

[70] M. Braun, T. Stetz, R. Bründlinger, C. Mayr, K. Ogimoto, H. Hatta, H. Kobayashi, B. Kroposki, B. Mather, M. Coddington *et al.*, "Is the distribution grid ready to accept large-scale photovoltaic deployment? state of the art, progress, and future prospects," *Progress in photovoltaics: Research and applications*, vol. 20, no. 6, pp. 681–697, 2012.

[71] A. B. Pedersen, A. Aabrandt, J. Ostergaard, and B. Poulsen, "Generating geospatially realistic driving patterns derived from clustering analysis of real ev driving data," in *Innovative Smart Grid Technologies-Asia (ISGT Asia), 2014 IEEE*. IEEE, 2014, pp. 686–691.

[72] J. Taylor, A. Maitra, M. Alexander, D. Brooks, and M. Duvall, "Evaluations of plug-in electric vehicle distribution system impacts," in *IEEE PES General Meeting*. IEEE, 2010, pp. 1–6.

[73] G. Graditi, M. L. Di Silvestre, R. Gallea, and E. R. Sanseverino, "Heuristic-based shiftable loads optimal management in smart micro-grids," *IEEE Transactions on Industrial Informatics*, vol. 11, no. 1, pp. 271–280, 2014.

[74] J. A. Jardini, C. M. Tahan, M. Gouvea, S. U. Ahn, and F. Figueiredo, "Daily load profiles for residential, commercial and industrial low voltage consumers," *IEEE Transactions on Power Delivery*, vol. 15, no. 1, pp. 375–380, 2000.

[75] J. V. Paatero and P. D. Lund, "A model for generating household electricity load profiles," *International Journal of Energy Research*, vol. 30, no. 5, pp. 273–290, 2006.

[76] C. Fünfgeld and R. Tiedemann, *Anwendung der repräsentativen VDEW-Lastprofile: step-by-step*. VDEW, 2000.

[77] J. A. P. Lopes, F. J. Soares, and P. M. R. Almeida, "Integration of electric vehicles in the electric power system," *Proceedings of the IEEE*, vol. 99, no. 1, pp. 168–183, 2011.

[78] P. Grahn, J. Munkhammar, J. Widén, K. Alvehag, and L. Söder, "Phev home-charging model based on residential activity patterns," *IEEE Transactions on power Systems*, vol. 28, no. 3, pp. 2507–2515, 2013.

[79] L. Zhao, S. Prousch, M. Hübner, and A. Moser, "Simulation methods for assessing electric vehicle impact on distribution grids," in *IEEE PES T&D 2010*. IEEE, 2010, pp. 1–7.

[80] K. Clement-Nyns, E. Haesen, and J. Driesen, "The impact of charging plug-in hybrid electric vehicles on a residential distribution grid," *IEEE Transactions on power systems*, vol. 25, no. 1, pp. 371–380, 2010.

[81] E. Sortomme, M. M. Hindi, S. J. MacPherson, and S. Venkata, "Coordinated charging of plug-in hybrid electric vehicles to minimize distribution system losses," *IEEE transactions on smart grid*, vol. 2, no. 1, pp. 198–205, 2011.

[82] L. Kelly, A. Rowe, and P. Wild, "Analyzing the impacts of plug-in electric vehicles on distribution networks in british columbia," in *2009 IEEE Electrical Power & Energy Conference (EPEC)*. IEEE, 2009, pp. 1–6.

[83] E. Gustafsson and F. Nordström, "Impact of electric vehicle charging on the distribution grid in uppsala 2030," 2017.

[84] S. Allard, P. C. See, M. Molinas, O. B. Fosso, and J. A. Foosnæs, "Electric vehicles charging in a smart microgrid supplied with wind energy," in *2013 IEEE Grenoble Conference*. IEEE, 2013, pp. 1–5.

[85] K. Herter, P. McAuliffe, and A. Rosenfeld, "An exploratory analysis of california residential customer response to critical peak pricing of electricity," *Energy*, vol. 32, no. 1, pp. 25–34, 2007.

[86] M. Messenger, "Strategic plan to reduce the energy impact of air conditioners," *California Energy Commission*, 2008.

[87] L. Yang, C. Dong, C. J. Wan, and C. T. Ng, "Electricity time-of-use tariff with consumer behavior consideration," *International Journal of Production Economics*, vol. 146, no. 2, pp. 402–410, 2013.

[88] A.-H. Mohsenian-Rad and A. Leon-Garcia, "Optimal residential load control with price prediction in real-time electricity pricing environments," *IEEE Trans. Smart Grid*, vol. 1, no. 2, pp. 120–133, 2010.

[89] P. Palensky and D. Dietrich, "Demand side management: Demand response, intelligent energy systems, and smart loads," *IEEE transactions on industrial informatics*, vol. 7, no. 3, pp. 381–388, 2011.

[90] M. H. Albadi and E. F. El-Saadany, "A summary of demand response in electricity markets," *Electric power systems research*, vol. 78, no. 11, pp. 1989–1996, 2008.

[91] Csaba Farkas, Kristóf I. Szabó, László Prikler, "Impact assessment of electric vehicle charging on a lv distribution system," *Proceedings of the 2011 3rd International Youth Conference on Energetics (IYCE)*, 2011.

[92] K. Yunus, H. Z. De La Parra, and M. Reza, "Distribution grid impact of plug-in electric vehicles charging at fast charging stations using stochastic charging model," in *Power Electronics and Applications (EPE 2011), Proceedings of the 2011-14th European Conference on.* IEEE, 2011, pp. 1–11.

[93] P. S. Moses, S. Deilami, A. S. Masoum, and M. A. Masoum, "Power quality of smart grids with plug-in electric vehicles considering battery charging profile," in *Innovative Smart Grid Technologies Conference Europe (ISGT Europe), 2010 IEEE PES.* IEEE, 2010, pp. 1–7.

[94] M. Neaimeh, R. Wardle, A. M. Jenkins, J. Yi, G. Hill, P. F. Lyons, Y. Hübner, P. T. Blythe, and P. C. Taylor, "A probabilistic approach to combining smart meter and electric vehicle charging data to investigate distribution network impacts," *Applied Energy*, vol. 157, pp. 688–698, 2015.

[95] R. Wardle, K. A. Capova, P. Matthews, S. Bell, G. Powells, and H. Bulkeley, "Insight report: Electric vehicles," *Customer-Led Netwoork Revolution*, 2015.

[96] L. Abramowski and A. Holmström, "Res 2005-2006, the national travel survey," *SIKA, Tech. Rep.*, 2007.

[97] J. Link, "Elektromobilität und erneuerbare energien: Lokal optimierter einsatz von netzgekoppelten fahrzeugen," Ph.D. dissertation, Technischen Universität Dortmund, 2012.

[98] M. Roozbehani, M. Dahleh, and S. Mitter, "On the stability of wholesale electricity markets under real-time pricing," in *49th IEEE Conference on Decision and Control (CDC).* IEEE, 2010, pp. 1911–1918.

[99] D. Westermann, M. Agsten, and S. Schlegel, "Empirical bev model for power flow analysis and demand side management purposes," in *2010 Modern Electric Power Systems*. IEEE, 2010, pp. 1–6.

[100] C. Jiang, R. Torquato, D. Salles, and W. Xu, "Method to assess the power-quality impact of plug-in electric vehicles," *IEEE Transactions on Power Delivery*, vol. 29, no. 2, pp. 958–965, 2014.

[101] L. Menz, S. Kehl, F. Grill, and A. Gerlicher, "Challenges in implementing intelligent charging strategies," in *Internet of Things*. VDE, 2016, pp. 6–12.

[102] S. Schey, D. Scoffield, and J. Smart, "A first look at the impact of electric vehicle charging on the electric grid in the ev project," *World Electric Vehicle Journal*, vol. 5, no. 3, pp. 667–678, 2012.

[103] M. Metz and C. Doetsch, "Electric vehicles as flexible loads–a simulation approach using empirical mobility data," *Energy*, vol. 48, no. 1, pp. 369–374, 2012.

[104] P. Poonpun and W. T. Jewell, "Analysis of the cost per kilowatt hour to store electricity," *IEEE Transactions on energy conversion*, vol. 23, no. 2, pp. 529–534, 2008.

[105] M. Hayn, V. Bertsch, and W. Fichtner, "Electricity load profiles in europe: The importance of household segmentation," *Energy Research & Social Science*, vol. 3, pp. 30–45, 2014.

[106] S. You, J. Hu, A. B. Pedersen, P. B. Andersen, C. N. Rasmussen, and S. Cha, "Numerical comparison of optimal charging schemes for electric vehicles," in *2012 IEEE power and energy society general meeting*. Ieee, 2012, pp. 1–6.

[107] W. W. Recker, M. G. McNally, and G. S. Root, "Travel/activity analysis: pattern recognition, classification and interpretation," *Transportation Research Part A: General*, vol. 19, no. 4, pp. 279–296, 1985.

[108] J. D. Mazimpaka and S. Timpf, "Trajectory data mining: A review of methods and applications," *Journal of Spatial Information Science*, vol. 2016, no. 13, pp. 61–99, 2016.

[109] H. Jeung, Q. Liu, H. T. Shen, and X. Zhou, "A hybrid prediction model for moving objects," in *2008 IEEE 24th International Conference on Data Engineering*. IEEE, 2008, pp. 70–79.

[110] H. Barbosa, M. Barthelemy, G. Ghoshal, C. R. James, M. Lenormand, T. Louail, R. Menezes, J. J. Ramasco, F. Simini, and M. Tomasini, "Human mobility: Models and applications," *Physics Reports*, 2018.

[111] S. K. Das, D. J. Cook, A. Battacharya, E. O. Heierman, and T.-Y. Lin, "The role of prediction algorithms in the mavhome smart home architecture," *IEEE Wireless Communications*, vol. 9, no. 6, pp. 77–84, 2002.

[112] M. Hoeynck and B. W. Andrews, "Sensor-based occupancy and behavior prediction method for intelligently controlling energy consumption within a building," Feb. 4 2010, uS Patent App. 12/183,361.

[113] L. Song, D. Kotz, R. Jain, and X. He, "Evaluating next-cell predictors with extensive wi-fi mobility data," *IEEE Transactions on Mobile Computing*, vol. 5, no. 12, pp. 1633–1649, 2006.

[114] S.-M. Qin, H. Verkasalo, M. Mohtaschemi, T. Hartonen, and M. Alava, "Patterns, entropy, and predictability of human mobility and life," *PloS one*, vol. 7, no. 12, p. e51353, 2012.

[115] M. C. Gonzalez, C. A. Hidalgo, and A.-L. Barabasi, "Understanding individual human mobility patterns," *Nature*, vol. 453, no. 7196, p. 779, 2008.

[116] C. Song, T. Koren, P. Wang, and A.-L. Barabási, "Modelling the scaling properties of human mobility," *Nature Physics*, vol. 6, no. 10, p. 818, 2010.

[117] C. M. Schneider, V. Belik, T. Couronné, Z. Smoreda, and M. C. González, "Unravelling daily human mobility motifs," *Journal of The Royal Society Interface*, vol. 10, no. 84, p. 20130246, 2013.

[118] D. Brockmann, L. Hufnagel, and T. Geisel, "The scaling laws of human travel," *Nature*, vol. 439, no. 7075, p. 462, 2006.

[119] C. Song, Z. Qu, N. Blumm, and A.-L. Barabási, "Limits of predictability in human mobility," *Science*, vol. 327, no. 5968, pp. 1018–1021, 2010.

[120] K. Laasonen, "Clustering and prediction of mobile user routes from cellular data," in *European Conference on Principles of Data Mining and Knowledge Discovery*. Springer, 2005, pp. 569–576.

[121] F. Calabrese, M. Diao, G. Di Lorenzo, J. Ferreira Jr, and C. Ratti, "Understanding individual mobility patterns from urban sensing data: A mobile phone trace example," *Transportation research part C: emerging technologies*, vol. 26, pp. 301–313, 2013.

[122] Y. Chon, H. Shin, E. Talipov, and H. Cha, "Evaluating mobility models for temporal prediction with high-granularity mobility data," in *Pervasive computing and communications (PerCom), 2012 IEEE international conference on*. IEEE, 2012, pp. 206–212.

[123] Q. Lv, Y. Qiao, N. Ansari, J. Liu, and J. Yang, "Big data driven hidden markov model based individual mobility prediction at points of interest," *IEEE Transactions on Vehicular Technology*, vol. 66, no. 6, pp. 5204–5216, 2017.

[124] J. Duch and A. Arenas, "Community detection in complex networks using extremal optimization," *Physical review E*, vol. 72, no. 2, p. 027104, 2005.

[125] B. Hillier, A. Turner, T. Yang, and H.-T. Park, "Metric and topo-geometric properties of urban street networks: some convergences, divergences and new results," *Journal of Space Syntax Studies*, 2009.

[126] R. Kitamura, C. Chen, R. M. Pendyala, and R. Narayanan, "Micro-simulation of daily activity-travel patterns for travel demand forecasting," *Transportation*, vol. 27, no. 1, pp. 25–51, 2000.

[127] L. Mari, E. Bertuzzo, L. Righetto, R. Casagrandi, M. Gatto, I. Rodriguez-Iturbe, and A. Rinaldo, "Modelling cholera epidemics: the role of waterways, human mobility and sanitation," *Journal of the Royal Society Interface*, vol. 9, no. 67, pp. 376–388, 2011.

[128] R. Di Taranto, S. Muppirisetty, R. Raulefs, D. Slock, T. Svensson, and H. Wymeersch, "Location-aware communications for 5g networks: How location information can improve scalability, latency, and robustness of 5g," *IEEE Signal Processing Magazine*, vol. 31, no. 6, pp. 102–112, 2014.

[129] H. Farooq and A. Imran, "Spatiotemporal mobility prediction in proactive self-organizing cellular networks," *IEEE Communications Letters*, vol. 21, no. 2, pp. 370–373, 2016.

[130] P. Baumann, *Human Mobility and Application Usage Prediction Algorithms for Mobile Devices*. Verlag Dr. Hut, 2016.

[131] A. Monreale, F. Pinelli, R. Trasarti, and F. Giannotti, "Wherenext: a location predictor on trajectory pattern mining," in *Proceedings of the 15th ACM SIGKDD international conference on Knowledge discovery and data mining*. ACM, 2009, pp. 637–646.

[132] Y. Chon, E. Talipov, H. Shin, and H. Cha, "Mobility prediction-based smartphone energy optimization for everyday location monitoring," in *Proceedings of the 9th ACM conference on embedded networked sensor systems*. ACM, 2011, pp. 82–95.

[133] Douglas C. Schmidt, "Google data collection," *Digital Content Next*, August 15, 2018.

[134] A. Küpper, *Location-based services: fundamentals and operation*. John Wiley & Sons, 2005.

[135] J. Krumm and E. Horvitz, "Predestination: Inferring destinations from partial trajectories," in *International Conference on Ubiquitous Computing*. Springer, 2006, pp. 243–260.

[136] S. Hasan, C. M. Schneider, S. V. Ukkusuri, and M. C. González, "Spatiotemporal patterns of urban human mobility," *Journal of Statistical Physics*, vol. 151, no. 1-2, pp. 304–318, 2013.

[137] B. Kapicioglu, D. S. Rosenberg, R. E. Schapire, and T. Jebara, "Collaborative place models," in *Twenty-Fourth International Joint Conference on Artificial Intelligence*, 2015.

[138] C. Kang, S. Gao, X. Lin, Y. Xiao, Y. Yuan, Y. Liu, and X. Ma, "Analyzing and geo-visualizing individual human mobility patterns using mobile call records," in *2010 18th international conference on geoinformatics*. IEEE, 2010, pp. 1–7.

[139] D. Ashbrook and T. Starner, "Learning significant locations and predicting user movement with gps," in *Proceedings. Sixth International Symposium on Wearable Computers,*. IEEE, 2002, pp. 101–108.

[140] D. Ashbrook, "Using gps to learn significant locations and predict movement across multiple users," *Personal and Ubiquitous computing*, vol. 7, no. 5, pp. 275–286, 2003.

[141] F. Cathey and D. J. Dailey, "A prescription for transit arrival/departure prediction using automatic vehicle location data," *Transportation Research Part C: Emerging Technologies*, vol. 11, no. 3-4, pp. 241–264, 2003.

[142] F. Giannotti, M. Nanni, F. Pinelli, and D. Pedreschi, "Trajectory pattern mining," in *Proceedings of the 13th ACM SIGKDD international conference on Knowledge discovery and data mining*. ACM, 2007, pp. 330–339.

[143] F. Calabrese, G. Di Lorenzo, and C. Ratti, "Human mobility prediction based on individual and collective geographical preferences," in *13th international*

IEEE conference on intelligent transportation systems. IEEE, 2010, pp. 312–317.

[144] H. He, Y. Qiao, S. Gao, J. Yang, and J. Guo, "Prediction of user mobility pattern on a network traffic analysis platform," in *Proceedings of the 10th International Workshop on Mobility in the Evolving Internet Architecture*. ACM, 2015, pp. 39–44.

[145] H. Zang and J. C. Bolot, "Mining call and mobility data to improve paging efficiency in cellular networks," in *Proceedings of the 13th annual ACM international conference on Mobile computing and networking*. ACM, 2007, pp. 123–134.

[146] I. O. Nunes, P. O. V. de Melo, and A. A. Loureiro, "Group mobility: Detection, tracking and characterization," in *2016 IEEE International Conference on Communications (ICC)*. IEEE, 2016, pp. 1–6.

[147] J. Froehlich and J. Krumm, "Route prediction from trip observations," SAE Technical Paper, Tech. Rep., 2008.

[148] J. J.-C. Ying, E. H.-C. Lu, W.-C. Lee, T.-C. Weng, and V. S. Tseng, "Mining user similarity from semantic trajectories," in *Proceedings of the 2nd ACM SIGSPATIAL International Workshop on Location Based Social Networks*. ACM, 2010, pp. 19–26.

[149] T. M. T. Do, O. Dousse, M. Miettinen, and D. Gatica-Perez, "A probabilistic kernel method for human mobility prediction with smartphones," *Pervasive and Mobile Computing*, vol. 20, pp. 13–28, 2015.

[150] M. G. Demissie, G. H. de Almeida Correia, and C. Bento, "Exploring cellular network handover information for urban mobility analysis," *Journal of Transport Geography*, vol. 31, pp. 164–170, 2013.

[151] G. Goulet-Langlois, H. N. Koutsopoulos, Z. Zhao, and J. Zhao, "Measuring regularity of individual travel patterns," *IEEE Transactions on Intelligent Transportation Systems*, vol. 19, no. 5, pp. 1583–1592, 2018.

[152] L. A. Adamic, "Zipf, power-laws, and pareto-a ranking tutorial," *Xerox Palo Alto Research Center, Palo Alto, CA, http://ginger. hpl. hp. com/shl/papers/ranking/ranking. html*, 2000.

[153] I. Burbey, "Predicting future locations and arrival times of individuals," Dissertation, Virginia Polytechnic Institute and State University, Blacksburg, Virginia, 26 April, 2011.

[154] L. Song, U. Deshpande, U. C. Kozat, D. Kotz, and R. Jain, "Predictability of wlan mobility and its effects on bandwidth provisioning," in *INFOCOM 2006. 25th IEEE International Conference on Computer Communications. Proceedings.* IEEE, 2006, pp. 1–13.

[155] C. M. Bishop, *Pattern Recognition and Machine Learning.* Springer Science+Business Media, 2006.

[156] I. A. Basheer and M. Hajmeer, "Artificial neural networks: fundamentals, computing, design, and application," *Journal of microbiological methods*, vol. 43, no. 1, pp. 3–31, 2000.

[157] C. M. Bishop *et al.*, *Neural networks for pattern recognition.* Oxford university press, 1995.

[158] D. S. Wickramasuriya, C. A. Perumalla, K. Davaslioglu, and R. D. Gitlin, "Base station prediction and proactive mobility management in virtual cells using recurrent neural networks," in *Wireless and Microwave Technology Conference (WAMICON), 2017 IEEE 18th.* IEEE, 2017, pp. 1–6.

[159] J. Capka and R. Boutaba, "Mobility prediction in wireless networks using neural networks," in *IFIP/IEEE International Conference on Management of Multimedia Networks and Services.* Springer, 2004, pp. 320–333.

[160] V. Etter, M. Kafsi, E. Kazemi, M. Grossglauser, and P. Thiran, "Where to go from here? mobility prediction from instantaneous information," *Pervasive and Mobile Computing*, vol. 9, no. 6, pp. 784–797, 2013.

[161] J. Scott, A. Bernheim Brush, J. Krumm, B. Meyers, M. Hazas, S. Hodges, and N. Villar, "Preheat: controlling home heating using occupancy prediction," in *Proceedings of the 13th international conference on Ubiquitous computing*. ACM, 2011, pp. 281–290.

[162] G. Smith, R. Wieser, J. Goulding, and D. Barrack, "A refined limit on the predictability of human mobility," in *Pervasive computing and communications (PerCom), 2014 IEEE international conference on*. IEEE, 2014, pp. 88–94.

[163] C. Arndt, *Information measures: information and its description in science and engineering*. Springer Science & Business Media, 2012.

[164] I. Burbey and T. L. Martin, "Predicting future locations using prediction-by-partial-match," in *Proceedings of the first ACM international workshop on Mobile entity localization and tracking in GPS-less environments*. ACM, 2008, pp. 1–6.

[165] E. L. Ikanovic and A. Mollgaard, "An alternative approach to the limits of predictability in human mobility," *EPJ Data Science*, vol. 6, no. 1, p. 12, 2017.

[166] A. Cuttone, S. Lehmann, and M. C. González, "Understanding predictability and exploration in human mobility," *EPJ Data Science*, vol. 7, no. 1, p. 2, 2018.

[167] Z. Zhao, H. N. Koutsopoulos, and J. Zhao, "Individual mobility prediction using transit smart card data," *Transportation research part C: emerging technologies*, vol. 89, pp. 19–34, 2018.

[168] L. Hurtado, A. Syed, P. Nguyen, and W. Kling, "Multi-agent based electric vehicle charging method for smart grid-smart building energy management," in *2015 IEEE Eindhoven PowerTech*. IEEE, 2015, pp. 1–6.

[169] R. Follmer, D. Gruschwitz, B. Jesske, and S. Quandt, "Mobilitaet in deutschland 2008: Mid 2008-struktur, aufkommen, emissionen, trends-ergebnisbericht," *The Transportation Research Board*, 2010.

[170] L. Calearo, A. Thingvad, K. Suzuki, and M. Marinelli, "Grid loading due to ev charging profiles based on pseudo-real driving pattern and user behaviour," *IEEE Transactions on Transportation Electrification*, 2019.

[171] G. Pasaoglu, D. Fiorello, A. Martino, G. Scarcella, A. Alemanno, A. Zubaryeva, and C. Thiel, "Driving and parking patterns of european car drivers - a mobility surve," in *Report EUR 25627 EN*.

[172] D. Bochan, "Development of an energy demand simulation model for battery electric vehicles (unpublished master's thesis)," Master's thesis, Stuttgart Media University, 2018.

[173] P. Besse, B. Guillouet, J.-M. Loubes, and R. François, "Review and perspective for distance based trajectory clustering," *arXiv preprint arXiv:1508.04904*, 2015.

[174] K. Torkkola, K. Zhang, H. Li, H. Zhang, C. Schreiner, and M. Gardner, "Traffic advisories based on route prediction," in *Proceedings of Workshop on Mobile Interaction with the Real World*, 2007, pp. 33–36.

[175] M. Schwandt, "Automated vehicle trip data collection in the context of charging strategies for electric vehicles (unpublished master's thesis)," Master's thesis, Stuttgart Media University, 2017.

[176] M. A. Bayir, M. Demirbas, and N. Eagle, "Mobility profiler: A framework for discovering mobility profiles of cell phone users," *Pervasive and Mobile Computing*, vol. 6, no. 4, pp. 435–454, 2010.

[177] M. Weyn and F. Schrooyen, "A wi-fi assisted gps positioning concept," *ECUMICT, Gent, Belgium*, 2008.

[178] A. Jahangiri and H. A. Rakha, "Applying machine learning techniques to transportation mode recognition using mobile phone sensor data." *IEEE Trans. Intelligent Transportation Systems*, vol. 16, no. 5, pp. 2406–2417, 2015.

[179] B. Wang, L. Gao, and Z. Juan, "Travel mode detection using gps data and socioeconomic attributes based on a random forest classifier," *IEEE Transactions on Intelligent Transportation Systems*, vol. 19, no. 5, pp. 1547–1558, 2018.

[180] V. Van Acker, B. Van Wee, and F. Witlox, "When transport geography meets social psychology: toward a conceptual model of travel behaviour," *Transport Reviews*, vol. 30, no. 2, pp. 219–240, 2010.

[181] T. Gnann, P. Plötz, S. Funke, and M. Wietschel, "What is the market potential of plug-in electric vehicles as commercial passenger cars? a case study from germany," *Transportation Research Part D: Transport and Environment*, vol. 37, pp. 171–187, 2015.

[182] D. Ambuhl and L. Guzzella, "Predictive reference signal generator for hybrid electric vehicles," *IEEE transactions on vehicular technology*, vol. 58, no. 9, pp. 4730–4740, 2009.

[183] E. Apostolaki-Iosifidou, P. Codani, and W. Kempton, "Measurement of power loss during electric vehicle charging and discharging," *Energy*, vol. 127, pp. 730–742, 2017.

[184] G. A. McCoy and J. G. Douglass, "Premium efficiency motor selection and application guide–a handbook for industry," Washington State University Energy Program, Tech. Rep., 2014.

[185] M. Allen, "Real-world range ramifications: Heating and air conditioning," *FleetCarma.*, 2014.

[186] C. McLaren, J. Null, J. Quinn *et al.*, "Heat stress from enclosed vehicles: moderate ambient temperatures cause significant temperature rise in enclosed vehicles," *Pediatrics-English Edition*, vol. 116, no. 1, p. e109, 2005.

[187] J. Rugh, A. Pesaran, and K. Smith, "Electric vehicle battery thermal issues and thermal management techniques (presentation)," National Renewable Energy Lab.(NREL), Golden, CO (United States), Tech. Rep., 2013.

[188] I. Almanjahie, "Temperature variations in a parked car," *Masters in Math. Stat. Sc, University of Western Australia*, 2008.

[189] M. Mitschke and H. Wallentowitz, *Dynamik der kraftfahrzeuge*. Springer, 1972, vol. 4.

[190] A. Kreim, "Modellierung und parameteroptimierung einer permanenterregten synchronmaschine unter berücksichtigung von lastzyklen," Ph.D. dissertation, Technische Universität Berlin, 2015.

[191] L. Menz, R. Herberth, S. Körper, C. Luo, F. Gauterin, A. Gerlicher, and Q. Wang, "Identifying atypical travel patterns for improved medium-term mobility prediction," *IEEE Transactions on Intelligent Transportation Systems*, pp. 1–12, 2019.

[192] A. Sadilek and J. Krumm, "Far out: Predicting long-term human mobility." in *AAAI*, 2012.

[193] Y. Chun and D. A. Griffith, "Modeling network autocorrelation in space–time migration flow data: an eigenvector spatial filtering approach," *Annals of the Association of American Geographers*, vol. 101, no. 3, pp. 523–536, 2011.

[194] L. Menz, R. Herberth, C. Luo, F. Gauterin, A. Gerlicher, and Q. Wang, "An improved method for mobility prediction using a markov model and density estimation," in *2018 IEEE Wireless Communications and Networking Conference (WCNC)*. IEEE, 2018, pp. 1–6.

[195] A. Aabrandt, P. B. Andersen, A. B. Pedersen, S. You, B. Poulsen, N. O'Connell, and J. Østergaard, "Prediction and optimization methods for electric vehicle charging schedules in the edison project," in *2012 IEEE PES Innovative Smart Grid Technologies (ISGT)*. IEEE, 2012, pp. 1–7.

[196] J. Zuzanek and B. J. Smale, "Life-cycle and across-the-week allocation of time to daily activities," in *Time use research in the social sciences*. Springer, 2002, pp. 127–153.

[197] C. Zhang and Y. Ma, *Ensemble machine learning: methods and applications*. Springer, 2012.

[198] M. Kim and D. Kotz, "Periodic properties of user mobility and access-point popularity," *Personal and Ubiquitous Computing*, vol. 11, no. 6, pp. 465–479, 2007.

[199] N. Eagle and A. S. Pentland, "Reality mining: sensing complex social systems," *Personal and ubiquitous computing*, vol. 10, no. 4, pp. 255–268, 2006.

[200] S. Boriah, V. Chandola, and V. Kumar, "Similarity measures for categorical data: A comparative evaluation," in *Proceedings of the 2008 SIAM International Conference on Data Mining*. SIAM, 2008, pp. 243–254.

[201] P. J. Rousseeuw, "Silhouettes: A graphical aid to the interpretation and validation of cluster analysis," *Journal of Computational and Applied Mathematics*, vol. 20, pp. 53 – 65, 1987.

[202] J. E. Beck and B. P. Woolf, "High-level student modeling with machine learning," in *International Conference on Intelligent Tutoring Systems*. Springer, 2000, pp. 584–593.

[203] S. Gambs, M.-O. Killijian, and M. N. del Prado Cortez, "Towards temporal mobility markov chains," in *1st International Workshop on Dynamicity Collocated with OPODIS 2011, Toulouse, France*, 2011, pp. 2–pages.

[204] S. Gambs, M.-O. Killijian, and del Prado Cortez, "Next place prediction using mobility markov chains," in *Proceedings of the First Workshop on Measurement, Privacy, and Mobility*. ACM, 2012, p. 3.

[205] P. Baumann, "Adaptive sensor cooperation for predicting human mobility," *Ubicomp '14 ADJUNCT*, September 2014.

[206] M. Balmer, K. Meister, K. Nagel, and K. Axhausen, *Agent-based simulation of travel demand: Structure and computational performance of MATSim-*

T. ETH, Eidgenössische Technische Hochschule Zürich, IVT Institut für Verkehrsplanung und Transportsysteme, 2008.

[207] B. W. Silverman, *Density estimation for statistics and data analysis*. Routledge, 2018.

[208] A. Z. Zambom and R. Dias, "A review of kernel density estimation with applications to econometrics," *arXiv preprint arXiv:1212.2812*, 2012.

[209] E. Parzen, "On estimation of a probability density function and mode," *The annals of mathematical statistics*, vol. 33, no. 3, pp. 1065–1076, 1962.

[210] J. S. Simonoff, *Smoothing methods in statistics*. Springer Science & Business Media, 2012.

[211] C. A. Hoare, "Quicksort," *The Computer Journal*, vol. 5, no. 1, pp. 10–16, 1962.

[212] M. Sokolova, N. Japkowicz, and S. Szpakowicz, "Beyond accuracy, f-score and roc: a family of discriminant measures for performance evaluation," in *Australasian joint conference on artificial intelligence*. Springer, 2006, pp. 1015–1021.

[213] H. Qin and W. Zhang, "Charging scheduling with minimal waiting in a network of electric vehicles and charging stations," in *Proceedings of the Eighth ACM international workshop on Vehicular inter-networking*. ACM, 2011, pp. 51–60.

[214] O. Sundstrom and C. Binding, "Flexible charging optimization for electric vehicles considering distribution grid constraints," *IEEE Transactions on Smart Grid*, vol. 3, no. 1, pp. 26–37, 2011.

[215] S. I. Vagropoulos, G. A. Balaskas, and A. G. Bakirtzis, "An investigation of plug-in electric vehicle charging impact on power systems scheduling and energy costs," *IEEE Transactions on power systems*, vol. 32, no. 3, pp. 1902–1912, 2017.

[216] E. Graham-Rowe, B. Gardner, C. Abraham, S. Skippon, H. Dittmar, R. Hutchins, and J. Stannard, "Mainstream consumers driving plug-in battery-electric and plug-in hybrid electric cars: A qualitative analysis of responses and evaluations," *Transportation Research Part A: Policy and Practice*, vol. 46, no. 1, pp. 140–153, 2012.

[217] J. Schmutzler, C. Wietfeld, and C. A. Andersen, "Distributed energy resource management for electric vehicles using iec 61850 and iso/iec 15118," in *2012 IEEE Vehicle Power and Propulsion Conference*. IEEE, 2012, pp. 1457–1462.

[218] T. Franke and J. F. Krems, "What drives range preferences in electric vehicle users?" *Transport Policy*, vol. 30, pp. 56–62, 2013.

[219] N. Rauh, T. Franke, and J. F. Krems, "Understanding the impact of electric vehicle driving experience on range anxiety," *Human factors*, vol. 57, no. 1, pp. 177–187, 2015.

[220] A. Thingvad and M. Marinelli, "Influence of v2g frequency services and driving on electric vehicles battery degradation in the nordic countries," in *on 31st International Electric Vehicles Symposium & Exhibition & International Electric Vehicle Technology Conference*, 2018.

Appendix A

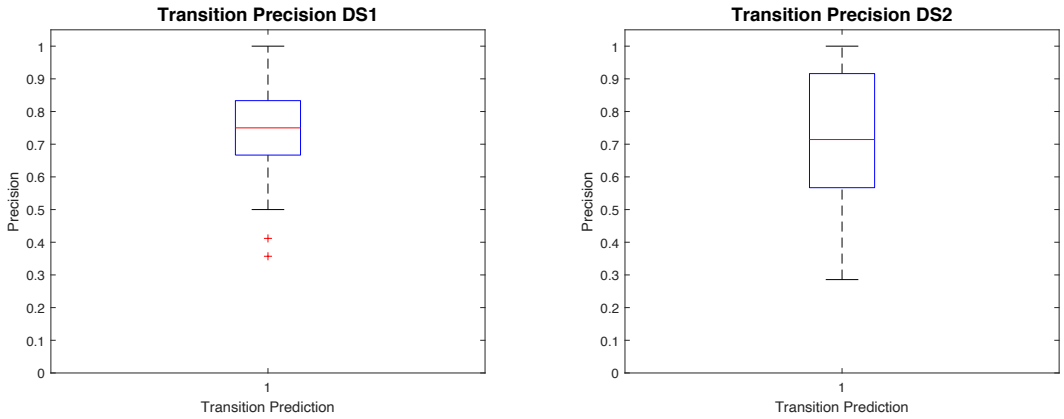

(a) (b)

Figure A1: Transition precision for DS1 and DS2 with MM/KDE

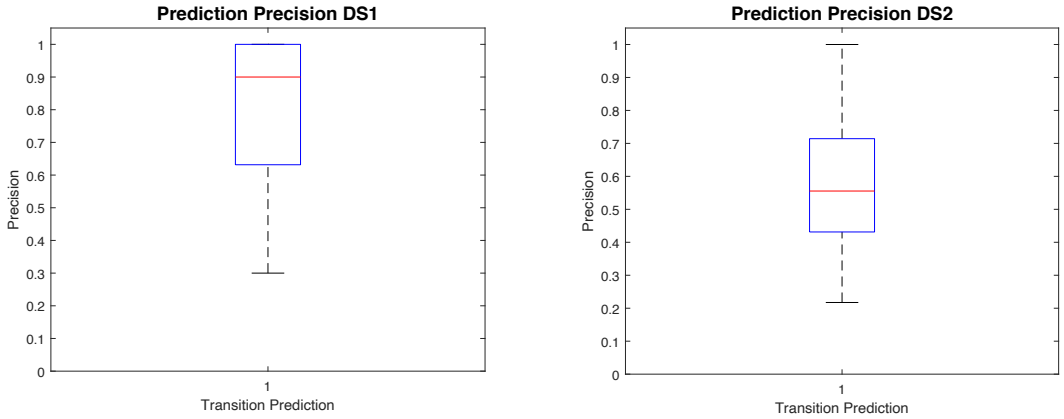

(c) (d)

Figure A2: Transition precision for DS1 and DS2 with Mode

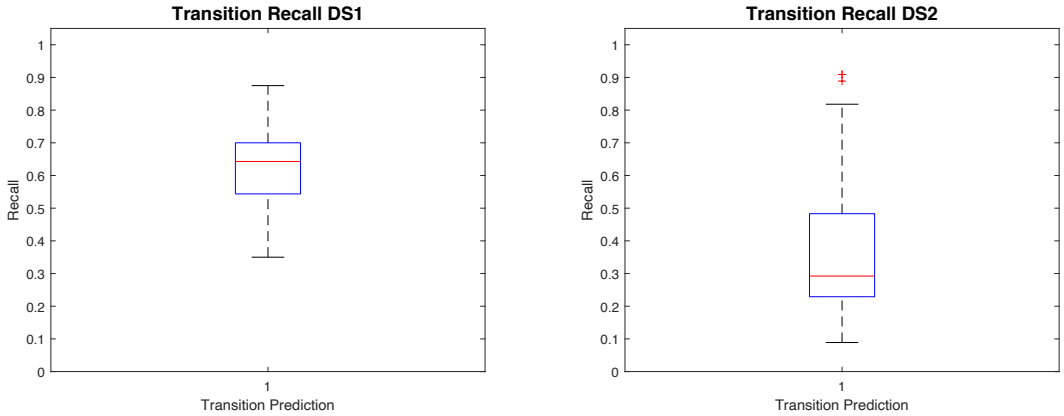

(e) (f)

Figure A3: Transition recall for DS1 and DS2 with with MM/PDF

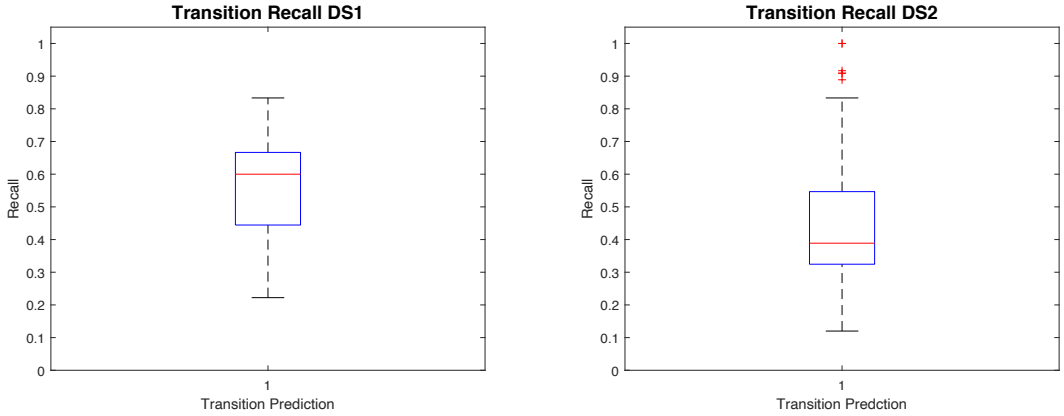

(g) (h)

Figure A4: Transition recall for DS1 and DS2 with with Mode

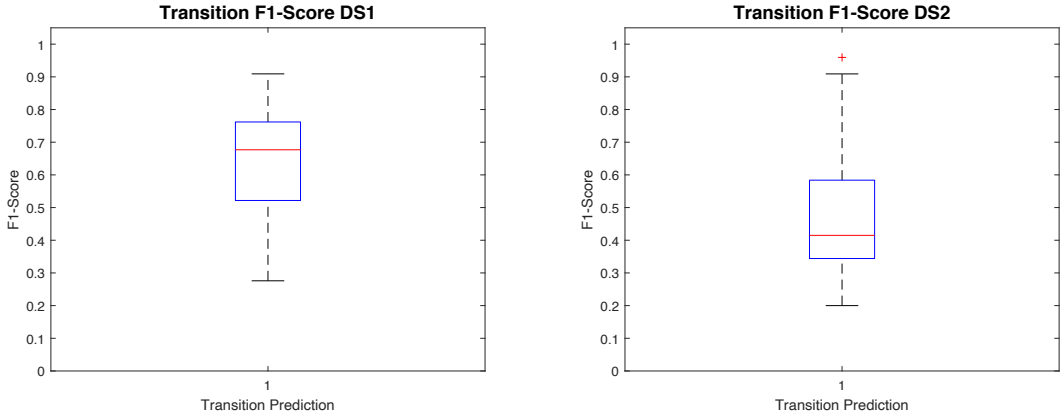

(i) (j)

Figure A5: Transition F1 Score for DS1 and DS2 with with MM/PDF

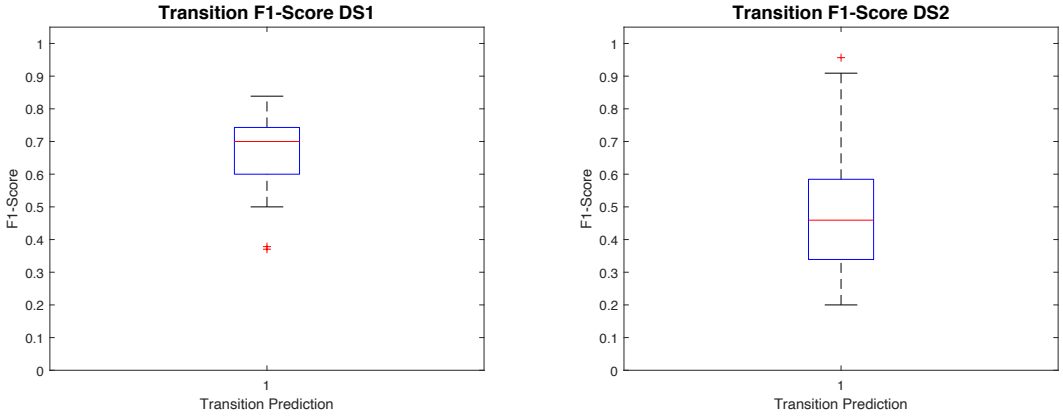

(k) (l)

Figure A6: Transition F1-score for DS1 and DS2 with Mode

Appendix B

Table B1 shows the number of scheduled charging events which corresponds with the number of times a user would have to plug in the vehicle or place it above an AWC ground plate, assuming the availability of Tariff 1. Table B2 and B3 illustrate the framework's results regarding the costs and number of charging events for Tariff 2 and Tariff 3 respectively.

Table B1: Scheduling results for user profiles (Price curve 1)

	Total costs [Euro]			Average price per kWh [Euro]			Total charged energy [kWh]			Number of charging events		
User	Comf.	Flx.	Cst.	Comf.	Flx.	Cst.	Comf.	Flx.	Cos.	Comf.	Flx.	Cst.
1	25.58	32.83	25.58	0.35	0.34	0.34	76	89.44	76	1	8	1
2	72.41	84.71	84.71	0.34	0.33	0.33	214.00	253.00	253.00	**3**	**7**	**7**
3	15.47	35.83	28.19	**0.33**	**0.33**	**0.32**	47.10	109.00	87.70	**1**	**8**	**2**
4	28.20	40.18	40.18	0.34	0.33	0.33	82.10	121.00	121.00	**1**	**10**	**10**
5	-	24.20	-	-	0.33	-	-	73.10	-	-	4	-
6	14.88	26.51	10.78	0.34	0.34	0.34	44.10	78.60	32.10	2	4	2
7	28.56	42.10	42.10	0.34	0.33	0.33	82.90	126.00	126.00	1	8	1
8	10.46	27.54	19.53	0.32	0.33	0.32	32.30	84.40	60.50	1	3	1
9	21.23	35.65	27.10	**0.34**	**0.34**	**0.33**	63.00	106.00	80.90	3	5	3
10	26.36	34.74	34.74	0.34	0.33	0.33	77.80	105.00	105.00	1	3	1
11	38.10	48.66	38.10	0.32	0.32	0.32	119.00	149.00	119.00	2	4	2
12	54.19	66.26	66.26	0.33	0.33	0.33	161.00	198.00	198.00	**3**	**5**	**4**

Table 1: Table B2: Scheduling results for user profiles (Price curve 2)

	Total costs [Euro]			Average price per kWh [Euro]			Total charged energy [kWh]			Number of charging events		
User	Comf.	Flx.	Cst.	Comf.	Flx.	Cst.	Comf.	Flx.	Cos.	Comf.	Flx.	Cst.
1	26.70	30.49	16.06	**0.35**	**0.34**	**0.22**	76.00	89.2	74.5	1	8	1
2	64.70	80.79	64.70	0.30	0.32	0.30	214.00	253.00	214.00	**3**	**7**	**7**
3	16.05	33.77	28.24	**0.34**	**0.31**	**0.26**	47.10	109.00	109.00	**1**	**8**	**3**
4	27.12	39.93	38.36	**0.33**	**0.33**	**0.32**	82.10	121.00	121.00	**1**	**10**	**3**
5	-	19.23	-	-	0.26	-	-	73.10	-	-	4	-
6	15.14	27.30	15.14	0.34	0.35	0.34	44.10	78.60	32.10	2	4	2
7	29.05	41.39	28.86	**0.35**	**0.33**	**0.29**	82.90	126.00	99.20	**1**	**8**	**2**
8	10.69	28.07	19.11	0.33	0.33	0.33	32.30	84.40	58.20	**1**	**3**	**2**
9	22.54	32.70	18.21	**0.36**	**0.32**	**0.29**	63.00	103.00	62.30	3	5	3
10	15.72	32.41	13.37	0.20	0.31	0.20	77.80	105.00	67.30	1	7	1
11	40.07	45.01	44.71	0.33	0.30	0.30	119.00	149.00	149.00	**2**	**5**	**4**
12	55.28	66.82	66.82	0.34	0.34	0.34	161.00	198.00	198.00	**3**	**5**	**5**

Table B3: Scheduling results for user profiles (Price curve 3, Cost Curve 3 Electric Vehicle Time-of-Use Plans - SUMMER (June 1 - October 31) (23 - 54 Cent))

	Total costs [Euro			Average price per kWh [Euro]			Total charged energy [kWh]			Number of charging events		
User	Comf.	Flx.	Cst.	Comf.	Flx.	Cst.	Comf.	Flx.	Cos.	Comf.	Flx.	Cst.
1	22.90	26.38	26.38	0.30	0.30	0.30	76.00	89.20	74.50	**1**	**8**	**8**
2	65.13	72.41	72.41	0.30	0.29	0.29	214.00	253.00	214.00	**3**	**7**	**6**
3	13.36	29.20	23.24	**0.28**	**0.27**	**0.26**	47.10	109.00	109.00	**1**	**8**	**3**
4	26.65	33.68	33.68	0.32	0.28	0.28	82.10	121.00	121.00	**1**	**10**	**10**
5	-	21.34	-	-	0.29	-	-	73.10	-	-	4	-
6	13.91	22.78	9.08	**0.29**	**0.29**	**0.28**	44.10	78.60	32.10	2	4	2
7	24.98	35.19	35.19	0.30	0.28	0.28	82.90	126.00	99.20	**1**	**8**	**8**
8	8.94	23.11	15.38	0.26	0.27	0.26	32.30	84.40	58.20	**1**	**3**	**2**
9	18.25	30.47	18.25	0.29	0.29	0.29	63.00	103.00	62.30	3	5	3
10	25.21	29.38	29.38	0.32	0.28	0.28	77.80	105.00	67.30	**1**	**7**	**7**
11	32.26	41.37	32.26	0.27	0.28	0.27	119.00	149.00	149.00	2	5	2
12	45.23	55.02	55.02	0.28	0.28	0.28	161.00	198.00	198.00	**3**	**5**	**5**